

Copyright
By
Brian James Petruzzi
2010

The thesis committee for Brian James Petruzzi
certifies that this is the approved version of the following thesis:

Stabilizing Techniques for Curved Steel I-Girders During Construction

**APPROVED BY
SUPERVISING COMMITTEE:**

Todd A. Helwig, Supervisor

Michael D. Engelhardt

Stabilizing Techniques for Curved Steel I-Girders During Construction

by

Brian James Petruzzi, B.S.C.E

Thesis

Presented to the Faculty of the Graduate School of

The University of Texas at Austin

in Partial Fulfillment

of the Requirements

for the Degree of

Master of Science in Engineering

The University of Texas at Austin

May 2010

Dedication

To my parents, whose love and support have made this possible and to my sister, who has always inspired me to be the best person I can be.

Acknowledgements

I would like to thank the Texas Department of Transportation for funding an abundance of projects at Fergusson Structural Engineering Laboratory and allowing students such as myself the opportunity to conduct research. I have enjoyed my time at The University of Texas a great deal and attribute a large amount of that enjoyment to my experiences and friendships developed at FSEL.

I also feel very fortunate to have been placed on an incredible research team. All four of the professors who have been involved in the curved girder research project, Todd Helwig, Eric Williamson, Karl Frank, and Michael Engelhardt, have provided me endless guidance and support which was invaluable to the success and completion of this thesis. The advice given to me by Dr. Helwig and Dr. Engelhardt throughout the writing process was greatly appreciated and this thesis is better because of it. I would particularly like to thank the PhD student on the project, Jason Stith, for being an incredible mentor. Jason's hard work, thoroughness, and curiosity in his own research was inspirational to me I immensely enjoyed all of the time spent with him over the past two years. I attribute much of my research success at UT to him and wish him the best in the future.

Lastly I would like to thank my parents, Jim and Carol, and my sister, Heather, who have always supported me in the decisions I have made in all aspects of my life. Although they may not agree with everything I do, it is because of their continued support and love that I have the confidence, ability, and most of all the opportunity to come to Texas to complete my Master's Degree. They are greatly appreciated and I owe them everything.

Brian J. Petruzzi

May 7, 2010

Stabilizing Techniques for Curved Steel I-Girders During Construction

Brian James Petruzzi, M.S.E.

The University of Texas at Austin, 2010

SUPERVISOR: Todd Helwig

There are many issues and challenges to deal with when designing a curved I-girder bridge. These challenges primarily deal with the many performance stages that curved I-girder bridges have such as the erection, construction, and in-service stages. When design engineers assess the stability of a bridge system, they typically evaluate the system in its final configuration with all cross frames attached and the hardened concrete deck placed. The evaluation of girder stability during erection and early stages of construction stages is difficult because of the limited presence of bracing in the system. Due to a lack of readily available analytical tools, many contractors do not conduct detailed analytical evaluations of the bridge behavior during early stages of the construction when stability is often critical. Instead, many contractors use rules of thumb and experience to ensure stability during erection. Erection and construction practices typically vary among contractors and consistent erection methods are a rarity. Although some rules of thumb may be quite conservative, others are much less so. Therefore, coming up with design guidelines based on parametric studies rather than rules of thumb are desirable to help allow the contractor and the designer to work together to prevent issues that may occur due to the lack of communication between the two professions.

Lastly, many challenges arise due to the complex geometry of curved I-girders. To prevent excessive rotation in erected girders, three points of vertical support are often

provided. Two of these points usually consist of permanent supports in the form of bridge piers or abutments. The third point of support may consist of a temporary support in the form of a shore tower or holding crane. Cases where a holding crane may be satisfactory over a shore tower are also not well understood.

To improve the understanding of lifting practices and temporary support requirements, parametric studies were conducted using the finite element program ANSYS. Field data consisting of displacement, stress, and girder rotations gathered from two tests were used to validate both the linear and geometric non-linear three-dimensional FEA models. Upon validation, the finite element model was used to conduct linear and geometric non-linear analyses to determine critical factors in curved I-girder bridges during construction. Specifically, serviceability limit states were studied for the lifting of curved girders. For partially constructed states, parametric studies were conducted to determine optimal locations to place temporary supports as well as to investigate stability differences between using a shore tower and a holding crane. Recommendations are presented to provide guidance for the lifting of curved I-girders as well as to maximize stability of partially constructed bridges.

Table of Contents

CHAPTER 1 Introduction.....	1
1.1 Overview	1
1.2 Scope of Study.....	4
1.3 Thesis Overview.....	5
CHAPTER 2 Background and Literature Review	6
2.1 Introduction	6
2.2 Recent Work by Others	6
2.2.1 Effects of Web Plumbness on Girder Rotation.....	6
2.2.2 Girder Lateral Torsional Buckling.....	7
2.2.3 Flange Local Buckling.....	9
2.3 Work Previously Completed on TxDOT Project 0-5574.....	10
2.3.1 Girder Lifting Field Tests	10
2.3.2 Finite Element Analysis of Lifting of Curved Girders	11
2.3.3 Nationwide Survey of Erectors.....	12
2.3.4 Development of Analysis Tools.....	12
2.4 Summary	13
CHAPTER 3 Non-Linear Analysis of Lifting of Curved Steel I-Girders	14
3.1 Introduction	14
3.2 Modeling Approaches	15
3.3 Research Objectives	17
3.4 Previous Work on Lifting of Curved Girders for Project 0-5574	17
3.4.1 Rigid Body Girder Rotations	19
3.4.2 Buckling Expressions for Girder Stability.....	20
3.5 Study Description.....	29
3.5.1 Finite Element Modeling Technique	29
3.5.2 Parameter Descriptions	30
3.5.3 Parameter Ranges.....	31
3.6 Results of Parametric Studies.....	33

3.6.1	Overview.....	33
3.6.2	Using Eigenvalues to Predict Instability of Curved Girders.....	33
3.6.3	Additional Failure Criteria for Lifting of Horizontally Curved I-Girders 35	
3.6.4	Controlling Girder Rotation during Lifting.....	40
3.6.5	Preferred Lifting Locations.....	50
3.7	Conclusions.....	57
3.7.1	Eigenvalues.....	57
3.7.2	Rotation Limits.....	57
3.7.3	Lifting Location Limits.....	58
3.7.4	Preferred Lifting Locations.....	58
CHAPTER 4 Parametric Studies on the Behavior of Partially Constructed Bridges with Curved Steel I-Girders.....		60
4.1	Introduction.....	60
4.2	Background on Shore Towers and Holding Cranes.....	61
4.3	Study Objectives and Description.....	64
4.3.1	Parameter Descriptions.....	64
4.3.2	Parameter Ranges.....	65
4.4	Results of Parametric Studies.....	67
4.4.1	Shore Tower Location.....	67
4.4.2	Holding Crane Location.....	71
4.4.3	Holding Crane Lifting Load.....	73
4.5	Load Height Effects.....	77
4.5.1	Shore Towers.....	77
4.5.2	Holding Cranes.....	79
4.6	Critical Stages During Construction.....	82
4.7	Conclusions.....	85
CHAPTER 5 Conclusions and Recommendations.....		87
5.1	Introduction.....	87

5.2	Non-Linear Analysis of Lifting of Curved Steel I-Girders	88
5.3	Partially Constructed Bridges.....	89
APPENDIX A Parametric Study Summary for the Lifting of Curved Steel I-Girders		91
A.1	Parametric Study Summary.....	91
A.1.1	Study One.....	92
A.1.2	Study Two.....	98
A.1.3	Study Three.....	105
A.1.4	Study Four.....	109
A.1.5	Study Five.....	112
A.1.6	Study Six.....	116
APPENDIX B Parametric Study Summary for Partially Constructed Bridges during Erection.....		120
B.1	Parametric Study Summary.....	120
B.1.1	Study One.....	121
B.1.2	Study Two.....	127
B.1.3	Study Three.....	133
References.....		145
Vita.....		147

List of Tables

Table 2.1: Guidelines for the Stability of a Steel I-girder.....	8
Table B.1: Case 1 Temporary Support Location and Corresponding Reaction	134
Table B.2: Case 2 Temporary Support Location and Corresponding Reaction	134
Table B.3: Case 3 Temporary Support Location and Corresponding Reaction	134

List of Figures

Figure 1.1: Curved Bridge Collapse [Photo Courtesy ILDOT].....	3
Figure 2.1: Parameter Definitions for Girder Lifting Studies.....	11
Figure 3.1: Effect of Radius of Curvature on Eigenvalue, λ for Different Lift Locations (Schuh, 2008).....	18
Figure 3.2: Location of Center of Gravity and Line of Support for Straight and Curved Girders.....	20
Figure 3.3: C_L vs. a/L for a Flange Width to Depth Ratio [Prismatic] (Schuh)	25
Figure 3.4: C_L vs. a/L for a Span to Depth Ratio [Prismatic] (Schuh)	25
Figure 3.5: C_b vs. a/L for a Flange Width to Depth Ratio [Non-Prismatic] (Farris)	26
Figure 3.6: C_b vs. a/L for Span to Depth Ratio [Non-Prismatic](Farris).....	26
Figure 3.7: Effect of Radius of Curvature on Eigenvalue, λ (Stith, Schuh and Farris, Guidance for Erection and Construction of Curved I-girder Bridges, FHWA/TX- 09/0-5574).....	29
Figure 3.8: Definition of Parameters	31
Figure 3.9: Flange Lateral Displacements for $b_f/D = 1/3$	34
Figure 3.10: Flange Lateral Displacements for $b_f/D = 1/6$	34
Figure 3.11: Lifting Configuration for Figure 3.12 through Figure 3.15	37
Figure 3.12: Flange Lateral Displacements [$a/L = 0.25$; $b_f/D = 1/3$; $R = 500'$]	38
Figure 3.13: Flange Lateral Displacements [$a/L = 0.25$; $b_f/D = 1/3$; $R = 8000'$ (Straight)]	38
Figure 3.14: Flange Lateral Displacements [$a/L = 0.25$; $b_f/D = 1/6$; $R = 500'$]	39
Figure 3.15: Flange Lateral Displacements [$a/L = 0.25$; $b_f/D = 1/6$; $R = 8000'$ (Straight)]	39
Figure 3.16: Rotations at the End of the Girder for Different Lifting Locations.....	42
Figure 3.17: Rotations at Middle of Girder for Different Lifting Locations	43
Figure 3.18: Eccentricity for Prismatic Girders Lifted at Different Locations.....	44
Figure 3.19: Flange Rotation [$a/L = 0.30$; $b_f/D = 1/3$; $R = 500'$]	45

Figure 3.20: Cross Sectional Twist.....	46
Figure 3.21: Example Torsion Diagram for Prismatic Girder [$a/L = 0.23$].....	47
Figure 3.22: Summation of Area under Torque Diagram for Different Lift Locations....	48
Figure 3.23: Eigenvalue and Inverted Torque Diagram	49
Figure 3.24: Summation of Area under Torque Diagram for a/L equal to 0.17 – 0.25	50
Figure 3.25: Components of Timoshenko’s LT Buckling Equation.....	51
Figure 3.26: Cross Sectional Property Designations	51
Figure 3.27: Rotations at End of Girder for Different Lifting Locations	53
Figure 3.28: Rotations at Middle of Girder for Different Lifting Locations	54
Figure 3.29: Subtended Angle [Θ] Definition	55
Figure 3.30: Optimal Lifting Location as a Function of Subtended Angle, Theta, to Cause End Rotation of 1.5 Degrees [$b_f/D = 1/5$].....	56
Figure 4.1: Shore Towers under Partially Constructed Bridges	61
Figure 4.2: Temporary Top Flange Bracing to Restrain Girder Rotation.....	62
Figure 4.3: Holding Crane and its Attachment to the Top Flange of a Girder	63
Figure 4.4: Girder Geometric Parametrics.....	65
Figure 4.5: Temporary Support Location Parameter Definitions	66
Figure 4.6: Top Flange Rotational Support Options Considered	67
Figure 4.7: Location of Maximum Positive Moment; Simple Span with Cantilever	69
Figure 4.8: Vertical Reactions for Various Locations along a Girder [$L = 185'$, $b = 51'$]70	
Figure 4.9: Top Flange Out-of-Plane Displacements for Various Shore Tower Positions	71
Figure 4.10: Top Flange Out-of-Plane Displacements for Various Holding Crane Locations.....	72
Figure 4.11: Out of Plane Deflections for Varying Crane Loads	74
Figure 4.12: Geometry Used for Figure 5.18, Figure 5.19, and Figure 5.20.....	75
Figure 4.13: Optimal Load (36.5 kips) and Optimal Location (80 feet).....	75
Figure 4.14: Non-Optimal Load (40 kips) and Optimal Location (80 feet)	76
Figure 4.15: Optimal Load (37.6 kips) and Non-Optimal Location (100 feet)	76

Figure 4.16: Disturbing Force Caused by a Lack of Bracing on the Top Flange	77
Figure 4.17: Linear and Non-Linear Displacements along a Girder for a Girder with a Disturbing Force	78
Figure 4.18: Restoring Force Caused by Lack of Bracing.....	79
Figure 4.19: Displacements along a Girder Supported by a Holding Crane based on Linear versus Nonlinear Geometry Analysis	80
Figure 4.20: Displacements along a Girder Supported by a Shore Tower based on Linear versus Nonlinear Geometry Analysis - Amplified Displacement Scale.....	81
Figure 4.21: Displacements along a Girder Supported by a Holding Crane based on Linear versus Nonlinear Geometry Analysis - Amplified Displacement Scale	82
Figure 4.22: Single Girder Segment Lifted for a Particular Cross Section	83
Figure 4.23: One, Two, Three, and Four Girder Erected Systems – Temporary Support at 80'	84
Figure A.1: Parameter Definitions.....	92
Figure A.2: $b_f/D = 1/3 : a/L = 0.15$:	94
Figure A.3: $b_f/D = 1/3 : a/L = 0.21$:	94
Figure A.4: $b_f/D = 1/3 : a/L = 0.34$:	95
Figure A.5: $b_f/D = 1/4 : a/L = 0.15$:	95
Figure A.6: $b_f/D = 1/4 : a/L = 0.21$:	96
Figure A.7: $b_f/D = 1/4 : a/L = 0.34$:	96
Figure A.8: $b_f/D = 1/6.667 : a/L = 0.15$:	97
Figure A.9: $b_f/D = 1/6.667 : a/L = 0.21$:	97
Figure A.10: $b_f/D = 1/6.667 : a/L = 0.34$:	98
Figure A.11: $b_f/D = 1/3 : a/L = 0.20$:	100
Figure A.12: $b_f/D = 1/3 : a/L = 0.25$:	100
Figure A.13: $b_f/D = 1/3 : a/L = 0.30$:	101
Figure A.14: $b_f/D = 1/4 : a/L = 0.20$:	101
Figure A.15: $b_f/D = 1/4 : a/L = 0.25$:	102
Figure A.16: $b_f/D = 1/4 : a/L = 0.30$:	102

Figure A.17: $b_f/D = 1/6.7 : a/L = 0.20$:	103
Figure A.18: $b_f/D = 1/6.7 : a/L = 0.25$:	103
Figure A.19: $b_f/D = 1/6.7 : a/L = 0.30$:	104
Figure A.20: Rotations : $L = 125' : R = 500'$	106
Figure A.21: Rotations : $L = 125' : R = 1000'$	106
Figure A.22: Rotations : $L = 125' : R = 8000'$ (~Str)	107
Figure A.23: Rotations : $L = 80' : R = 500'$	107
Figure A.24: Rotations : $L = 80' : R = 1000'$	108
Figure A.25: Rotations : $L = 80' : R = 8000'$ (~Str)	108
Figure A.26: End Rotations : $R = 500' : D = 96''$	110
Figure A.27: Middle Rotations : $R = 500' : D = 96''$	110
Figure A.28: End Rotations : $R = 500' : D = 60''$	111
Figure A.29: Middle Rotations : $R = 500' : D = 60''$	111
Figure A.30: Load to Reach Serviceability Limit vs. Interior Angle, Θ ($b_f/D = 1/4$)	113
Figure A.31: Load to Reach Serviceability Limit vs. Interior Angle, Θ ($b_f/D = 1/4$)	113
Figure A.32: Load to Reach Serviceability Limit vs. Interior Angle, Θ ($b_f/D = 1/5$)	114
Figure A.33: Load to Reach Serviceability Limit vs. Interior Angle, Θ ($b_f/D = 1/5$)	114
Figure A.34: Load to Reach Serviceability Limit vs. Interior Angle, Θ ($b_f/D = 1/6$)	115
Figure A.35: Load to Reach Serviceability Limit vs. Interior Angle, Θ ($b_f/D = 1/6$)	115
Figure A.36: Serviceability Limits – $b_f/D = 1/4 : D = 60'' : b = 15'' : R = 1800'$	117
Figure A.37: Serviceability Limits – $b_f/D = 1/6 : D = 60'' : b = 9'' : R = 1800'$	117
Figure A.38: Serviceability Limits – $b_f/D = 1/4 : D = 60'' : b = 15'' : R = 500'$	118
Figure A.39: Serviceability Limits – $b_f/D = 1/6 : D = 60'' : b = 10'' : R = 500'$	118
Figure A.40: Serviceability Limits – $b_f/D = 1/6 : D = 90'' : b = 15'' : R = 500'$	119
Figure B.1: Parameter Definitions	121
Figure B.2: Shore Tower at 40 ft	122
Figure B.3: Shore Tower at 60 ft	122
Figure B.4: Shore Tower at 80 ft	123
Figure B.5: Shore Tower at 100 ft	123

Figure B.6: Shore Tower at 120 ft	124
Figure B.7: Shore Tower at 140 ft	124
Figure B.8: Shore Tower at 160 ft	125
Figure B.9: Shore Tower at 205 ft	125
Figure B.10: Shore Tower at 225 ft	126
Figure B.11: Shore Tower at 245 ft	126
Figure B.12: Holding Crane with 20 kip Vertical Force	128
Figure B.13: Holding Crane with 25 kip Vertical Force	128
Figure B.14: Holding Crane with 30 kip Vertical Force	129
Figure B.15: Holding Crane with 35 kip Vertical Force	129
Figure B.16: Holding Crane with 40 kip Vertical Force	130
Figure B.17: Holding Crane with 45 kip Vertical Force	130
Figure B.18: Holding Crane with 47.8 kip Vertical Force	131
Figure B.19: Holding Crane with 50 kip Vertical Force	131
Figure B.20: Holding Crane with 55 kip Vertical Force	132
Figure B.21: Holding Crane with 60 kip Vertical Force	132
Figure B.22: Shore Tower Reaction vs. Location [% L_{total}]	135
Figure B.23: Case 1: $x = 70$ ft : $F = 49.5$ kips : 0.15 Cantilever.....	136
Figure B.24: Case 1: $x = 80$ ft : $F = 46.0$ kips : 0.15 Cantilever.....	136
Figure B.25: Case 1: $x = 90$ ft : $F = 44.7$ kips : 0.15 Cantilever.....	137
Figure B.26: Case 1: $x = 100$ ft : $F = 45.7$ kips : 0.15 Cantilever.....	137
Figure B.27: Case 1: $x = 110$ ft : $F = 48.8$ kips : 0.15 Cantilever.....	138
Figure B.28: Case 2: $x = 66$ ft : $F = 44.3$ kips : 0.22 Cantilever.....	139
Figure B.29: Case 2: $x = 76$ ft : $F = 40.7$ kips : 0.22 Cantilever.....	139
Figure B.30: Case 2: $x = 86$ ft : $F = 39.1$ kips : 0.22 Cantilever.....	140
Figure B.31: Case 2: $x = 96$ ft : $F = 39.6$ kips : 0.22 Cantilever.....	140
Figure B.32: Case 2: $x = 106$ ft : $F = 42.1$ kips : 0.22 Cantilever.....	141
Figure B.33: Case 3: $x = 56$ ft : $F = 32.5$ kips : 0.30 Cantilever.....	142
Figure B.34: Case 3: $x = 66$ ft : $F = 28.4$ kips : 0.30 Cantilever.....	142

Figure B.35: Case 3: $x = 76$ ft : $F = 26.3$ kips : 0.30 Cantilever.....	143
Figure B.36: Case 3: $x = 86$ ft : $F = 25.9$ kips : 0.30 Cantilever.....	143
Figure B.37: Case 3: $x = 96$ ft : $F = 27.3$ kips : 0.30 Cantilever.....	144

CHAPTER 1

Introduction

1.1 OVERVIEW

The research reported in this thesis addresses questions and problems that arise in the construction of curved steel I-girder bridges. This work is a part of Texas Department of Transportation (TxDOT) Research Project 0-5574 on *Curved Plate Girder Design for Safe and Economical Construction*. There are many issues and challenges to deal with when designing a curved I-girder bridge for safety and serviceability during various stages of construction up through the final in-service condition. This research project examines issues related to safety and serviceability of curved I-girders during lifting operations as well as the safety and serviceability of partially constructed bridges curved I-girder bridges.

When design engineers assess the stability of a bridge system, they typically evaluate the system in its final in-service configuration with all cross frames attached and the hardened concrete deck in-place. However, the most critical stage for stability of the bridge often occurs during erection and the early stages of construction before all cross-frames are in place and before the concrete deck has hardened. Figure 1.1 is a photo of a curved steel I-girder bridge that collapsed during construction.

Traditionally, design engineers and contractors/erectors work independently in the design and construction of most bridges. Design engineers are generally responsible for assuring that the bridge is able to withstand all strength and serviceability limit states in the final in-service configuration. Contractors and erectors, on the other hand, are generally responsible for the stability of the bridge during erection and construction. To minimize problems during construction, the Texas Department of Transportation (TxDOT) has implemented many preferred practices within their designs that are based upon experience. The TxDOT preferred practices sometimes differ and are generally more conservative from those recommended by the American Association of State and

Highway Transportation Officials (AASHTO). One key area of difference is in the recommended value for the ratio of flange width to girder depth, b_f/d . TxDOT preferred practices recommend designing curved I-girders with a target value for b_f/d of 1/3. AASHTO, on the other hand, permits b_f/d values as low as 1/6. Higher values of b_f/d , such as that recommended by TxDOT, produce girders with a higher torsional stiffness making them less likely to distort or fail from lateral torsional buckling. The recommendation to use b_f/d of 1/3 is therefore intended to mitigate girder stability problems during lifting or in early stages of construction before all the bracing is present. On the other hand, designing for b_f/d equal to 1/3 can increase the cost of the girder. Reducing the b_f/d value to the AASHTO limit of 1/6 can result in more economical girders, but can also result in more stability related problems during construction. The girders in the bridge collapse shown in Figure 1.1 had a very low value of b_f/d , as can be seen from the girder contained within the highlighted box. Consequently, the b_f/d value is a critical factor that affects both girder economy and girder stability. Accordingly, one of the questions being examined in this research project is whether the b_f/d value of 1/3 currently recommended by TxDOT can be reduced to provide more economical girders, while still minimizing stability problems during lifting and construction.



Figure 1.1: Curved Bridge Collapse [Photo Courtesy ILDOT]

Many challenges arise in assessing stability during construction due to the complex geometry of curved I-girders. The center of gravity of a curved I-girder is eccentric to the centerline of the girder. Therefore, the girder rotates until the center of gravity of the girder lines up with the lifting points to maintain static equilibrium (Farris 2008). To prevent excessive rotation in partially erected systems, three points of vertical support are often provided. Two of these points usually consist of permanent supports in the form of bridge piers or abutments. The third point of support may consist of a temporary support in the form of a shore tower or holding crane. The boundary conditions at these supports are often difficult to characterize and to properly model with commercially available bridge software. In addition to unclear boundary conditions, many questions must be considered in evaluating stability during construction. How many cross frames will be attached before the next girder is lifted and how many should be attached to prevent buckling? Once the girders are in place, which segments of concrete should be placed first, and how much time needs to elapse to ensure sufficient

composite action before placing the next section? Developing tools to address these questions is an additional goal of TxDOT Research Project 0-5574.

1.2 SCOPE OF STUDY

As described earlier, this thesis is a part of a TxDOT Research Project 0-5574 on *Curved Plate Girder Design for Safe and Economical Construction*. The focus of the research study is to study the behavior and safety of curved steel I-girder bridges during construction. Included within the overall scope of this project is the development of recommendations and tools for evaluating safety and serviceability of curved I-girders through all stages of the erection process as well as during casting of the concrete deck. Research activities included field instrumentation of steel I-girders during lifting operations and curved steel I-girder bridges at various stages of construction. The field data was used to develop an improved understanding of behavior during construction and to validate finite element models. To better understand the behavior of the curved girders throughout all of the performance stages, extensive parametric studies were conducted using the finite element program ANSYS. Finally, two PC based tools, *UT Lift* and *UT Bridge* were created to help analyze both the lifting and partially constructed stages of construction. *UT Lift*, a macro-enabled spread sheet analyzes the behavior of curved I-girders during lifting. *UT Bridge* is a full three-dimensional finite element program for analyzing bridge systems during the erection sequence and deck placement. Research conducted in earlier phases of Project 0-5574 is reported by Schuh (2008), Farris (2008) and Stith (2010). Further background on this work is provided in Chapter 2 of this thesis.

The purpose of research conducted for this thesis was to extend and supplement other work on Project 0-5774 by Schuh (2008), Farris (2008) and Stith (2010). More specifically, the research reported in this thesis has two primary objectives. The first objective is to extend previous work on lifting of curved I-girders by Schuh (2008) and Farris (2008). The previous work evaluated the stability of curved I-girders during lifting through the use of eigenvalue buckling analysis. However, it is unclear if eigenvalue analysis provides an accurate prediction of instability for curved girders. Consequently, in this thesis, the behavior of curved I-girders during lifting is evaluated using nonlinear

geometry analyses. The purpose of this nonlinear analysis was to evaluate the suitability of eigenvalue analyses for curved girders and to provide additional insights into problems that can arise during lifting operations. The second objective of the research reported herein was to examine how the use and placement of temporary shore towers and holding cranes affect the structural performance of partially constructed curved steel I-girder bridges.

1.3 THESIS OVERVIEW

Background information on previous research conducted on the behavior and analyses of curved steel I-girder bridges during construction is provided in Chapter 2. This includes research conducted under TxDOT Project 0-5574 as well as work by others.

The results of a parametric finite element study on the lifting of curved I-girders based on geometric nonlinear analyses are provided in Chapter 3. The behavior of girders during lifting predicted by nonlinear analyses is compared with eigenvalue buckling analyses. The results of the nonlinear analyses are also used to evaluate serviceability criteria for lifting and to develop recommendations on preferred lifting locations.

The results from parametric finite element studies on partially constructed bridges are highlighted in Chapter 4. This parametric study focuses on identifying when a temporary support is required to stabilize a girder. In addition, advantages and disadvantages are discussed for both shore towers and holding cranes. A summary of all of the work presented in this thesis is provided in the final chapter.

CHAPTER 2

Background and Literature Review

2.1 INTRODUCTION

As described in Chapter 1, the research summarized in this thesis was conducted as part of TxDOT Research Project 0-5574 on *Curved Plate Girder Design for Safe and Economical Construction*. A significant amount of research has already been completed under this project, and has been documented in the M.S. theses by Schuh (2008) and Farris (2008) and in the PhD dissertation by Stith (2010). Prior to TxDOT Project 0-5574, there has been considerable previous research on the behavior of curved steel I-girders that support the objectives of this research project. Extensive reviews of previous research have been documented by Schuh (2008), Farris (2008) and Stith (2010), and will not be repeated here. Material presented in this chapter will therefore only summarize on recent research efforts conducted by others since 2007. In addition, the previous work completed on TxDOT Project 0-5574 will also be summarized.

2.2 RECENT WORK BY OTHERS

This section provides a review of recent research pertinent to curved girders that has been published since the original literature review was completed by Schuh (2008), Farris (2008), and Stith (2010). Most of the studies that were reviewed investigated the behavior of erected steel I-girders and concrete deck placement. No recent research was found on the behavior of steel I-girders during the lifting process when the only source of support comes from the crane.

2.2.1 Effects of Web Plumbness on Girder Rotation

Recent work by Howell and Earls (2007) examined the effects that web out of plumbness on the constructability of a bridge. The authors note that the self weight of a girder alone will typically cause a curved girder to roll off of two supports. The reason for the instability is because the girder's center of gravity is not in line with the web. In

order to prevent the girder from rolling over, erectors attempt to brace the girder at a third point by either introducing a temporary support into the system, placing cables and wood blocks at permanent supports to prevent rotation, or erecting two girders at one time when possible. Currently, there is no guidance in AASHTO on the allowable magnitude of web rotation. The goal of the work by Howell and Earls was to quantify the effects that web out-of-plumbness have on the girder behavior and to determine a suitable limit. To quantify the effects, they computed girder flange stresses, vertical deflections, girder distortion, and cross-frame forces with only steel dead load. Using finite element analysis, the researchers modeled a six girder, three span continuous bridge with no skew angles, and a radius of curvature of just over 500 feet. They changed the web out-of-plumbness from zero degrees to five degrees in one degree increments. The results of the study showed that the lateral deflections increased up to 250% for five degrees out of plumbness and up to 100% for just two degrees of out of plumbness. The cross frame forces were affected the most in the vicinity of the support locations. From the analyses conducted, it was concluded that controlling the web plumbness is crucial in the construction of bridges and that a more robust level of analysis may be needed for the construction of complex curved steel I-girder bridges.

2.2.2 Girder Lateral Torsional Buckling

Recent work on lateral torsional buckling of steel I-girders during bridge erection is reported by Zhao et al (2009). Zhao et al discuss the validity of commonly used guidelines for girder stability related to the ratio L/b . The unbraced length of the girder is represented by L and b is the flange width. The Handbook for Construction Engineers provides L/b ranges for both cantilevers and simply supported sections that state whether a system is stable, may be stable, or temporary supports are required as listed in Table 2.1 (American Bridge Division).

System Stability	Cantilever	Simply Supported
Stable	$L/b < 30$	$L/b < 60$
May be Stable	$30 \leq L/b < 40$	$60 \leq L/b < 80$
Temporary Supports Required	$40 \leq L/b$	$80 \leq L/b$

Table 2.1: Guidelines for the Stability of a Steel I-girder

Zhao used the AASHTO LRFD (2007) design guidelines and finite element analyses to evaluate the validity of these guidelines. The AASHTO LRFD states that a steel girder under bending will remain stable if lateral torsional buckling is prevented as shown in Eq. 2.1.

$$f_{bu} \leq \phi_f F_{cr} \quad \text{Eq. 2.1}$$

$$f_{bu} = \frac{M_u C}{I}$$

This formulation is only valid for simple bending and therefore can only be applied to straight girders. Through this simple equation, a closed form solution of the maximum unbraced length, L_{max} , can be determined for both a simply supported beam and a cantilever as seen in Eq. 2.2 where r_t is the effective radius of gyration for lateral torsional buckling, C_b is the moment gradient modifier, R_b is the web load shedding factor, E is the modulus of elasticity, I is the moment of inertia, ϕ_f is the resistance factor for flexure, w_u is the girder self weight along the span, and d is the girder depth.

$$L_{max} = 1.28 \sqrt[4]{\frac{\phi_f C_b R_b \pi^2 E I r_t^2}{w_u d}} \quad \text{Eq. 2.2}$$

Using the closed form solution for L_{max} , a parametric study was conducted where the girder's cross sectional properties were varied and a resulting L_{max} was determined. The same cross sections were then modeled in ABAQUS and the results were presented as a series of curves that show $(L/b)_{max}$ versus web depth for numerous cross sections. From the results, it was determined that for both cantilevers and simply supported beams, the lower limits given by the handbook are reasonable, but that the upper limits can be slightly increased. Through the parametric studies, it was also determined that the most

important factors to control girder stability are the compression flange width and the web depth.

In addition to looking at commonly used rules of thumb for girder stability, Zhao et al (2009) also discussed optimal places to brace a cantilevered steel I-girder during erection to minimize both vertical and lateral deflections and prevent lateral-torsional buckling (Q. Zhao, B. Yu and E. G. Burdette). Using ABAQUS, Zhao et al modeled a cantilever and factored the self weight in accordance to the AASHTO code (1.5 x dead load). With no bracing, the section buckled under its own factored self weight. Bracing was then placed at the top flange, bottom flange, and both flanges and the location and magnitude of the maximum lateral displacements along the girder were computed. It was determined that although it was best to brace both the top and bottom flange, that the response of the girder was almost the same by just bracing the top, tension flange. Bracing just the bottom (compression) flange resulted in lower deflections than no bracing, but didn't prevent the girder from buckling. As a result, it was concluded that bracing the top, tension flange is an efficient and effective way to prevent lateral torsional buckling in erection situations where a girder is cantilevered past a support.

2.2.3 Flange Local Buckling

Madhavan and Davidson (2009) conducted a study on flange local buckling in curved I-girders. This research examined the effect that the curvature and warping stresses had on the local buckling behavior of the compression flange. Traditionally, only bending stresses are considered in local flange buckling. Yet, due to the curved geometry, skewed supports, eccentricity of the deck weight on overhand brackets, deck forms, screed rails, utilities, and wind loads, additional torsional and lateral bending stresses can be introduced into the girder. The current 2007 AASHTO LRFD Specification implements a unified approach for the flexural design of both tangential and horizontally curved I-girder bridges with lateral bending loads to prevent local buckling. The code states that for all girder slenderness ratios, a “one-third” rule is applied that accounts for lateral bending in the flange. The “one-third” rule takes the maximum stress that a cross section can handle before local buckling will occur, and reduces it by a factor

of $f_l/3$ where f_l is the factored lateral flange bending stress at the section being considered. Using theoretical equations to evaluate definitions for slenderness limits, Madhavan and Davidson were able to conclude that the “one-third” rule adopted by AASHTO in 2007 is accurate for compact sections, but is increasingly conservative for both non-compact and slender sections.

2.3 WORK PREVIOUSLY COMPLETED ON TXDOT PROJECT 0-5574

There are many aspects of TxDOT Project 0-5574 that were completed before and in conjunction with the work described in this thesis. In order for the parametric studies in this thesis to be completed on girder lifting and partially constructed bridges, a validated three dimensional finite element model in ANSYS was needed. To validate the ANSYS model, two independent field tests were completed to compare with ANSYS predictions. Numerous eigenvalue and linear-elastic analyses were also previously completed using the validated ANSYS model to investigate the stability of curved steel I-girders during lifting. A nationwide survey of bridge erectors was also conducted to establish typical industry lifting procedures and limits. Lastly, two analysis tools, UT Lift and UT Bridge, were developed to assist designers and contractors to analyze curved I-girders during lifting and to analyze partially constructed bridges. A brief discussion of this previous work is described below.

2.3.1 Girder Lifting Field Tests

The literature review showed that very little research work has previously been done on the lifting of horizontally curved I-girders. As a result, two tests were conducted as part of TxDOT Project 0-5574 to better understand the behavior of curved steel I-girders during lifting and to provide data to validate an ANSYS model for girder lifting. In the first set of tests, a bridge located near Austin Bergstrom International Airport on SH 130 at US 71 was instrumented and monitored during lifting. The data collected in this test was difficult to interpret because the girder support conditions on the ground prior to lifting were not well defined (Schuh). Therefore, a second set of tests were conducted in San Angelo, Texas at a Hirschfeld Steel Company bridge girder

storage site. Using a crane at the storage site, a curved steel I-girder was instrumented and displacements, rotations, and stresses were monitored during lifting. In this test, well-defined girder support conditions were provided. As a result, high quality data was obtained in this test. Further details of these tests are provided by Schuh (2008).

To the author's knowledge, there is no other experimental data available that records both rotations and stresses of curved steel I-girders during lifting.

2.3.2 Finite Element Analysis of Lifting of Curved Girders

The first finite element parametric study to be conducted on TxDOT Project 0-5574 was by Schuh and identified the effects of changing various parameters during the lifting of curved girders. Schuh conducted eigenvalue buckling analyses to quantify the effects of changing variables such as the radius of curvature (R), flange width to girder depth ratio (b_f/d), span to depth ratio (L/d), and lift point location (a/L). These parameters are illustrated in Figure 2.1.

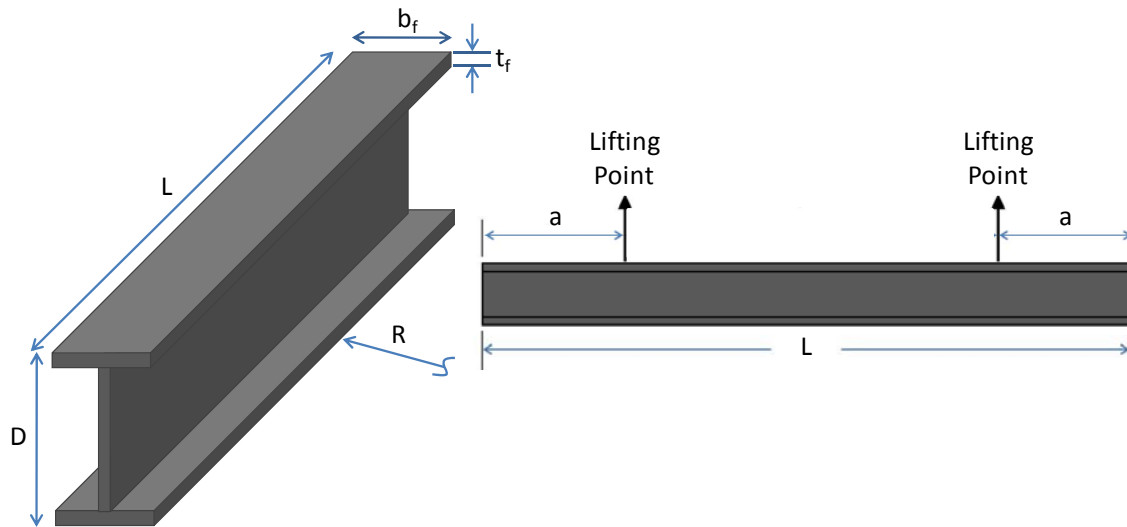


Figure 2.1: Parameter Definitions for Girder Lifting Studies

The results from the parametric studies showed that the radius of curvature had little effect on the eigenvalue of the system. For a given a/L , R , and b_f/d , as the span to depth ratio (L/d), increases, the eigenvalue buckling capacity decreases rapidly. The variable that had the largest effect on the eigenvalue was the lift point location, a/L .

When a girder is lifted at extreme locations ($a/L = 0.1$ or $a/L = 0.4$), the eigenvalue is the lowest and eigenvalues are highest at $a/L = 0.25$ (Schuh).

Using eigenvalue buckling analyses, Schuh (2008) developed recommendations for computing the buckling capacity of prismatic curved I-girders during lifting using conventional formulas for lateral torsional buckling. Farris (2008) extended the work by Schuh, and used eigenvalue buckling analyses to study the stability of non-prismatic curved I-girders during lifting.

2.3.3 Nationwide Survey of Erectors

Farris also conducted a nationwide survey of steel bridge erection contractors, inspectors and engineers. The primary purpose of the survey was to determine common methodologies used in the lifting of curved, steel I-girders such as typical spreader beam length, lift point locations, use of shore towers, and the length of girders lifted. The industry survey was conducted to provide the researchers with a better understanding of typical industry practices. The range of parameters used in practice, were used to assist in planning the parameters that were studied on the research project so that solutions could be developed for commonly encountered problems. Complete details of the survey and survey responses are documented by Farris (2008).

2.3.4 Development of Analysis Tools

As a part of TxDOT Project 0-5574, two PC-based tools were developed to assist with analysis of curved steel I-girder bridges during critical stages of the construction process. One of these tools, called "UT Bridge," is a three dimensional finite element program that contains a graphical user interface (GUI) that allows bridge engineers to input a curved, I-girder bridge and quickly evaluate the stability of the system during girder erection and concrete deck placement based upon information commonly found in bridge plans. In addition to UT Bridge that evaluates girder stability during partially constructed configurations, the tool "UT Lift" was also developed for analysis of curved steel I-girders during lifting. UT Lift is a macro-enabled Microsoft Excel based spreadsheet that allows the user to input the properties of a girder being lifted and quickly

evaluate both strength and serviceability limit states. Both UT Bridge and UT Lift are described in Stith (2010).

2.4 SUMMARY

This chapter provided a brief review of recently completed research pertinent to curved I-girders completed at other universities as well as previous work completed on TxDOT Project 0-5574. The material presented in the chapter supplements the background information provided by Stith (2010) Schuh (2008), and Farris (2008).

The research reported in this thesis extends previous work conducted on TxDOT Project 0-5574 in two areas. As described above, Schuh (2008) and Farris (2008) examined the stability of curved I-girders during lifting through the use of eigenvalue buckling analyses. To extend this work, additional parametric studies of girder lifting were conducted using nonlinear geometrical analyses for comparison with predictions on curved girder behavior provided by the eigenvalue buckling analyses. The purpose of the nonlinear analysis, which is described in Chapter 3, was to evaluate the ability of eigenvalue buckling analysis to predict instability of curved I-girders and to also evaluate proposed limits on girder rotation during lifting. The second area addressed by this thesis, described in Chapter 4, was the analysis of partially constructed bridges with a focus on the role of temporary shore towers and holding cranes.

CHAPTER 3

Non-Linear Analysis of Lifting of Curved Steel I-Girders

3.1 INTRODUCTION

Lifting of curved steel I-girders is an issue of significant concern in the construction of steel bridges. Improper lifting practices can lead to safety concerns and serviceability problems that can adversely impact construction operations. Despite the importance of lifting operations, there is little work available from past research that can provide engineers and erectors with guidance on criteria for lifting. In as such, there is a lack of analysis tools and design criteria for lifting. Rather, bridge erectors have largely relied on experience and rules of thumb to guide lifting operations (Beckmann and Mertz 2005). To address the lack of analysis tools and guidance on lifting of curved steel I-girders, research on this topic was conducted as part of Texas Department of Transportation (TxDOT) Research Project 0-5574, “Curved Plate Girder Design for Safe and Economical Construction.” As part of TxDOT Project 0-5574, considerable research has already been completed on lifting of curved steel I-girders, and is reported in Schuh (2008) and Farris (2008). The work described in this chapter is a continuation of this research for TxDOT Project 0-5574, and builds on the work of Schuh and Farris.

Two critical issues of concern in lifting of curved steel I-girders are safety and serviceability. From a safety perspective, lateral torsional buckling of the girder is the primary limit state of concern. Buckling of a girder during lifting can result in injuries or fatalities. Thus, assuring the stability of a curved steel I-girder is critical in planning a lifting operation. However, even if stability and safety are assured, serviceability problems can occur due to excessive deformations of a girder during lifting. For example, excessive rotation or deflection of a lifted girder can make connecting the girder to other portions of the bridge that have already been erected very difficult. Such serviceability problems, while not affecting safety, can cause costly delays in construction. Serviceability is of particular concern with curved girders, as the curved geometry can

lead to large rotations of a lifted girder due to rigid body movements of the girder combined with cross sectional torsional rotations.

3.2 MODELING APPROACHES

There are several possible approaches for conducting a structural analysis of curved steel I-girders during lifting for the purposes of assessing safety and serviceability. One approach is to conduct a first order structural analysis to compute the moment diagram for the lifted girder as well as deflections and rotations. To check stability of the girder, the moment in the girder can be compared to a critical buckling moment. The critical buckling moment can be computed using formulas provided in AASHTO or other codes, which are generally based on classical formulas for elastic lateral torsional buckling of a straight beam. Buckling solutions are discussed in greater detail later in this thesis. However, this approach leads to difficulties in that formulas for the buckling moment for a beam since the engineer must identify the unbraced length of the beam, which is unclear since there is no clear bracing present. Assessing the buckling strength also may necessitate using a C_b factor to account for moment gradient. Again, since the C_b factor is generally dependent on the unbraced length, there is significant uncertainty on the proper C_b factor during lifting. The applicability of conventional beam buckling formulas to curved girders is not well understood. Finally, many bridge girders are nonprismatic, and the correct treatment of nonprismatic girders in formulas for critical buckling moment is also unclear.

The deflections and rotations computed from a first order analysis can be used to assess serviceability criteria. However, it is unclear if a first order analysis provides an accurate prediction of the actual deflections and rotations of a curved girder during lifting. That is, it is unclear if second-order geometric effects may significantly affect girder deformations during lifting.

As an alternative to using buckling formulas, a first order structural analysis can be combined with an eigenvalue analysis to estimate the buckling moment. An eigenvalue analysis does not require the engineer to define the unbraced length or to compute a C_b factor. However, it is unclear if an eigenvalue analysis can accurately

predict instability of a curved girder since the girder tends to laterally deflect and twist from the applied load.

The most accurate approach for predicting the behavior of a curved steel I-girder during lifting is to conduct an analysis that explicitly models nonlinear geometry. A nonlinear analysis evaluates equilibrium in the deformed configuration of the girder, and provides the most realistic prediction of deflections and rotations, and of internal forces and stresses. A geometric nonlinear analysis is also sometimes referred to as a second-order analysis, in that it includes second-order geometric effects.

An additional consideration in the analysis of curved steel I-girders is the representation of the girder in the analysis model. At the simplest level, beam elements can be used to model the girder. At a more advanced level, continuum finite elements, such as shell elements can be used to model the girder. Shell finite element models increase the complexity of modeling, but can provide more accurate results. Further, shell finite element models can predict local buckling of the flanges and web as well as local effects at lift points and at changes in the cross-section for nonprismatic girders. Such local effects generally cannot be captured using beam elements. Note that either beam elements or shell finite elements can be used to conduct a first order analysis, an eigenvalue analysis, or a nonlinear geometry analysis.

A final issue in girder modeling is consideration of material inelasticity. Significant yielding in the girder will affect the distribution of the internal forces and stresses, deflections, rotations, and stability of the girder. In general, a key design criterion for girder lifting is to prevent yielding of the girder during the lifting operation to prevent permanent deformations. Consequently, an elastic analysis is generally satisfactory for girder lifting. It is, of course, important to check the internal forces and stresses predicted by the analysis to ensure that the girder does, in fact, remain elastic. All of the analyses described in this chapter utilized elastic materials.

3.3 RESEARCH OBJECTIVES

The previous studies by Schuh (2008) and Farris (2008) used eigenvalue analysis to develop recommendations for evaluating girder stability using simplified buckling formulas. However, the validity of eigenvalue analyses for curved girders is unclear. Consequently, the primary objective of the research described in this chapter is to assess the validity of eigenvalue analyses for predicting instability of curved girders during lifting and to extend the work previously conducted by Schuh and Farris. To accomplish this objective, a geometric nonlinear analysis of curved girders during lifting using a three-dimensional finite element model was conducted and compared to the results of first-order and eigenvalue analysis. In addition to assessing the usefulness of eigenvalue analyses, this research also examined additional issues involved in lifting of curved steel girders.

Prior to describing the nonlinear analysis of curved steel I-girders during lifting, the results of previous research on girder lifting conducted as part of TxDOT Project 0-5574 will be reviewed.

3.4 PREVIOUS WORK ON LIFTING OF CURVED GIRDERS FOR PROJECT 0-5574

As part of TxDOT Project 0-5574, an extensive series of analyses were conducted on lifting of curved steel I-girders (Schuh (2008), Farris (2008), Stith et al. (2009), and Stith (2010)). In this previous work, the stability of curved steel I-girders during lifting was evaluated by the use of eigenvalue analyses on a three-dimensional finite element model of the girder using the ANSYS finite element computer program. Shell elements were used to represent the flanges and web of the girder. The model used for this analysis, as well as validation of the model by field testing of lifted curved girders is described by Schuh (2008) and Stith (2010). The results of the eigenvalue analyses were then used by Schuh and Farris to develop recommendations for the calculation of buckling moments.

Analysis by Schuh (2008) showed that radius of curvature had little effect on the eigenvalue for a curved girder during lifting. This is illustrated in Figure 3.1 **Error! Reference source not found.** below, which shows the eigenvalues for a 90 ft long girder

computed from the ANSYS model. Loading on the girder consisted of the girder self weight. The girder had a top flange width (b_f) of 18 in and a web depth (d) of 72 in (b_f/d ratio = 1/4). Four different radiuses of curvature were modeled ($R = 250$ ft, 500 ft, 1000 ft, and 8000 ft). The 8000 ft radius of curvature was included to approximate a straight girder. For each radius of curvature, the eigenvalue was obtained for seven different lift point locations (a/L) where a represents the distance from the end of the girder to the lift point location and L is the total length of the girder being lifted. The eigenvalue, λ , shown in Figure 3.1 represents a multiplier on the self-weight of the girder needed to cause buckling.

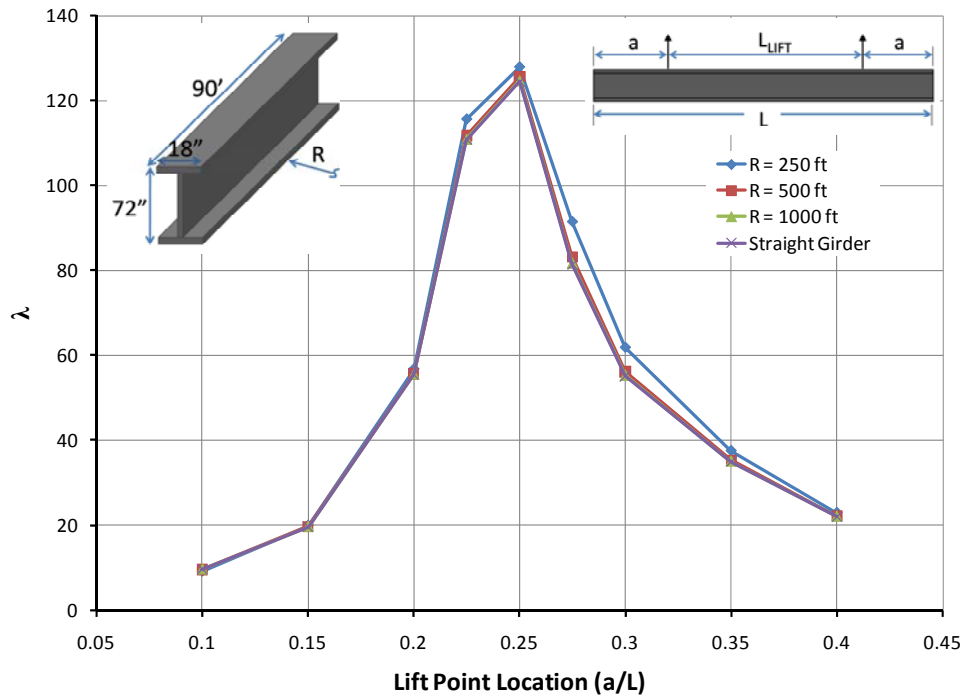


Figure 3.1: Effect of Radius of Curvature on Eigenvalue, λ for Different Lift Locations (Schuh, 2008)

From the results in Figure 3.1, it can be seen that regardless of the lift point location, the eigenvalues are nearly the same for the four different radiuses of curvature. The eigenvalue was therefore assumed to not be a function of the radius of curvature in the parametric studies subsequently conducted by Schuh (2008) and Farris (2008). The

graphs show that the resulting eigenvalues are very sensitive to the lifting location and ranged from approximately 10 to 125 for the various a/L ratios.

3.4.1 Rigid Body Girder Rotations

Because of the geometry of horizontally curved I-girders, a potential for significant rotations during lifting is present. Large rotations can contribute to instability of the girder during lifting and can also cause problems during fit up when attempting to connect two girders in the air or when attempting to connect cross frames. There are two sources of rotation when lifting a curved girder. One source is a rigid body rotation that occurs when the center of gravity of the curved girder is not located on the line of support defined by the lift points. The second source of rotation is deformation due to girder flexibility and includes both torsional deformations and weak axis bending of the girder.

The rigid body rotation depends on the girder geometry and lift locations, and does not depend on the stiffness of the girder. Straight girders do not develop rigid body rotations because their center of gravity lies between the line of support created by the lifting locations for any two points on a straight girder. However, for curved girders, rigid body rotation will occur if the girder's center of gravity is eccentric to the line of support between the lifting locations, as illustrated in Figure 3.2.

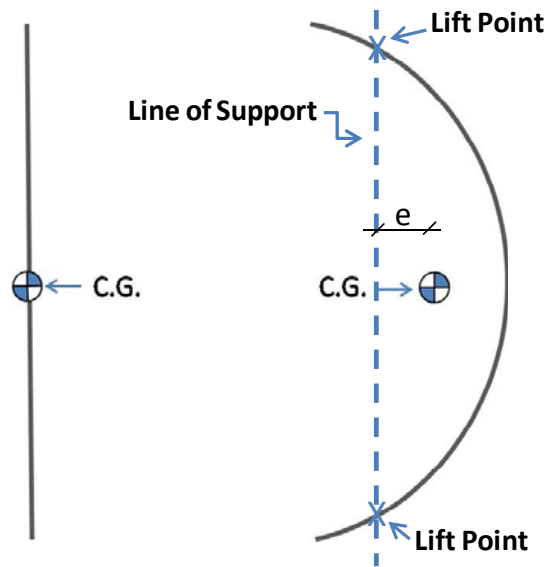


Figure 3.2: Location of Center of Gravity and Line of Support for Straight and Curved Girders

The eccentricity of the line of support and the center of gravity creates an additional torque that causes the girder to rotate until the line of support is coincident with the center of gravity. For more information on calculating this rigid body rotation, see the work done by Schuh (2008).

3.4.2 Buckling Expressions for Girder Stability

As discussed earlier, one approach for checking the stability of a girder during lifting is to use a buckling formula. With this approach, the bending moment in the lifted girder is computed using a first order analysis. This can normally be done by hand calculations or simple computer programs. The maximum moment in the girder is then compared to a critical moment that will cause lateral torsional buckling, computed using a buckling formula. Most buckling formulas are derived for uniform moment loading and the effects of moment gradient are accounted for with moment modification (C_b) factors, which are discussed below. The buckling solutions that are available in design codes and in the literature to predict elastic lateral torsional buckling of a girder often vary in the form of presentation. A classical formula for elastic buckling of doubly-symmetric

girders is the formula presented in Timoshenko and Gere (1961), which is shown as Eq. 3.1 below. This formula, referred to herein as the “Timoshenko Equation,” is the basis for most doubly-symmetric beam buckling formulas found in design codes, including AASHTO. This formula assumes the girder is straight, prismatic and is subject to a uniform moment along its length. At the girder ends, this formula assumes warping is permitted but that twist is fully restrained. Although Timoshenko originally stated that lateral movement was restrained at the ends, the assumption is not actually required to obtain the resulting expression. As a result, effective bracing need only control twist of the cross section; however bracing can also be provided to prevent lateral movement of the compression flange. The value of M_o computed from Eq. 3.1 is the critical moment that will cause elastic buckling of the girder for these conditions.

When the moment diagram along the unbraced length of the girder is not uniform, as is the case with a girder during lifting, a moment gradient factor, C_b , is typically applied to the uniform buckling moment from Eq. 3.1. Thus, the final formula for predicting elastic lateral torsional buckling of a girder is given by Eq. 3.2. To check girder stability, the buckling moment, M_{cr} computed by Eq. 3.2 is compared to the maximum moment computed in the girder, with application of an appropriate factor of safety.

As noted above, Eq. 3.2 is the basis for beam buckling formulas found in many design standards for steel structures, including AASHTO (2008) and AISC (2005). However, the use of Eq. 3.2 for checking stability of girders during lifting raises a number of questions and concerns, as follows:

- What unbraced length, L_b should be used in Eq. 3.2?

The unbraced length, L_b is defined as: “Length between points that are either braced against lateral displacement of the compression flange or braced against twist of the cross-section.” (AISC, 2005). For a girder during lifting, there are no points along the girder that are braced against lateral displacement or braced against twist of the cross-section. The primary source of stability in girders during lifting comes from the fact that the point of application of the

self weight lies below the vertical lifting locations. Consequently, it is very unclear how L_b should be determined for a girder during lifting.

- How should C_b be determined?

Various expressions for computing C_b are available in design codes and in the literature. All of these expressions require information on the shape of the moment diagram over the unbraced length. Since the unbraced length is not clearly defined for a girder during lifting, the calculation of C_b is also not clear. Further, in addition to C_b accounting for moment gradient over the unbraced length, this factor also accounts for load height effects. Most C_b factors are applicable for mid-height loading. When the loads are applied above or below mid-height, load height effects increase or decrease the buckling capacity. For gravity loading, loads applied above mid-height results in a reduction of the capacity relative to mid-height loading, while loads applied below mid-height result in an increase in the buckling capacity. In the case of a girder during lifting, where the girder is generally hanging from lifting hooks, conventional formulas for C_b do not properly account for this support conditions.

- Is Eq. 3.2 applicable to curved girders?

The Timoshenko Equation was derived for a straight girder. Its applicability to a curved girder is unclear.

- How can Eq. 3.2 be applied to a nonprismatic girder?

The Timoshenko Equation was derived for a prismatic girder. However, many bridge girders are nonprismatic. The correct application of Eq. 3.2 to nonprismatic girders is unclear.

$$M_o = \frac{\pi}{L_b} \sqrt{EI_y GJ + E^2 I_y C_w \left(\frac{\pi^2}{L_b^2} \right)} \quad \text{Eq. 3.1}$$

L_b = Unbraced Length of Girder (in)

E = Modulus of Elasticity (ksi)

I_y = Weak Axis Moment of Inertia (in⁴)

G = Shear Modulus (ksi)

J = Torsional Constant (in⁴)

C_w = Warping Constant (in⁶)

$$M_{cr} = C_b * \frac{\pi}{L_b} \sqrt{EI_y GJ + E^2 I_y C_w \left(\frac{\pi^2}{L_b^2} \right)} \quad \text{Eq. 3.2}$$

M_{cr} = Critical Buckling Moment

C_b = Moment Gradient Factor

Schuh and Farris developed recommendations on how Eq. 3.2 can be used to compute the buckling moment for a girder during lifting. The basic approach used in this work was to consider a wide range of parameters for lifted girders, including variations in length, cross-section properties, location of lift points, etc. For each case considered, an eigenvalue buckling analysis was conducted on a three-dimensional finite element model of the lifted girder using ANSYS. Moment gradient factors can be found analytically by conducting two analyses: one with moment gradient and one with uniform moment. The moment gradient factor is then found using the following expression in Eq. 3.3.

$$C_b = \frac{M_{cr}}{M_o} \quad \text{Eq. 3.3}$$

Where M_{cr} is the maximum moment at buckling within a specific unbraced length, L_b from the analysis with moment gradient; and M_o is the buckling moment from the corresponding analysis with uniform moment loading. Instead of conducting a second analysis with uniform moment loading, Eq. 3.1 can also be used for M_o . An important factor in defining C_b from the analysis is the selection of the unbraced length

that is used to define M_o and M_{cr} . The definition of L_b , is a major factor that differed in the work from Schuh and Farris.

Schuh (2008) considered prismatic girders while Farris (2008) considered nonprismatic girders. Schuh defined the unbraced length L_b to be taken as the larger of L_{Lift} and a , where L_{Lift} is the distance between lift point, and a is the overhang distance from the lift point to the end of the girder (Figure 3.3). In computing the C_b factor for nonprismatic girders (Figure 3.5, Figure 3.6), Farris (2008) defined the unbraced length L_b as the total length L of the girder. Further, Farris developed recommendations for an approach for using Eq. 3.2 for checking nonprismatic girders. Figure 3.3 through Figure 3.6 illustrate some of the results from these studies. For these figures, the moment gradient factor is represented by the symbol C_L for prismatic girders and C_b for nonprismatic girders. While there is not a significant difference in the desired effect of using C_L or C_b , the primary difference is the unbraced length that was used to define the values. Therefore, the magnitude of the range of C_L and C_b vary in the graphs. The C_b factors from the work of Farris are generally larger than the C_L values from Schuh, however Farris would use the full length of the segment in Eq. 3.1 while Schuh would use the larger of a or L_{Lift} .

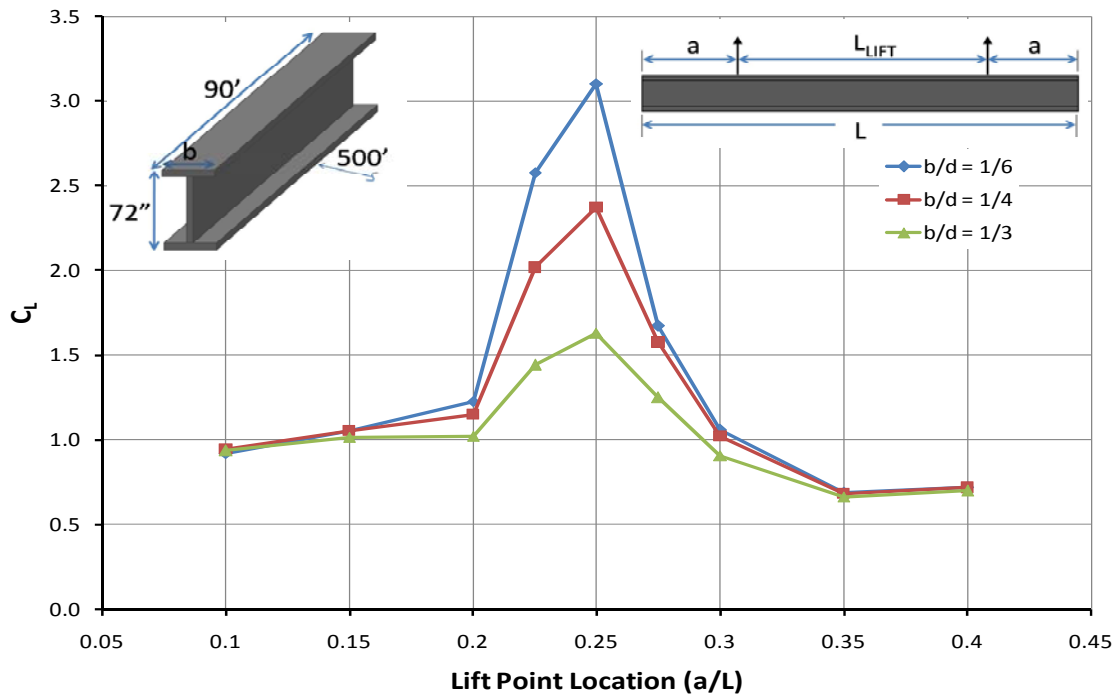


Figure 3.3: C_L vs. a/L for a Flange Width to Depth Ratio [Prismatic] (Schuh)

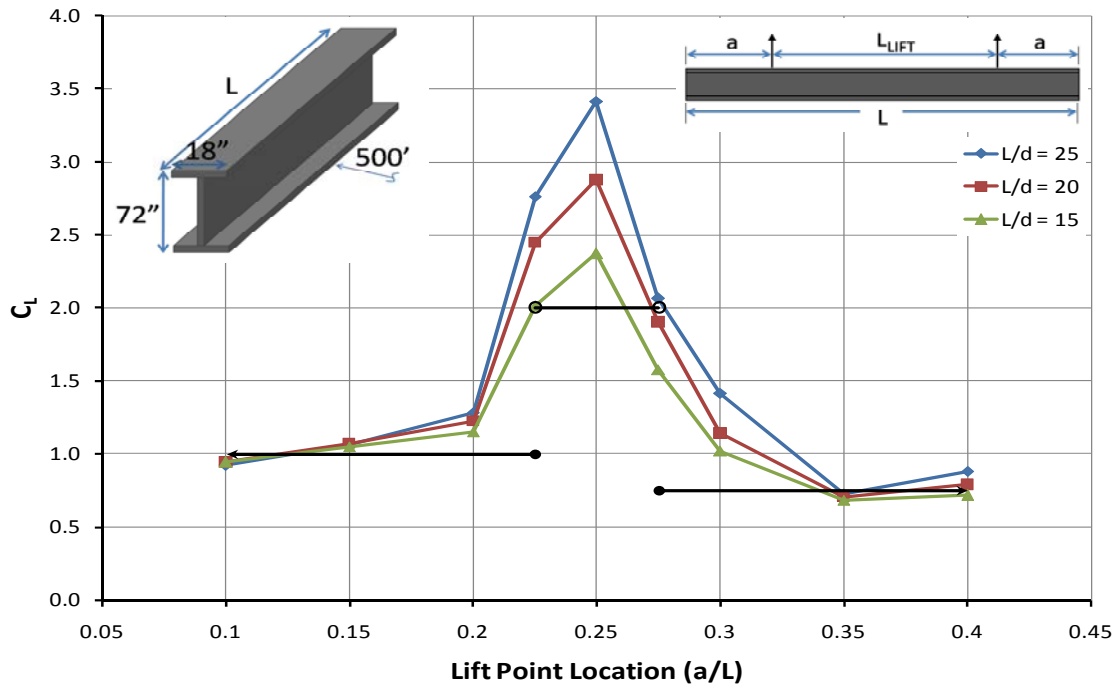


Figure 3.4: C_L vs. a/L for a Span to Depth Ratio [Prismatic] (Schuh)

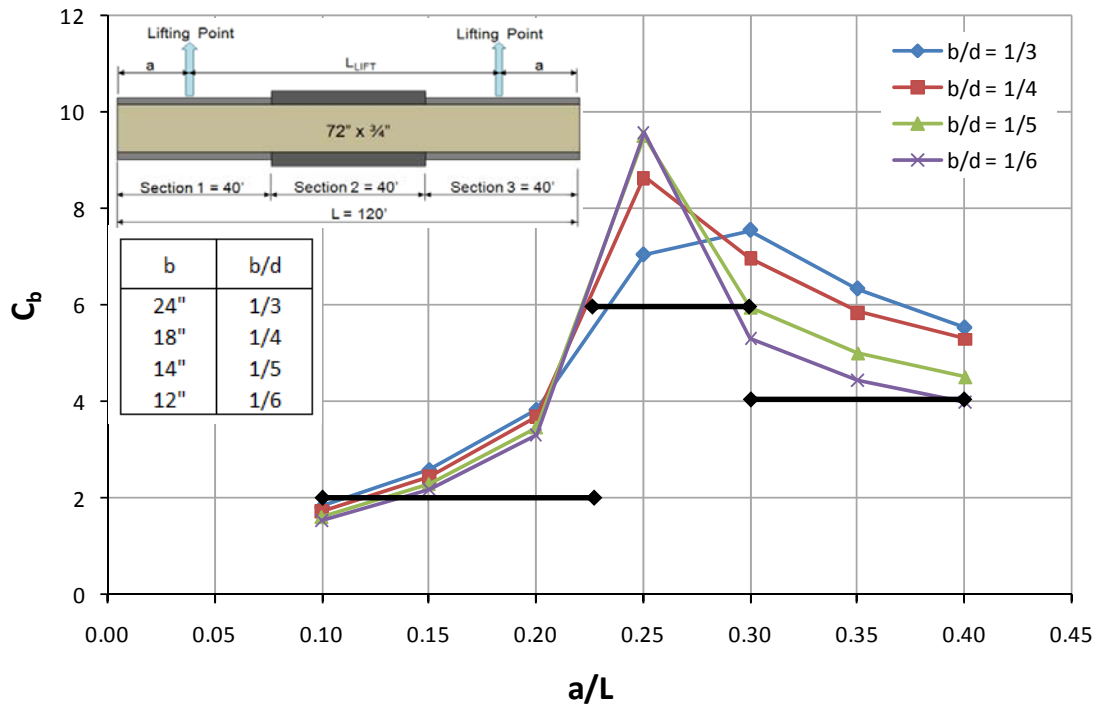


Figure 3.5: C_b vs. a/L for a Flange Width to Depth Ratio [Non-Prismatic] (Farris)

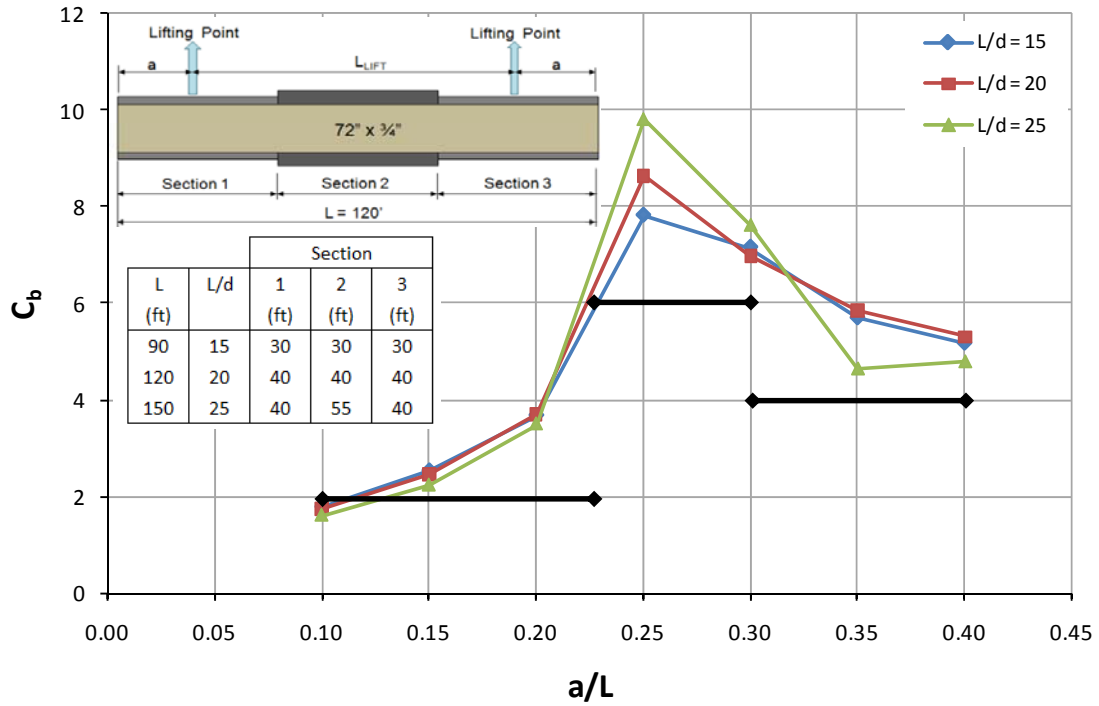


Figure 3.6: C_b vs. a/L for Span to Depth Ratio [Non-Prismatic](Farris)

For additional information on the development of the moment gradient factor, C_L , for prismatic girders, see Schuh (2008). For additional information on the development of the moment gradient factor, C_b , for non-prismatic girders, see Farris (2008). One of the consistent conclusions from these studies, as illustrated in Figure 3.3 to Figure 3.6, is that the best place to lift a girder from a stability stand point is at the quarter points where $a/L = 0.25$. This location will typically give the highest C_L or C_b factor resulting in the highest critical moment. Lifting at these locations, however, may not always be possible based on spreader beam availability, or based on the need to minimize rigid body rotations. Lifting at the quarter points may not align the girder's center of gravity with the line of support (Figure 3.2), which may in turn require moving the lift points away from the quarter points.

The C_L and C_b factors developed by Schuh and Farris can be used with Eq. 3.2 to check stability of curved girders during lifting. As noted above, however, it is important to use a definition for the unbraced length L_b that is consistent with the calibration process. It is also important to use these calibrated factors only within the range of parameters for which the calibrations were conducted.

3.4.2.1 Concerns with using Eigenvalue Solutions to Evaluate Curved Girder Stability

The recommendations by Schuh and Farris for calculating buckling moments for lifted girders are based on calibrations to eigenvalue buckling analyses. Implicit in this process were two assumptions. The first was that the eigenvalue buckling capacity was largely independent of radius of curvature. The second assumption was that eigenvalue analysis provides a reasonable prediction for instability of a curved girder.

There is reason to question these assumptions. With regard to the first assumption, additional analyses by Stith et al. (2009) showed some dependence of the eigenvalue on radius of curvature. A result of this analysis is shown in Figure 3.7. Note that while this analysis shows some dependence of the eigenvalue on the radius of curvature, the effect was still rather small. For the analysis shown in Figure 3.7, the difference in eigenvalue between a straight girder and a highly curved girder is less than 5-percent.

The second assumption is one of potentially greater concern. That is, it is unclear if instability of a curved girder is accurately predicted by an eigenvalue analysis. Work by Earls (2007) suggests that eigenvalue buckling analysis from finite element programs may provide misleading results for cases other than simple bifurcation buckling. In the case of horizontally curved girders, the initial curved geometry can be viewed as a large initial geometric imperfection. This suggests that instability of curved girders may not be well characterized as a bifurcation buckling problem, and consequently, may not be accurately predicted by an eigenvalue buckling analysis.

To address concerns on the applicability of eigenvalue buckling analysis for predicting instability of curved girder during lifting, a series of geometric nonlinear analyses were conducted. These analyses can provide a more accurate prediction of the behavior of curved girders during lifting. As described earlier, the objective of these nonlinear analyses is to evaluate the applicability of eigenvalue buckling analysis, extend the previous work by Schuh and Farris, and provide additional insights into the behavior of curved steel I-girders during lifting.

Results from the graphs above show that the best place to lift a girder from a stability stand point is at the quarter points where $a/L = 0.25$. This location will typically give the highest C_b factor resulting in the highest critical moment. As discussed previously, these results assume that the radius of curvature does not affect the solution to the problem. A more refined analysis was conducted and demonstrated that the radius of curvature actually did affect the eigenvalue buckling capacity of the system. The results are presented in Figure 3.7.

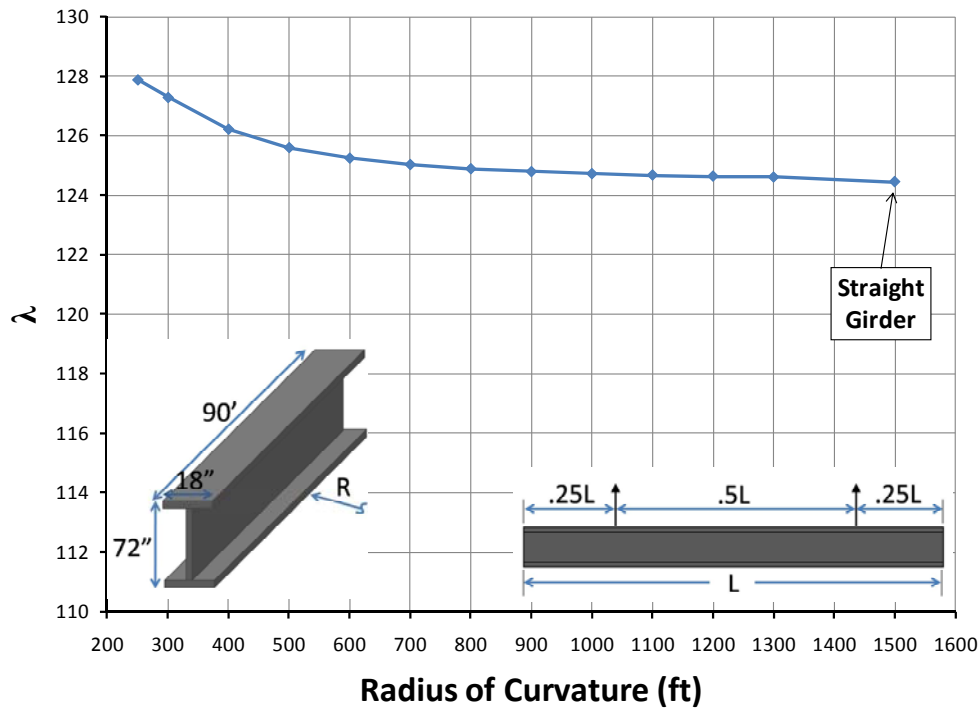


Figure 3.7: Effect of Radius of Curvature on Eigenvalue, λ (Stith, Schuh and Farris, Guidance for Erection and Construction of Curved I-girder Bridges, FHWA/TX-09/0-5574)

3.5 STUDY DESCRIPTION

3.5.1 Finite Element Modeling Technique

The nonlinear analysis of curved steel I-girders during lifting was conducted using the same basic ANSYS finite element model used by Schuh (2008) and Farris (2008) for the eigenvalue buckling analysis. As described earlier, this model used shell elements to represent the flanges and web of the girder. The details of this model, including the representation of the lifting equipment attached to the girder, and validation of the model from field tests is described by Schuh (2008). Using this validated FEA model, both linear-elastic and geometric non-linear elastic analysis were conducted to study curved girders during lifting.

Linear elastic materials were used in all analyses conducted. Within the context of an elastic analysis, a linear geometric analysis formulates equations of equilibrium using the initial undeformed geometry of the structure and loading. Such an analysis is accurate if deformations remain sufficiently small so as not to significantly alter the equations of equilibrium, and therefore not to significantly affect the predicted stresses and deformations.

In the case of a geometric nonlinear analysis, equations of equilibrium are formed in the deformed configuration of the structure. This provides a more accurate representation of actual behavior, since an actual structure must always be in equilibrium in any deformed state. For structures that undergo significant displacements, a nonlinear analysis will provide a more accurate prediction of stresses and deformations. For a geometric nonlinear FE analysis, various solution strategies are possible, but these generally involve applying load in increments and then iterating to find a solution within a specified tolerance.

3.5.2 Parameter Descriptions

Using the geometric nonlinear analysis capability of ANSYS, a parametric study was conducted on curved steel I-girders during lifting. These parametric studies were conducted on doubly symmetric, prismatic girders. The parameters that were investigated were the slenderness ratio (b_f/D) where b_f is the flange width and D is the web depth, the lifting location (a/L) where a is the distance from the lift point to the end of the girder and L is the girder length, the radius of curvature (R), and the girder cross sectional properties. The girder cross sectional properties that were varied include the web depth, D , the flange width, b_f , and the flange thickness, t_f . The parameters are illustrated defined in Figure 3.8.

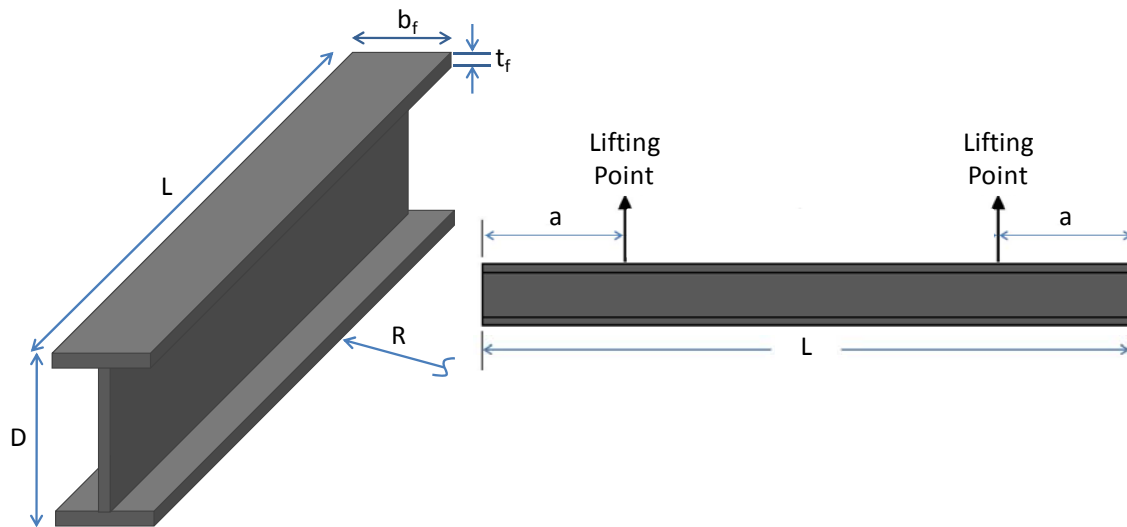


Figure 3.8: Definition of Parameters

3.5.3 Parameter Ranges

3.5.3.1 Flange Width to Depth Ratio (b_f/D)

The flange width to depth ratio (b_f/D) that the Texas Department of Transportation (TxDOT) recommends in their TxDOT Preferred Practices for Steel Bridge Design, Fabrication, and Erection is 1/3 (Texas Steel Quality Council, 2007). AASHTO on the other hand allows a bridge design engineer to use a flange width to depth ratio as little as 1/6 as seen in Equation 6.10.2.2-2 of the AASHTO LRFD Bridge Specification (AASHTO, 2008). In this study, the range of b_f/D ratios that were used was 0.15 to 0.33 (roughly 1/6 to 1/3) to study the behavior of the girders at these two limits. After a number of studies with varying values of b_f/D were conducted, $b_f/D = 1/3$ was used in subsequent studies. When changing the b_f/D ratio, the depth stayed constant and only the flange width varied. Additionally, when the flange widths were varied, the flange thicknesses also changed to maintain the same flange slenderness ($b_f/2t_f$). For example, if the flange width doubled in size from 9 in to 18 in, the flange thicknesses also doubled in size from 0.5 in to 1.0 in. For all parametric studies completed, the top and bottom flange dimensions were identical.

3.5.3.2 Lift Location (a/L)

The lift location ratio (a/L) is used to create a non-dimensional variable able to be compared between all parametric studies regardless of the length of the girder. The variable a is the distance from the end of the girder being lifted to the lift point. The variable L is the total length of the girder being lifted. For this study, all of the lifting locations were symmetric about the center of the girder. At first, the values of the a/L ratio considered ranged from 0.15 to 0.34. After a number of studies were concluded, the range was reduced to 0.20 to 0.25. This was done because a/L values outside of this range were not practical since they resulted either in excessive initial rigid body rotation or in excessive cross sectional twist for most girders studied. This is discussed in greater detail in the results section.

3.5.3.3 Radius of Curvature

The radius of curvature (R) is the distance from the center of curvature to the centerline of the girder cross section. The radius of curvatures that were considered in this study ranged from 500 ft. to 8,000 ft. The 8000 ft. radius of curvature was intended to approximate a straight girder. Most bridges in Texas have a radius of curvature greater than 800 ft.

3.5.3.4 Girder Cross Section

The girder depth (D) refers to the depth of the web of the girder. The girder depths considered in this study were 60 in, 72 in, or 96 in with the majority of the girders having a depth of 60 in. The flange width (b_f) investigated in this study ranged from 9 in to 24 in. The flange thickness ranged from 0.5 in to 1.125 in.

The girder length (L) refers to the total length of the lifted girder lengths, which ranged from 80 ft to 225 ft. A majority of the girders studied had a length of either 80 ft or 125 ft.

3.6 RESULTS OF PARAMETRIC STUDIES

3.6.1 Overview

This section presents key results from the parametric studies on geometric nonlinear analysis of curved steel I-girders during lifting. Rather than presenting the results for each variable individually, results are presented in the context of important issues related to girder analysis and lifting.

3.6.2 Using Eigenvalues to Predict Instability of Curved Girders

One of the key objectives in this parametric study was to investigate how well eigenvalue analysis characterizes potential instability of curved girders during lifting. Some representative results from this evaluation are illustrated in Figure 3.9 and Figure 3.10. In Figure 3.9, three 125 ft long girders with a b_f/D ratio of $1/3$ were analyzed and their top flange and bottom flange out of plane displacements are plotted against multiples of the girders self weight. The depth of the web is 60 in and the width of the flanges is 20 in. The girder is lifted at a/L equal to 0.21. The three girders lifted have a radius of curvature of 500 ft, 1000 ft, and 8000 ft (straight). The out of plane displacements graphed in the remainder of this chapter are the result of the geometric nonlinear analysis. The dotted line represents the top flange out of plane displacement and the solid line represents the bottom flange out of plane displacement. The eigenvalue for the three girders is 25.4 and is also plotted. Although the magnitudes of the loads that are graphed are not generally practical, the purpose of this comparison is to determine if the eigenvalue provides a reasonable estimate of a limit for curved girders. In as such, the load level that is graphed is the eigenvalue for the problem. Recall that the radius of curvature does not have a significant effect on the eigenvalue. Consequently, the eigenvalue of 25.4 was computed for all three values of radius of curvature considered in this analysis. In Figure 3.10, three similar girders to the ones plotted in Figure 3.9 are shown, with the exception that the b_f/D ratio is $1/6$. The depth of the girders is still 60 in but the width of the flanges is now 9 in. Note that the horizontal scales are different for Figure 3.9 and Figure 3.10.

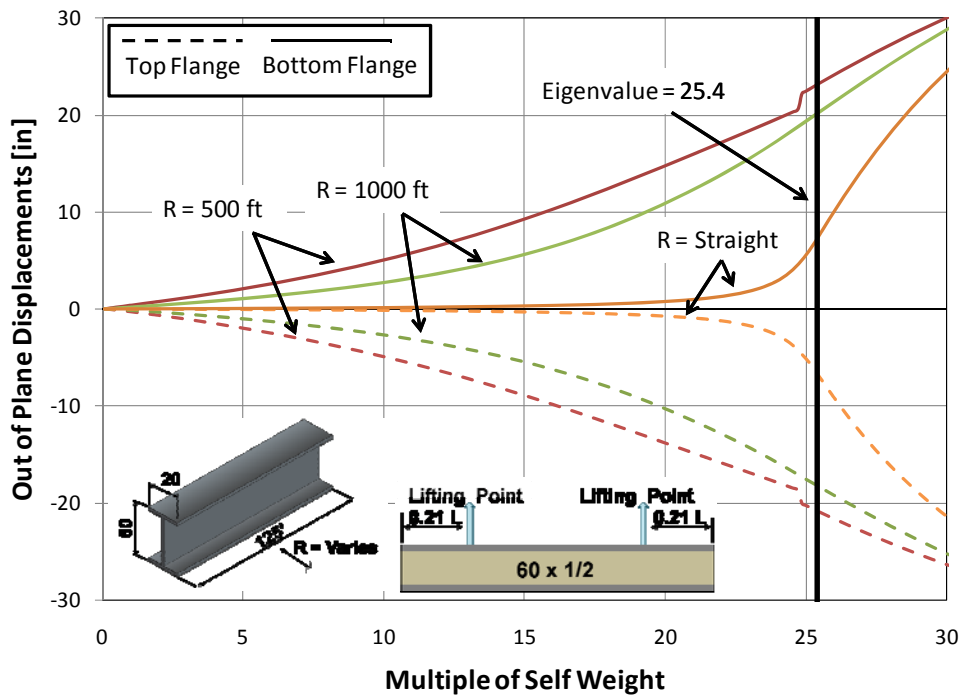


Figure 3.9: Flange Lateral Displacements for $b_f/D = 1/3$

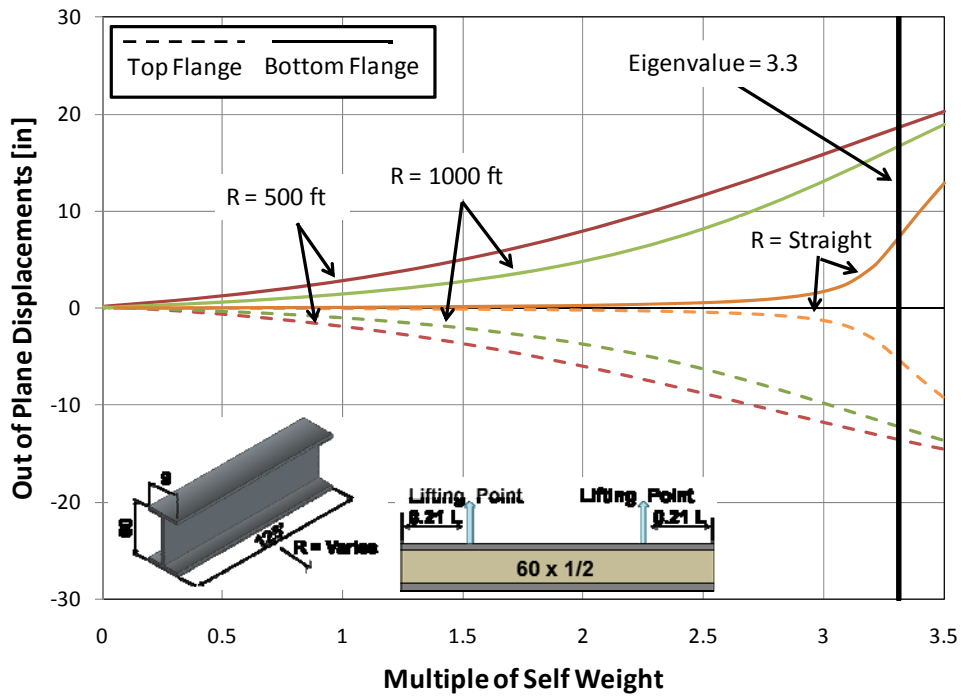


Figure 3.10: Flange Lateral Displacements for $b_f/D = 1/6$

Several observations can be made from Figure 3.9 and Figure 3.10. Looking at the displacements plotted on both figures, the straight girders exhibits a reasonably well defined bifurcation type behavior. That is, the lateral displacements initially remain very small as the load (represented by a multiple of self weight) increases, and then there is a load at which the lateral displacements increase rapidly. Further, the eigenvalue captures this phenomenon reasonably well. That is, the eigenvalue provides a good estimate of the load at which lateral displacements become large. Thus, the eigenvalue is a good predictor of elastic lateral torsional buckling for straight girders.

The lateral displacement plots for the curved girders, on the other hand, show a somewhat different type of behavior. These plots do not show a bifurcation type behavior. Rather, these plots show a continuous growth of lateral displacement from the start of loading, with no well defined bifurcation or critical load. Such a behavior is expected for a system with large initial geometric imperfections. As noted earlier, the curved geometry can be viewed as a large initial geometric imperfection from a stability perspective. When the load corresponding to the eigenvalue is reached for the curved girders, the out of plane displacements are significantly larger than for the straight girder. For example, for the straight girder with $b_f/D = 1/3$ (Figure 3.9), the out of plane displacement at the eigenvalue is about 7 inches. For the curved girder with a radius of 500 feet, the out of plane displacement at the same eigenvalue is about 22 inches. This large out of plane displacement would cause major problems with the girder erection.

Thus, the eigenvalue can provide a general indication of the load to cause lateral torsional buckling of straight girders, but is not practical for most curved steel I-girder during lifting. Therefore, additional checks are likely needed to assure that out of plane displacements are within reasonable serviceability limits and do not result in yielding of the girder.

3.6.3 Additional Failure Criteria for Lifting of Horizontally Curved I-Girders

As described above, the eigenvalue is not a good indicator of the potential for strength or serviceability problems during lifting of curved I-girders. Depending on the degree of curvature, large and potentially problematic out of plane displacements can

occur at loads well below the eigenvalue. Consequently, additional failure criteria need to be considered in the analysis of curved girders during lifting. In this section, two additional failure criteria are considered. These failure criteria are related to yielding of the girder and excessive rotation of the girder ends, and are described below.

From both a strength and serviceability point of view, yielding of the girder during lifting will be considered as a failure criterion. Yielding, in addition to causing permanent deformation of the girder, can also cause a loss of stiffness that may result in instability. Thus, using geometric nonlinear analyses, the stresses in the girder is examined to determine when yielding is expected. For the current analysis, failure is taken as the load at which peak girder stresses reach $F_y/2$, where F_y is taken as 50 ksi. The stress limit is taken as one-half of the yield stress to account for the presence of residual stresses in the girder. The stress limit of $F_y/2$ is somewhat arbitrary, but is considered reasonable for this analysis.

In addition to limiting stress in the girder, an additional limit is needed to avoid deformation related serviceability problems. However, it is more difficult to quantify a serviceability limit state for the lifting of curved girders. Setting this limit requires answering questions such as: how much deformation can be allowed at the end of a girder and still be able to complete the air splice. To help answer these questions, a nationwide survey was sent out to contractors and engineers to collect data on serviceability and other lifting issues (Farris, 2008). From the results of the survey, a serviceability criterion was established that rotations at the girder ends in excess of 1.5 degrees can result in fit-up problems. While this limit is subject to considerable judgment, this limit will be used in the analysis described below and a reasonable basis for minimizing serviceability problems.

To evaluate limit states related to yielding and girder end rotation, out of plane displacements are calculated with the only load on the girder being the self weight. Although wind may be present in the field, typically erectors and Departments of Transportations have strict guidelines on wind conditions that preclude girder erection. If it is too windy, then the lift will be postponed to a later time. Therefore, wind is not

considered in the following analysis. Because the eigenvalue is a multiple of the applied loads and the applied loads are only the self weight, the out of plane displacements will be plotted against multiples of self weight. In the following figures, both the top flange and bottom flange out of plane displacements are plotted at the middle of the girder, and at the end of the girder. Also shown on the plots is the self weight multiplier at which the different limit states are reached. The limit states shown are the end rotation = 1.5 degrees, peak stress = $F_y/2$ and the eigenvalue buckling load. The length of the girders lifted for all studies is 125 ft. The girders are all lifted symmetrically at $a/L = 0.25$ with a web depth of 60 in and a web thicknesses of 0.5 in. For Figure 3.12 and Figure 3.13 the $b_f/D = 1/3$ with a flange width of 20 in. and a flange thickness of 1.0 in. For Figure 3.14 and Figure 3.15 the b_f/D ratio = $1/6$ with a flange width of 9 in. and a flange thicknesses 0.5 in. For both b_f/D ratios, the results from a straight girder ($R = 8000$ ft) and a radius of curvature equal to 500 ft are presented.

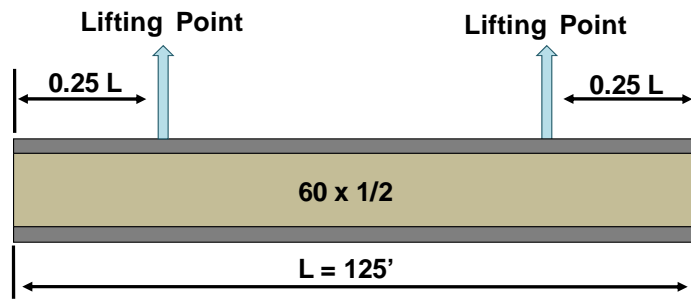


Figure 3.11: Lifting Configuration for Figure 3.12 through Figure 3.15

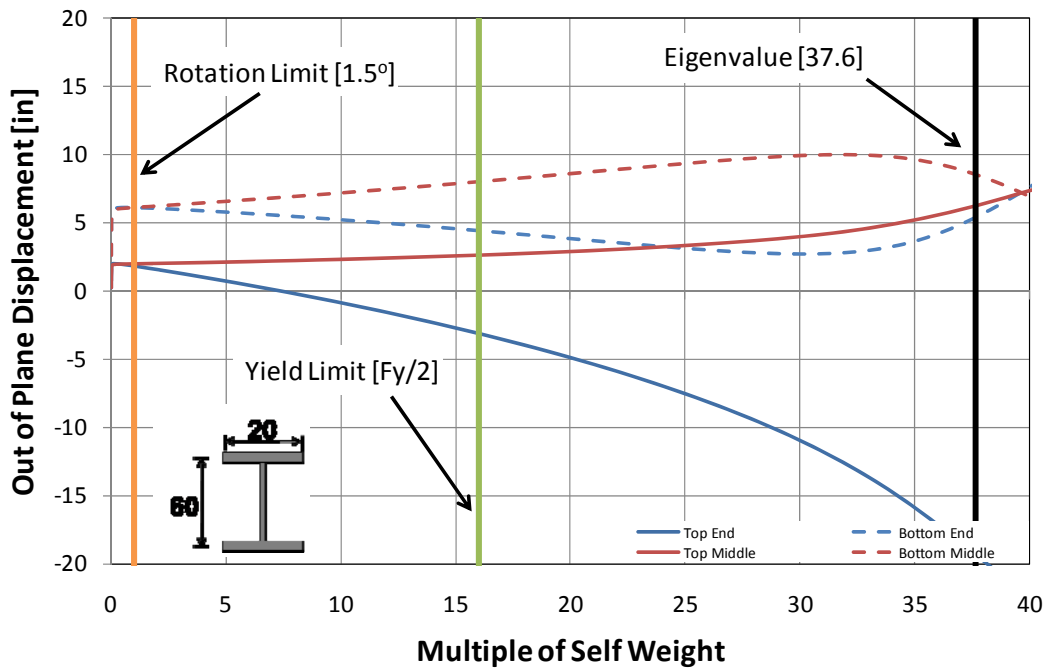


Figure 3.12: Flange Lateral Displacements [$a/L = 0.25$; $b_f/D = 1/3$; $R = 500'$]

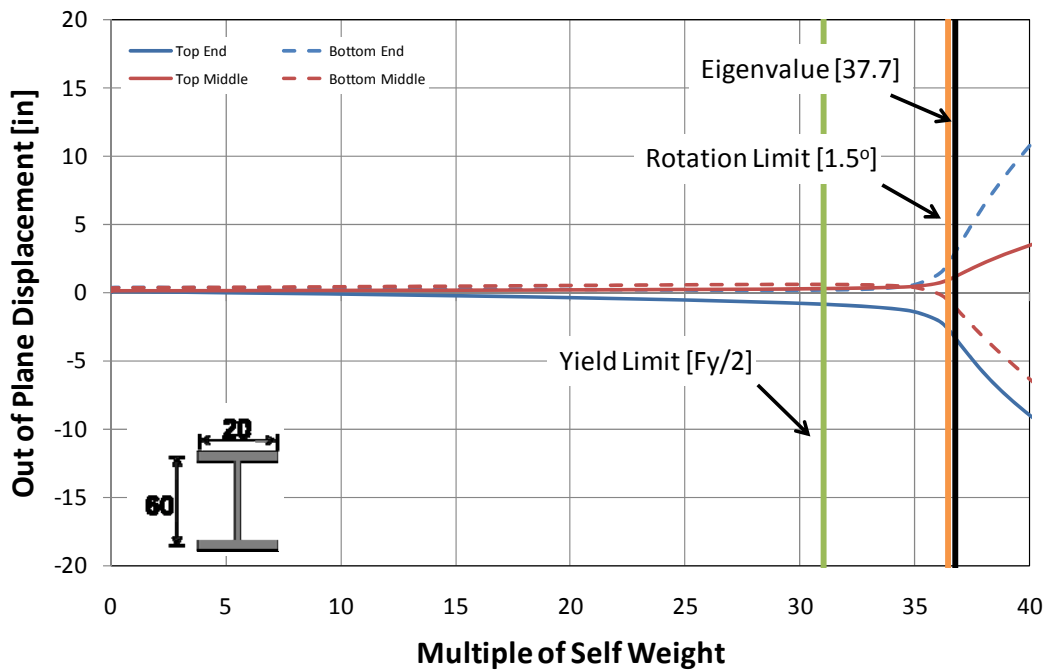


Figure 3.13: Flange Lateral Displacements [$a/L = 0.25$; $b_f/D = 1/3$; $R = 8000'$ (Straight)]

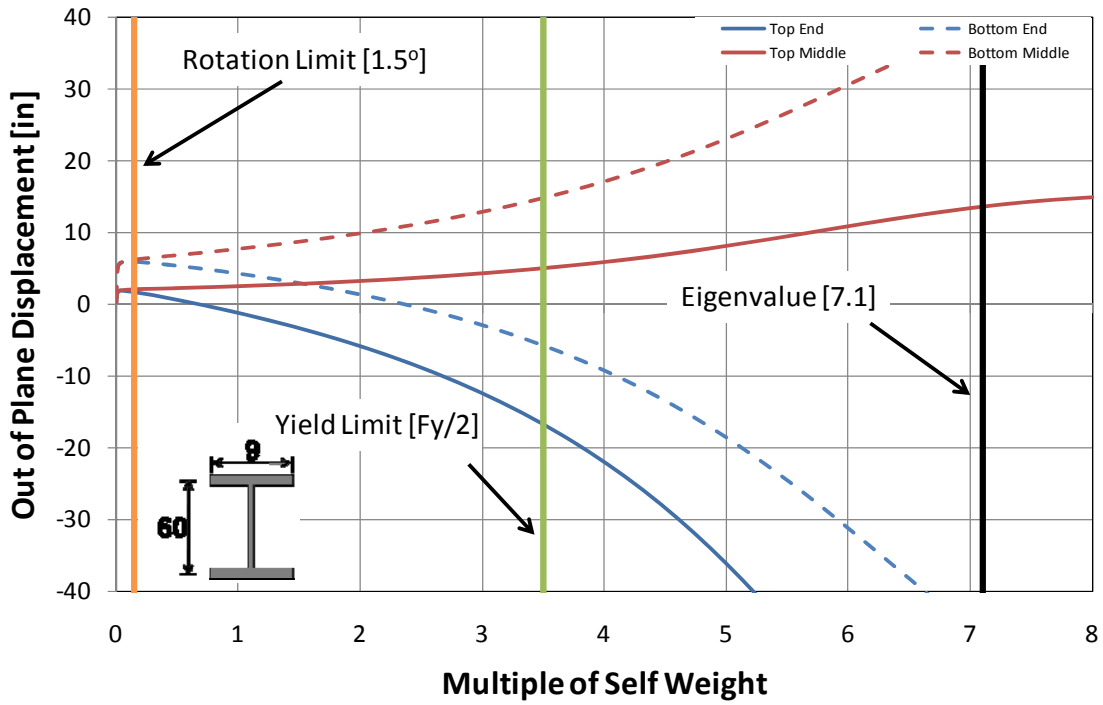


Figure 3.14: Flange Lateral Displacements [$a/L = 0.25$; $b/D = 1/6$; $R = 500'$]

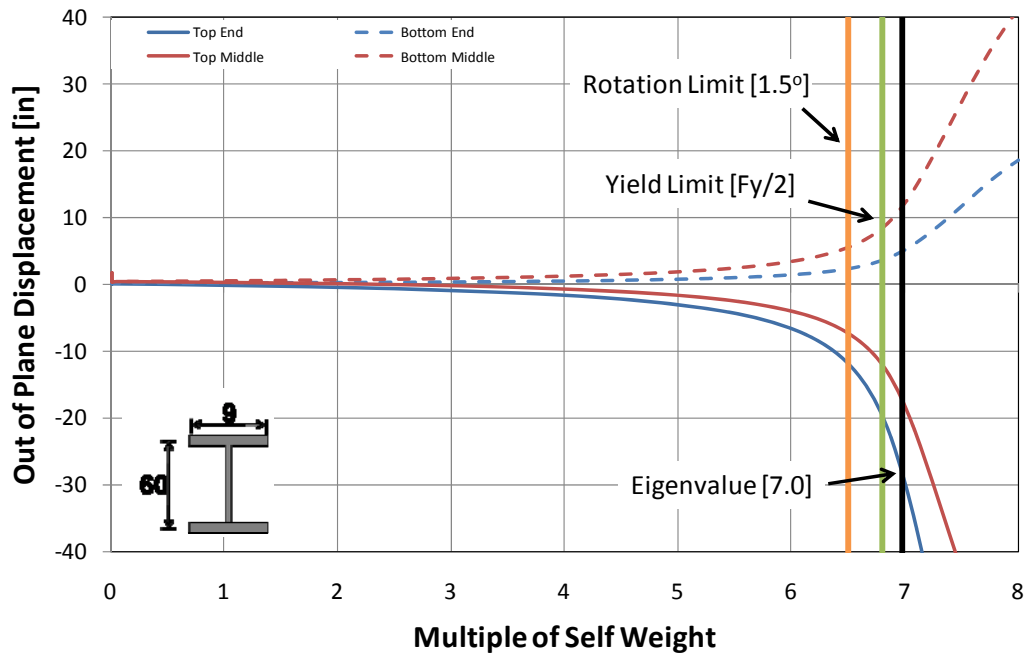


Figure 3.15: Flange Lateral Displacements [$a/L = 0.25$; $b/D = 1/6$; $R = 8000'$]
(Straight)]

As seen in Figure 3.13 and Figure 3.15 for the straight girder, the eigenvalue once again provides a reasonable indication of the load at which large out of plane displacements begin to occur, and provides a reasonable correlation with the load at which the yielding and end rotation limit states are exceeded. However, for the curved girder with a 500 ft. radius of curvature (Figure 3.12 and Figure 3.14) the girders deflected a large amount by the time it reaches the load corresponding to the eigenvalue. As a result, the load corresponding to the eigenvalue is significantly larger than the load at the yield or end rotation limit states. Thus, as noted in the previous section, the eigenvalue, by itself, may not be a reliable indicator of the potential for strength or serviceability problems during lifting of curved I-girders.

An important observation from the plots shown above is that the rotation limit controls in most situations. In three of the four plots above, the rotation limit is reached first, then the yield limit, and finally the eigenvalue. In additional studies shown in Appendix A, the only time it was found that the rotation limit state did not control was with straight girders. In these cases, the yield limit can be reached first. The rotation limit generally controlled for girders with a reasonable amount of curvature (approximately $R < 2000$ ft). It should also be noted that in Figure 3.14, there is a large initial rotation and therefore the 1.5 degree rotation limit is reached at less than the girder self weight. These analyses show the importance of controlling girder rotations when lifting curved girders.

3.6.4 Controlling Girder Rotation during Lifting

3.6.4.1 Overview

In order to control girder rotation, it is important to understand what contributes to the rotation of a girder. As discussed earlier, girder rotation has two different components: rigid body rotation and cross sectional twist. The rigid body rotation is independent of girder stiffness and is completely a function of the geometry of the girder and the lift locations. The cross sectional twist on the other hand is a function of the girder's St. Venant and warping torsional stiffness. Therefore, to control the rotations of

a girder, it is important to understand what factors influence the rigid body rotation and the cross sectional twist.

To investigate factors that influence rigid body rotation, a nonlinear analysis was conducted for a curved girder with a 500 ft. radius of curvature. In this analysis, rotations were calculated for a load corresponding to 0.1% the girder self weight. Because of the small load on the girder, rotations can be attributed primarily to girder rigid body rotation. Additionally, girder rotations were calculated for a load equal to 1.0% the girders self weight. The rotations calculated from the 0.1% self weight were then subtracted from the rotations calculated from a load equal to 1.0% self weight. These net rotations are then attributed primarily to the cross sectional twist of the girder. In Figure 3.16, a 125 ft long girder with a flange width of 15 in, flange thickness of 0.75 in, web depth of 60 in, web thickness of 0.5 in, and radius of curvature of 500 ft is lifted at different a/L locations and the rotations at the end of the girder are calculated. The resulting rigid body rotations, cross sectional twists, and total rotations are plotted for a/L equal to 0.20, 0.21, 0.23, and 0.25. The b_f/D ratio is 1/4.

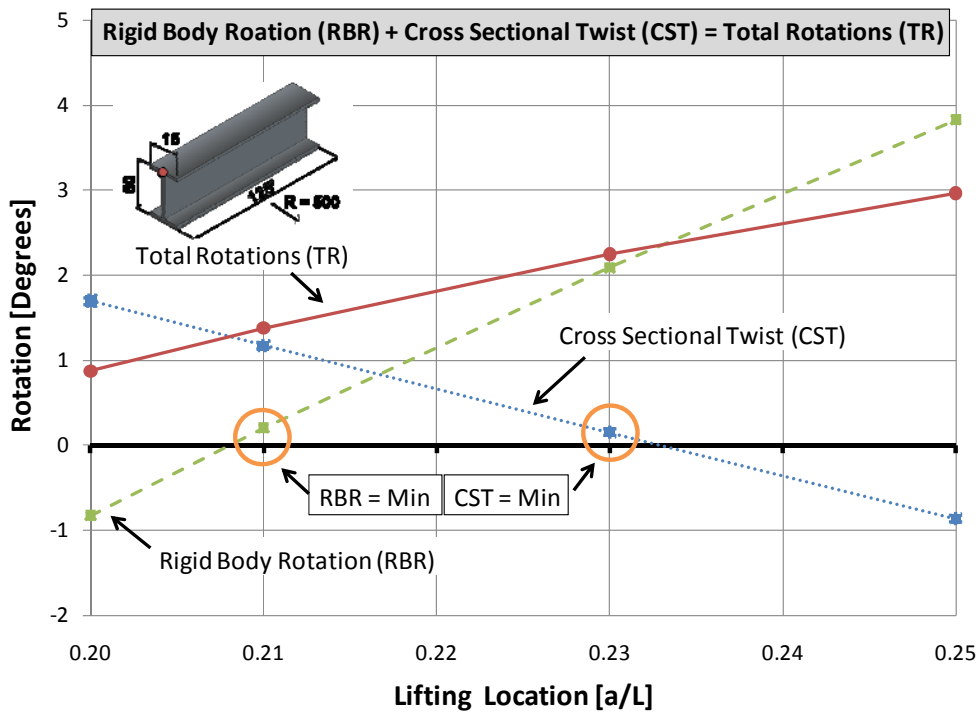


Figure 3.16: Rotations at the End of the Girder for Different Lifting Locations

$$[R = 500 \text{ ft} ; b/D = 1/4]$$

The results from Figure 3.16 show that the rigid body rotation is lowest at a/L of approximately 0.21. The cross sectional twist, on the other hand, is lowest at a/L of approximately 0.23. Therefore one might think the optimal place to lift a girder would be somewhere between 0.21 and 0.23 depending on the cross sectional properties and the stiffness of the given girder. Yet, in Figure 3.16, the lowest total rotation is found at $a/L = 0.20$. This is because the rigid body rotation and the cross section twist occur in different directions and tend to cancel each other at $a/L = 0.20$. Although the lowest total rotation is at $a/L = 0.20$, the highest cross sectional twist occurs for this lifting location. Therefore, there may be a concern that large rotations may be occurring at other points along the girder. The end rotations are important when connecting a splice, but being able to connect the cross frames elsewhere on the girder is also of concern. If the girder is rotated too much along the middle section of the girder, then cross frame fit up

may be a problem. Figure 3.17 plots rotations at the middle of the same girder that was analyzed for Figure 3.16.

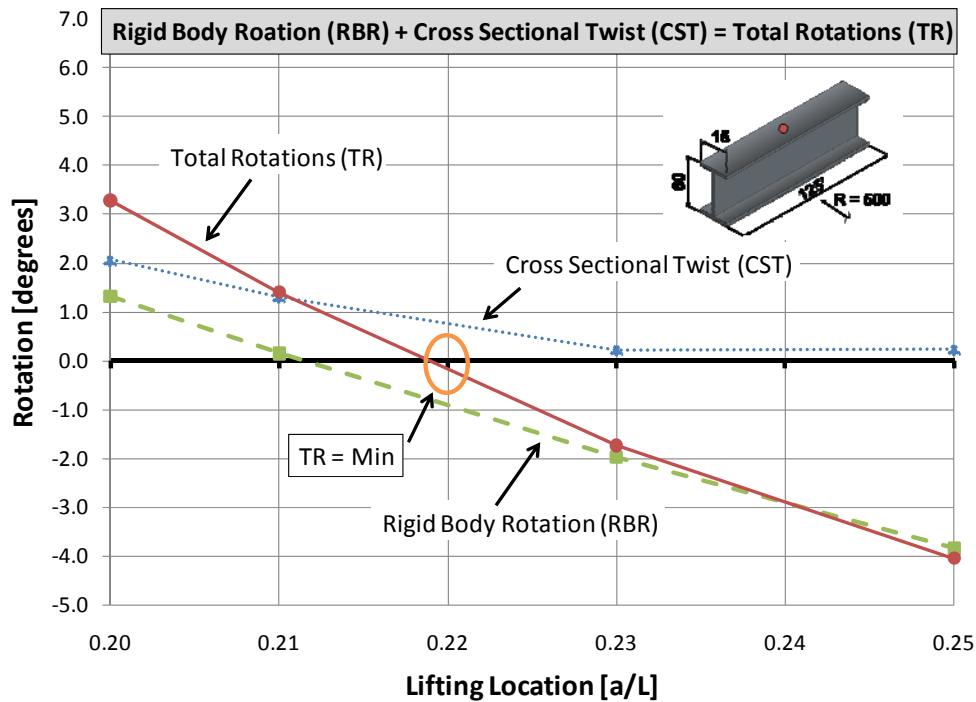


Figure 3.17: Rotations at Middle of Girder for Different Lifting Locations

$$[R = 500 \text{ ft} ; b_f/D = 1/4]$$

It can be seen in Figure 3.17 that the total rotation at the middle of the girder is the greatest at the two extremes: $a/L = 0.20$ and $a/L = 0.25$. The least total rotation at the middle of the girder occurs at $a/L \approx 0.22$. As was the case with the end of the girder, this is also where the rigid body rotation and cross sectional twist tend to cancel each other. However, the lift location that minimizes total rotation at the girder end ($a/L = 0.20$) is different than the lift location that minimized total rotation at the middle of the girder ($a/L = 0.22$). Therefore, it may be better for many lifting scenarios to lift the girder somewhere between $a/L = 0.20$ and 0.22 where the total rotations both at the end of the girder and at the middle of the girder are relatively low. Alternatively, an erector can choose to lift a girder at a location that will minimize total rotation at a specific point

along the girder where a critical fit up tolerance is needed. Further discussion of this issue is provided later.

3.6.4.2 Minimizing Rigid Body Rotation

This section examines the value of a/L that minimizes the rigid body rotation for a prismatic girder. As discussed earlier, the rigid body rotation is due to the line of support between the two lift points being eccentric to the center of gravity of the curved girder (Figure 3.2). Larger eccentricities lead to larger rigid body rotations. In Figure 3.18, the eccentricities for a prismatic girder are normalized to the maximum eccentricity for different lift locations ranging from $a/L = 0$ to 0.5. The values presented are the absolute values for the eccentricity.

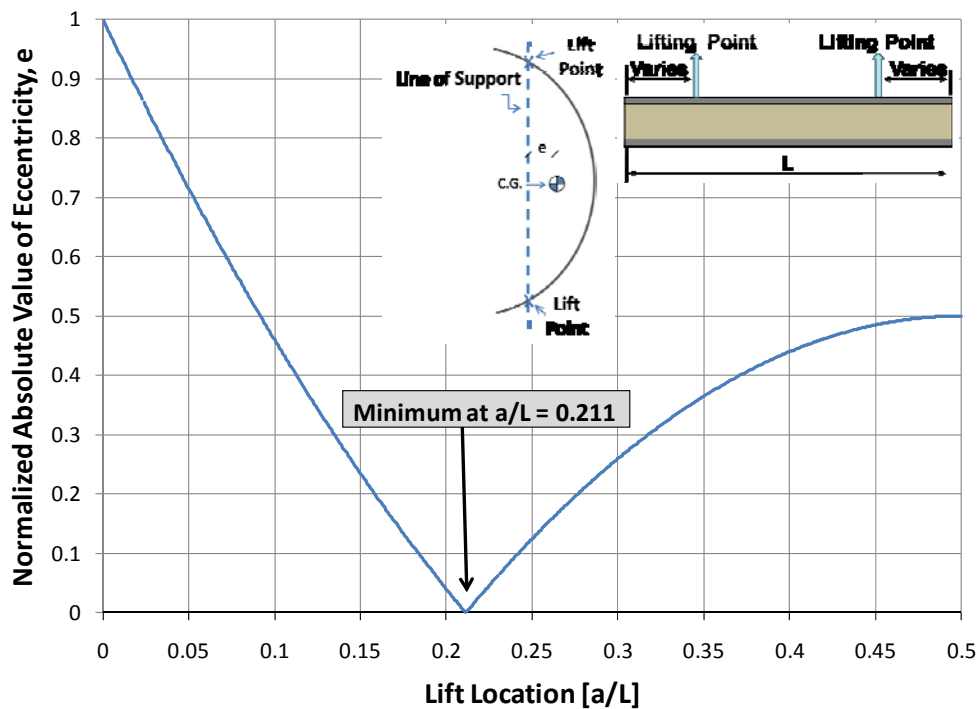


Figure 3.18: Eccentricity for Prismatic Girders Lifted at Different Locations

It can be seen from the results in Figure 3.18 that the smallest eccentricity occurs at $a/L = 0.211$. At this location, the line of support essentially passes through the center of gravity and therefore causes no rigid body rotation. These findings are valid for radius

of curvature values of approximately 100 ft or greater and are consistent with earlier results reported in Figure 3.16 and Figure 3.17 which showed that the smallest rigid body rotations occurred at a location of $a/L = 0.21$. Note that for nonprismatic girders, the value of a/L that results in no rigid body rotation will be different, but can be determined by computing the location of the center of gravity of the girder.

3.6.4.2.1 Rigid Body Rotation Limits

In the previous analysis shown in Figure 3.14, the rigid body rotation on the girder was large enough that the 1.5 degree rotation limit was exceeded at less than the full girder self weight. Clearly, if the lift locations are chosen so that rigid body rotation is large, it may be impossible to satisfy the 1.5 degree rotation limit regardless of girder stiffness. This is demonstrated in the analysis plotted in Figure 3.19. A stiff girder is lifted at a location $a/L = 0.30$. The cross sectional properties of the girder are similar to that of the girders lifted above with a b_f/D ratio = $1/3$, length = 125 ft, flange width = 20 in, web depth = 60 in, and a radius of curvature = 500 ft.

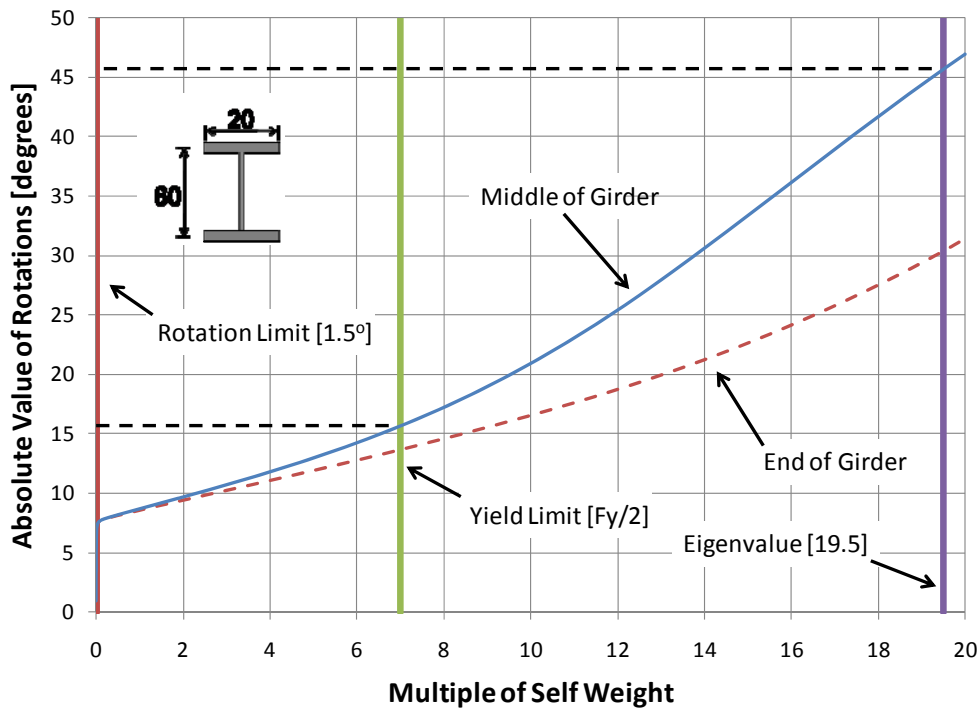


Figure 3.19: Flange Rotation [$a/L = 0.30$; $b_f/D = 1/3$; $R = 500'$]

For this girder, the rigid body rotation exceeds 1.5 degrees. Consequently, the 1.5 degree rotation limit can only be achieved if the direction of cross section twist is opposite to the rigid body rotation and reduces the total rotation to the 1.5 degree limit. However, as described above, even if rigid body rotations and cross section twist cancel each other at the girder ends, they may be additive near the middle of the girder, resulting in large rotations in the middle portions of the girder. Consequently, choosing a lifting location that results in a large rigid body rotation is likely to lead to serviceability problems at some point along the girder. As a result, it is important to understand how the lifted location can have a large effect on the rigid body rotation. Because of this, it is not recommended to lift a prismatic girder at a location greater than $a/L = 0.25$.

3.6.4.3 Minimizing Cross Sectional Twist

This section examines how the lift location a/L affects the cross section twist for a prismatic curved girder. Cross section twist refers to rotation of the girder due to an applied torsional moment, as shown in Figure 3.20. As used herein, the term cross section twist refers to the rotation resulting only from torsional flexibility of the girder, and does not include rigid body rotation.

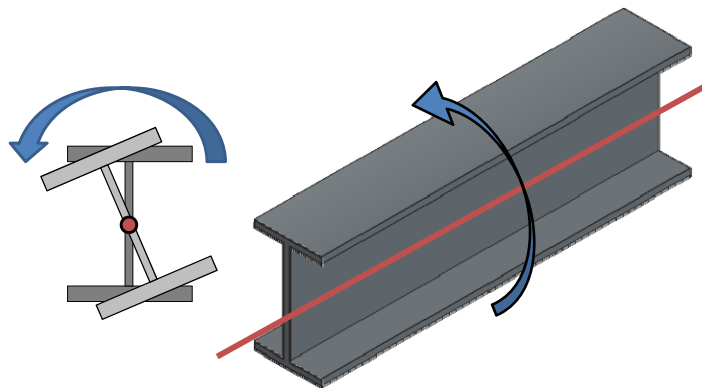


Figure 3.20: Cross Sectional Twist

For a curved girder during lifting, the torsional moment that produces cross section twist is generated by the girder's self weight. The distribution of torsional moment along the length of a lifted curved girder was evaluated by Stith (2010). An example of the analysis by Stith is shown in Figure 3.21. The torsional moment along the

length of the girder is graphed in the figure. The torsional moment is normalized by its maximum value. Note that this torsional moment is based on the undeformed geometry of the girder.

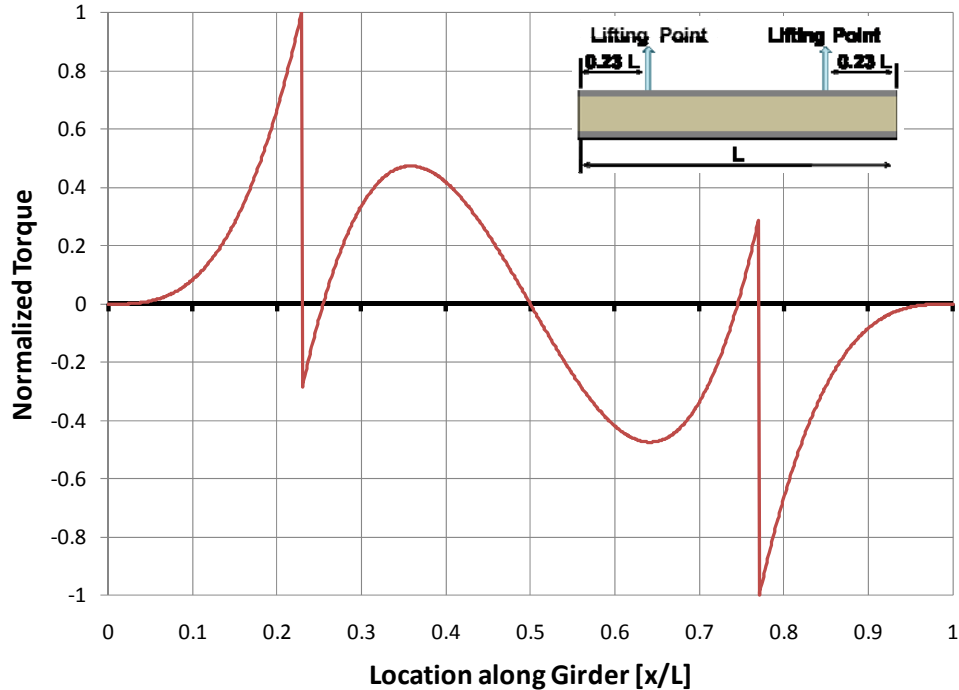


Figure 3.21: Example Torsion Diagram for Prismatic Girder [$a/L = 0.23$]

It should be noted that the radius of curvature will only change the magnitude of the torsion diagram, but not the shape. Therefore, for all configurations of a prismatic girder lifting at $a/L = 0.23$, the plot shown in Figure 3.21 represents the shape of the normalized torsion diagram. Note that the largest torsional moments occur at the lift locations.

The amount of cross section twist at the girder ends depends on the girder torsional stiffness as well as the magnitude and distribution of torque along the girder. However, for given cross section torsional properties, the amount of cross section twist at the girder ends is related to the absolute value of the area under the torsion diagram (Stith, 2010). More cross section twist will occur in the girder the larger the area is under the torsion diagram. In Figure 3.22, the summation using the absolute value of the area

under the torsion diagrams constructed for lift locations ranging from $a/L = 0$ to $a/L = 0.5$ is presented.

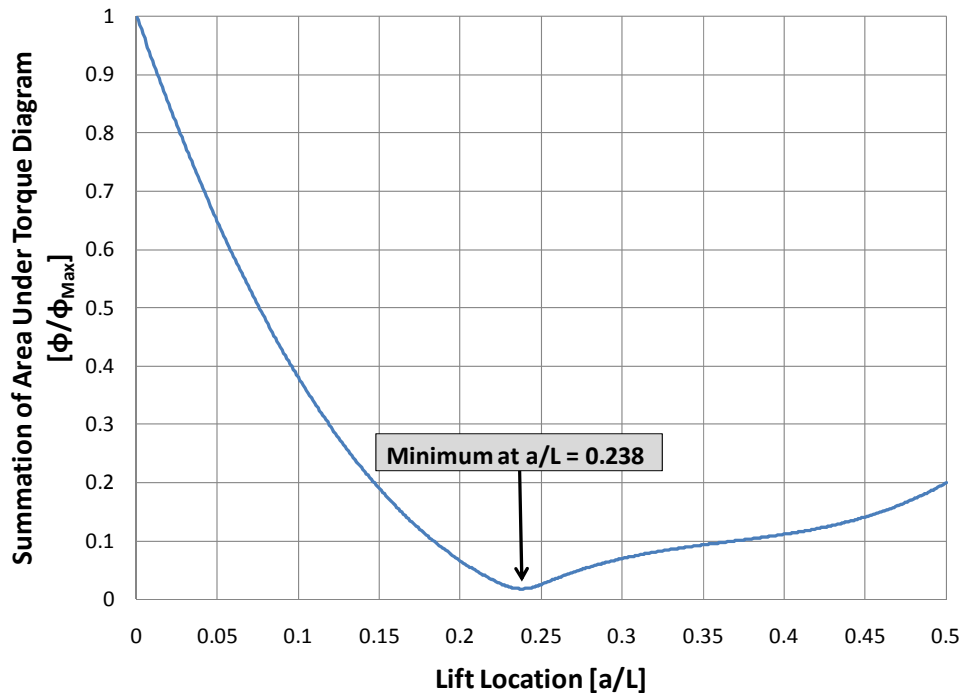


Figure 3.22: Summation of Area under Torque Diagram for Different Lift Locations

From Figure 3.22, it can be seen that the smallest total area occurs at $a/L = 0.238$. This indicates that the least amount of cross sectional twist in a prismatic girder segment occurs at a lift location a/L equal to 0.238. The results of Figure 3.22 are consistent with the results shown in Figure 3.16 and Figure 3.17 that show that the lift location $a/L = 0.23$ has the least amount of cross sectional twist.

As discussed earlier, another way to evaluate the stability of a system is to calculate the eigenvalue. Although the eigenvalue, by itself, may not be an accurate indicator of potential strength and serviceability problems for curved girders, it still provides a general indication of girder instability. In Figure 3.23, the diagram shown in Figure 3.22 is inverted and eigenvalues for prismatic girders are normalized to the maximum eigenvalue and plotted for different a/L locations.

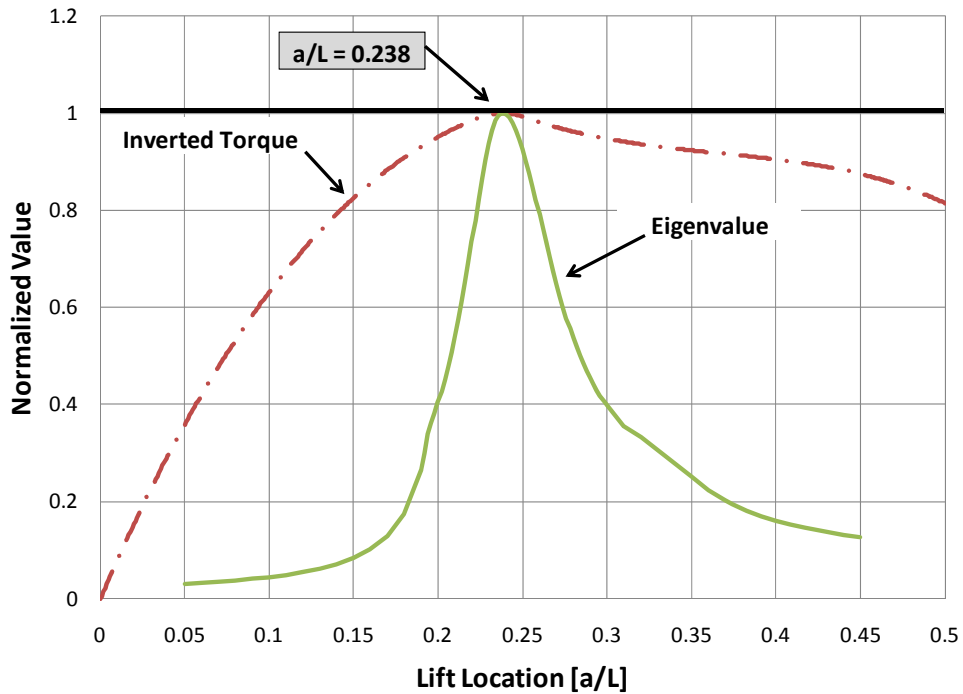


Figure 3.23: Eigenvalue and Inverted Torque Diagram

It can be seen that the maximum eigenvalue also occurs at $a/L = 0.238$. This is another indication that the system is most stable at $a/L = 0.238$ and that the least amount of cross sectional twist will occur at this lift location for most prismatic girders.

3.6.4.3.1 Cross Sectional Twist Limits

In Figure 3.24, the data shown in Figure 3.22 is replotted to only show the lift locations for the range of a/L equal to 0.17 to 0.25. The upper limit of 0.25 is used because large rigid body rotations will generally preclude lift locations beyond this limit, as discussed above.

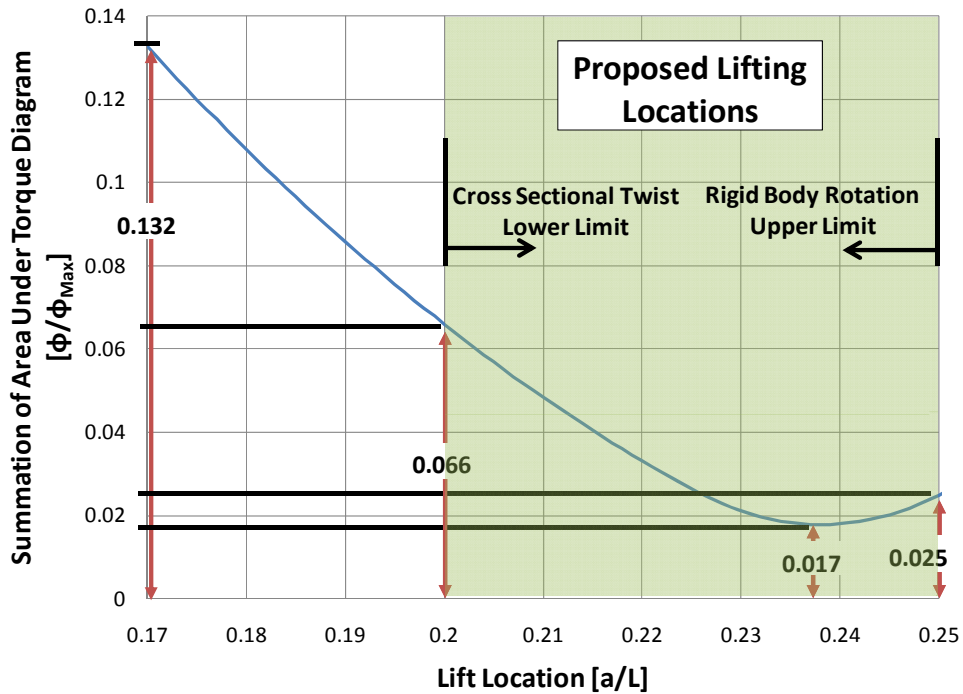


Figure 3.24: Summation of Area under Torque Diagram for a/L equal to 0.17 – 0.25

It can be seen in Figure 3.24 that the summed area under the normalized torque diagram at $a/L = 0.238$ is 0.017. At $a/L = 0.20$, the value more than triples to a value of 0.066. By the time the lift location is moved out to $a/L = 0.17$ the value is 0.132; almost eight times the value at $a/L = 0.238$. Between $a/L = 0.17$ and 0.20 the cross sectional twist generally dominates the behavior and leads to large rotations in horizontally curved I-girders. Therefore, it is recommended to lift a girder at a location between $a/L = 0.20$ and $a/L = 0.25$ to avoid excessive torsional deformations on the girder that lead to large twists of the cross section.

3.6.5 Preferred Lifting Locations

3.6.5.1 Slenderness Ratio [b_f/D]

A parameter that is sometimes used as an indicator of potential stability problems during girder lifting and erection is the ratio of girder flange width to depth b_f/D . To evaluate the significance of this parameter, it is instructive to consider the effect of cross-

section dimensions on the critical elastic lateral torsional buckling moment computed by Timoshenko's equation. This equation, shown in Figure 3.25, has two terms that contribute to the buckling resistance. As shown in the figure, these two terms are the St. Venant's torsional stiffness and the warping torsion stiffness.

$$M_o = \frac{\pi}{L_b} \sqrt{\underbrace{EI_y GJ}_{\text{Part 1}} + \underbrace{E^2 I_y C_w \left(\frac{\pi^2}{L_b^2} \right)}_{\text{Part 2}}}$$

Part 1 Part 2

Part 1: St. Venant's Stiffness
Part 2: Warping Stiffness

Figure 3.25: Components of Timoshenko's LT Buckling Equation

The flange width is important in determining many of the cross section properties that are found in both the St. Venant's stiffness and the warping stiffness terms. The moment of inertia (Eq. 3.4), I_y , the torsional constant (Eq. 3.5), J , and the warping torsional constant (Eq. 3.6), C_w , are all variables that are dependent on the flange width, b_f .

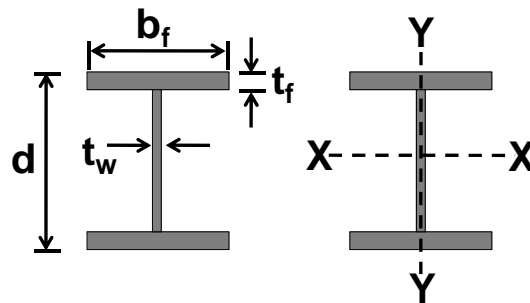


Figure 3.26: Cross Sectional Property Designations

$$I_y = \frac{t_f b_f^3}{6} \tag{Eq. 3.4}$$

$$J = \frac{2b_f t_f^3 + d' t_w^3}{3} \quad \text{Eq. 3.5}$$

$$d' = \text{Effective Depth} = d - t$$

$$C_w = \frac{I_y d'^2}{4} = \frac{(d')^2 b_f^3 t_f}{24} \quad \text{Eq. 3.6}$$

Because the thickness of the flange, t , and the width of the web, w , are small, the torsional constant, J , is generally small relative to the moment of inertia, I_y , and the torsional warping constant, C_w . Yet, both the moment of inertia and the torsional warping constant are dependent on the flange width cubed. Therefore, for a constant depth, doubling the slenderness ratio (b_f/D) from 1/6 to 1/3 can make each one of these terms eight times larger. Therefore, increasing the flange width will significantly increase the torsional stiffness and significantly increase the buckling moment.

As described earlier, current TxDOT preferred practices suggest limiting the value of b_f/D to 1/3. On the other hand, AASHTO permits a value of b_f/D as small as 1/6. Girders with a slenderness ratio closer to $b_f/D = 1/3$ have a significantly higher torsional stiffness and the rotation is more likely to be affected by rigid body rotation than by cross section twist. Therefore, it may be beneficial to lift these girders closer to $a/L = 0.211$ to minimize the rigid body rotation. For more slender girders closer to $b_f/D = 1/6$, cross sectional twist will play a much larger role in girder rotation. Therefore, it may be beneficial to lift these girders closer to $a/L = 0.238$ to minimize the cross sectional twist.

Highly curved girders with a slenderness ratio close to $b_f/D = 1/6$ may be problematic during lifting. Lifting these girders close to $a/L = 0.238$ to prevent excessive cross sectional twist will still lead to relatively large rigid body rotations. Yet, if the lift locations are chosen to minimize rigid body rotations, then large cross sectional twist will occur. This effect can be seen in Figure 3.27 where a girder with a flange width of 9 in, flange thickness of 0.5 in, web depth of 60 in, web thickness of 0.5 in, a length of 125 ft, and a radius of curvature of 500 ft is lifted.

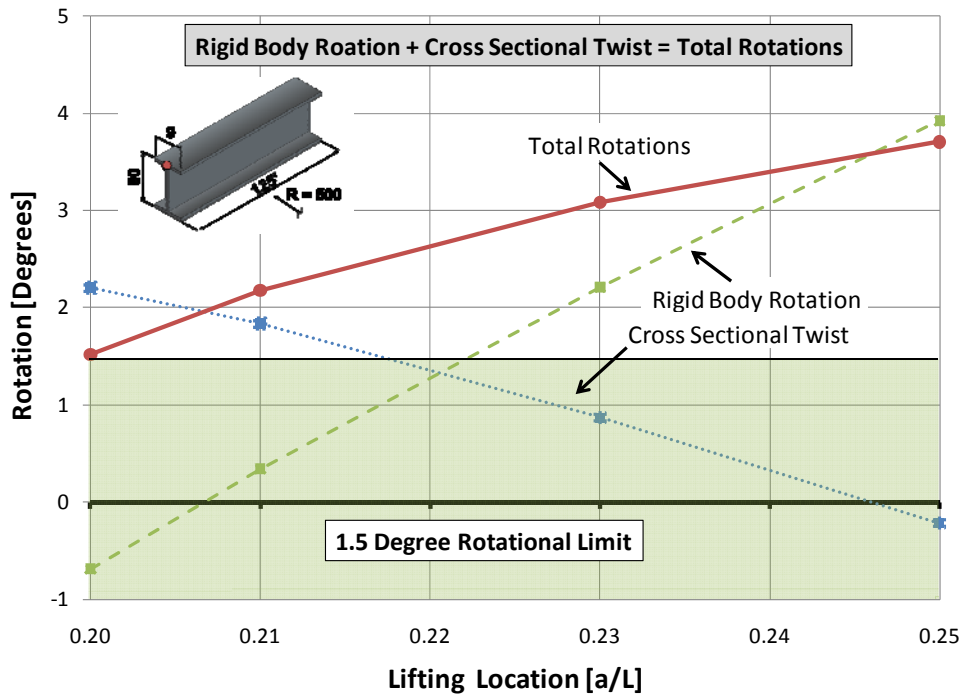


Figure 3.27: Rotations at End of Girder for Different Lifting Locations

$$[R = 500 \text{ ft}; b_f/D = 1/6]$$

It can be seen by looking at the total rotations in Figure 3.27 that no matter where the girder is lifted, the total rotations are above the 1.5 degree limit. In this case, lifting the girder at $a/L = 0.25$ creates the least amount of cross sectional distortion, yet, the rigid body rotation is almost 4 degrees. If the girder is lifted at $a/L = 0.21$, then the rigid body rotation is minimized, but the cross sectional twist is almost 2 degrees. Lifting the girder at $a/L = 0.2$ where the total rotation is the least creates the largest cross sectional twist as expected. Therefore, other locations on the girder should be checked to confirm that excessive deformations are not occurring. In Figure 3.28 the same girder is lifted and the rotations at the middle of the girder are plotted for different lift locations.

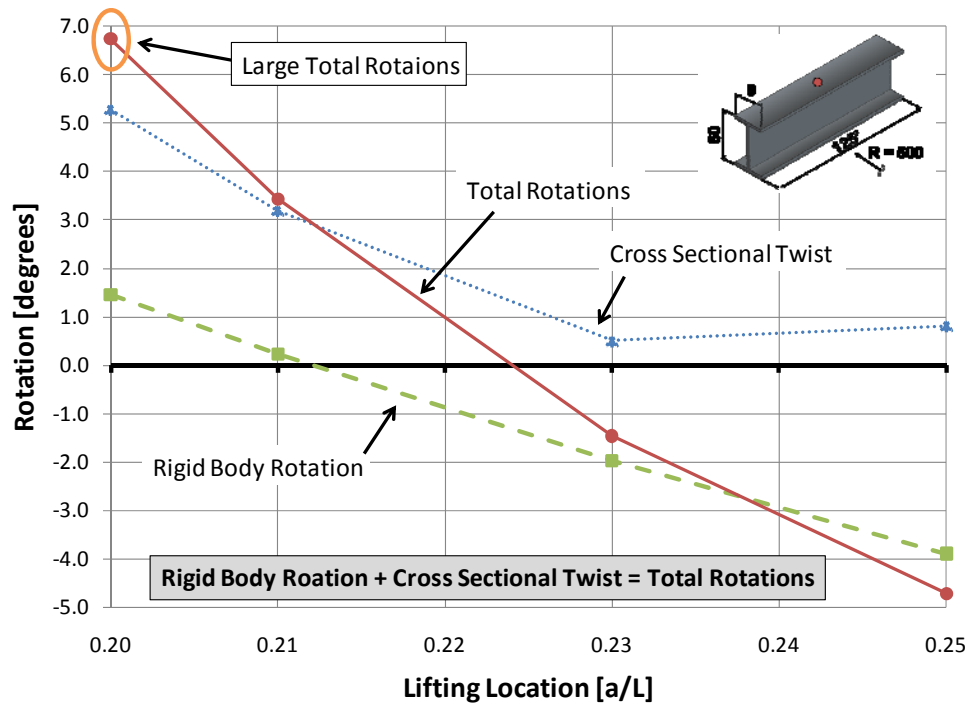


Figure 3.28: Rotations at Middle of Girder for Different Lifting Locations

$$[R = 500 \text{ ft} ; b_f/D = 1/6]$$

It can be seen in Figure 3.28 that at $a/L = 0.20$, the total rotation at the middle is almost 7 degrees. A majority of this is due to cross sectional twist as expected. It can therefore be concluded that the best place to lift the girder would be somewhere between $a/L = 0.21$ to 0.23 . Yet, as noted above, no location gives total rotations under the 1.5 degree limit. Therefore, due to serviceability issues during lifting, designing very slender members with a small top flange and a small radius of curvature is not recommended. With girders approaching $b_f/D = 1/6$, the best control over deformations will likely be to use two cranes with spreader bars so that the girder is supported at 4 lift points. Although parametric studies with 4 support points were not considered, isolated cases showed that the resistance to both rigid body deformations and torsional deformations were significantly improved.

3.6.5.2 Subtended Angle

A useful parameter when determining where to lift horizontally curved I-girders is the girder's subtended angle. The subtended angle, θ , is determined by the angle created by the arc formed by the girder as shown in Figure 3.29. If the radius of curvature of a girder is large, the subtended angle is generally small. When expressed in radian, the subtended angle is the arc length of the segment divided by the radius of curvature $[L/R]$.

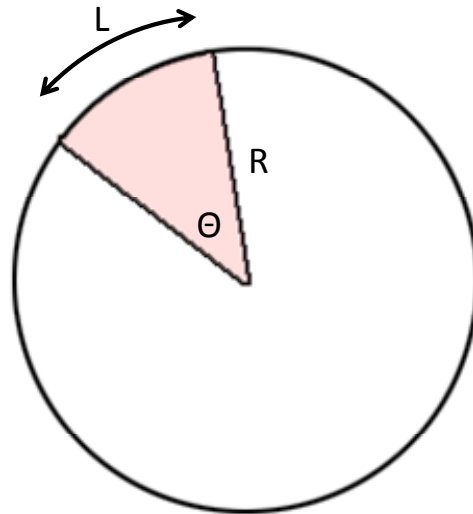


Figure 3.29: Subtended Angle [Θ] Definition

In Figure 3.30, a girder with a flange width of 12 in, flange thickness of 0.625 in, web depth of 60 in, web thickness of 0.5 in, and a length of 125 ft is lifted at four different lift locations: $a/L = 0.20, 0.21, 0.23,$ and 0.25 . For each of the lift locations, the girder was lifted with five different radii of curvature: $R = 1000$ ft, 1500 ft, 1800 ft, 2000 ft, and 2500 ft. Five different values for subtended angle are plotted for each lift location. The subtended angles are plotted versus the load in multiples of self weight that causes the girder to reach an end rotation of 1.5 degrees.

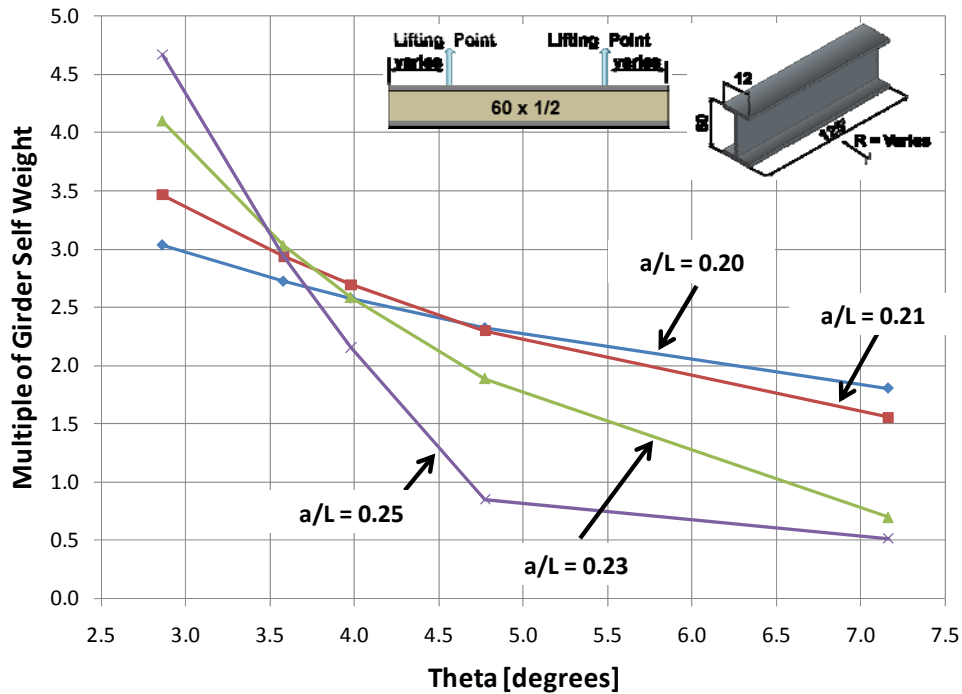


Figure 3.30: Optimal Lifting Location as a Function of Subtended Angle, Theta, to Cause End Rotation of 1.5 Degrees [$b/D = 1/5$]

From the results in Figure 3.30, it can be seen that there are different lift locations that provide the most stable system for different subtended angles. For a given length girder, larger subtended angles result from the smaller radius of curvature values. These girders are more vulnerable to rigid body rotations and therefore it is important to lift them so that the rigid body rotations are small. For a given length girder, smaller subtended angles result from larger values of the radius of curvature. In the limit of an infinite radius of curvature, i.e. a straight girder, the subtended angle is zero. Since rigid body rotations are less of a concern for straight girders, it is optimal to lift the girder where the least amount of cross sectional twist can occur. Based on these conclusions, the following recommendations have been made for prismatic, horizontally curved I girders: relatively straight girders (small subtended angles) should be lifted closer to $a/L = 0.238$ and highly curved girders (large subtended angles) should be lifted closer to $a/L = 0.211$.

It should be noted that when lifting closer to $a/L = 0.211$, the girder experiences more cross sectional twist. Therefore, deflections should be checked along the length of the girder to prevent fit up problems at locations other than at the end of the girder.

3.7 CONCLUSIONS

3.7.1 Eigenvalues

Eigenvalue buckling analyses provide an accurate prediction of instability for a straight girder during lifting. For curved girders, on the other hand, results from an eigenvalue buckling analysis are less useful. The eigenvalue provides a general indication of the load to cause instability of a curved girder. However, by the time the load corresponding to the eigenvalue is reached for a curved girder, very large lateral deflections and rotations may have already occurred. These large lateral deflections and rotations, in turn, can result in significant serviceability problems by making it difficult or impossible to connect the lifted girder to previously erected portions of the bridge. These large deformations can also lead to yielding of the girder. Thus, the eigenvalue, by itself, may not be a reliable indicator of the potential for strength or serviceability problems during lifting of curved I-girders. In general, the value of eigenvalue buckling analysis is diminished as the girder becomes more curved, i.e., as the radius of curvature is reduced.

3.7.2 Rotation Limits

As an alternative to an eigenvalue buckling analysis, computing the rotations of a curved girder during lifting can provide an improved approach for assuring safety and serviceability. Based on a nationwide survey of erectors and engineers, a rotation limit of 1.5 degrees at the end of the girder is recommended. The analyses conducted herein suggest that this rotation limit will generally be reached well before the eigenvalue is reached. There are two components that contribute to the total rotation of a girder: the rigid body rotation and the cross sectional twist. The rigid body rotation is only a function of geometry of the girder and the lift locations and is independent of girder stiffness. The cross sectional twist is a function of the girder stiffness. Both are a

function of the girder lift location. Consequently, it is recommended that in planning a lift for a curved steel I-girder that will not result in safety or serviceability problems, engineers should limit girder rotations to about 1.5 degrees and also check the eigenvalue. For girders with any significant curvature, the rotation limit is likely to be the controlling factor. However, for girders with only very slight curvature, the eigenvalue is likely to provide a useful prediction of instability. UT Lift, a macro enabled spreadsheet, was developed as a tool to calculate the rigid body rotation and predict the cross sectional twist using a first order analysis.

3.7.3 Lifting Location Limits

Because both the amount of rigid body rotation and the amount of cross sectional twist a girder is a function of the lift location, it is important to understand the upper and lower limits of the lift location to try to keep each one of these effects under the 1.5 degree rotational limit. It is recommended to lift a girder:

- At a location greater than $a/L = 0.20$: this will prevent excessive girder distortion due to cross sectional twist.
- At a location less than $a/L = 0.25$: this will prevent excessive rigid body rotations.

Adhering to the above guidelines will not ensure that when lifting a prismatic girder, that the rotations will stay under 1.5 degrees. Yet, the above guidelines are a good starting point to ensure the most stable lifting conditions for most prismatic girders.

3.7.4 Preferred Lifting Locations

The flange width significantly affects the stiffness of a girder. Therefore, for girders with b_f/D ratios close to $1/3$, the girders have a relatively high stiffness and the cross sectional distortions are less significant. For these girders, it is recommended to lift them closer to $a/L = 0.21$ to minimize the rigid body rotations on the system. For girders with a b_f/D ratio closer to $1/6$, it is recommended to lift them closer to $a/L = 0.24$ to help prevent excessive cross sectional distortion. Lifting very slender girders (where b_f/D is close to $1/6$) that have a small radius of curvature can be very problematic due to

excessive rigid body rotations and cross sectional distortions. Keeping their total rotations less than 1.5 degrees may not be possible in some cases and as a result should be avoided if possible due to serviceability issues during lifting. In girders with b_f/D approaching 1/6, the erector should consider using two cranes with spreader bars to distribute the support along the length.

CHAPTER 4

Parametric Studies on the Behavior of Partially Constructed Bridges with Curved Steel I-Girders

4.1 INTRODUCTION

The design of curved steel I-girder bridges necessitates considerations for safety and serviceability of the structure and structural elements at several stages. Important stages and elements that need to be considered include lifting of individual girder segments, the partially erected steel superstructure, the concrete deck placement, and finally the in-service stage. When bridge engineers assess the structural performance of a bridge system, they typically evaluate the system in its final in-service configuration. Yet, critical structural safety and serviceability issues often arise during the construction stages. A bridge structure can be particularly vulnerable to severe problems during construction because less bracing and continuity is present as compared to the final constructed bridge. Most often, contractors are responsible for the safety of the bridge during construction. However, structural design criteria and analysis tools for bridges during construction are not as well developed compared to that of the final fully constructed in-service bridge structure. Consequently, contractors often rely heavily on experience and on rules of thumb (Beckmann and Mertz 2005) to guide their assessment of structural safety during construction. Curved steel I-girder bridges can be particularly challenging during construction. The significant influence of torsion on the structural response of curved girders often makes their analysis more complex than for straight girders. Various issues related to the safety and serviceability of curved steel I-girder bridges during construction were investigated as part of TxDOT Research Project 0-5574 (2006), “Curved Plate Girder Design for Safe and Economical Construction.” One of the issues considered in this project was safety and serviceability of curved steel I-girders during lifting. These studies were described in the last chapter. An additional issue considered in TxDOT Project 0-5574 is the safety and serviceability of the steel

superstructure in a partially-constructed condition. A number of studies on partially constructed curved steel I-girder bridges for this project were conducted by Stith (2010). To support and supplement the work by Stith, a number of parametric finite element studies were conducted on partially constructed bridges, and are reported in this chapter. More specifically, the primary objective of the studies reported herein was to examine how the use and placement of temporary shore towers and holding cranes affect the structural performance of partially constructed bridges.

4.2 BACKGROUND ON SHORE TOWERS AND HOLDING CRANES

Shore towers or holding cranes are sometimes used to provide temporary support for one or more girders during construction of a curved steel I-girder bridge. These temporary supports are left in-place until the partially constructed bridge can safely stand without these supports. The temporary supports are often needed until a sufficient number of cross-frames have been connected to the girders and/or until girder splice connections have been completed. A shore tower is a temporary structure that is placed at a specific location along the girder to provide support to the girder at the bottom flange location. A shore tower acts essentially as a temporary bridge pier and can restrain both vertical and horizontal movement of the girder. Pictures of shore towers are shown in Figure 4.1.



Figure 4.1: Shore Towers under Partially Constructed Bridges

In addition to providing restraint to vertical and horizontal movement of a girder, the attachment of the girder to the shore tower can be designed to also restrain rotation of the girder. This can be accomplished by connecting the top flange of the girder to the shore tower with cables, timbers or other bracing. An example is shown in Figure 4.2. This figure shows photos of temporary bracing to restrain girder rotation at a permanent bridge pier. However, the same type of bracing can be used at a shore tower. In the photo on the left, an iron worker is positioning a timber brace to restrain the girder from rotating. In the photo on the right, both a timber brace, which can only resist compression, and a slender steel rod with a turnbuckle brace, which primarily resists tension, are used to prevent the girder from rotating in either direction.



Figure 4.2: Temporary Top Flange Bracing to Restrain Girder Rotation

Although shore towers are temporary structures, they are significant engineered structures in their own right. They must be designed to carry large loads at significant heights. Further, they must be designed to be quickly assembled on site to accommodate a variety of configurations and heights, and then to be quickly disassembled and moved to the next location. Shore towers can therefore be costly structures. Further, the time, labor, and equipment needed to assemble and disassemble a shore tower can impact the cost and schedule for constructing the bridge. Also, since a significant amount of time may be needed to assemble and disassemble a shore tower, their use may not be possible

if they are located on an existing in-service roadway where there is a lack of space and extended traffic closures are not permitted. Further, if the bridge crosses a waterway or other obstacles, the use of a shore tower may be impractical or impossible.

The use of a holding crane is another option for providing temporary support of girders during construction. Whereas a single shore tower can support several girders at one time (Figure 4.2), a holding crane typically supports only a single girder. Further, whereas the bottom flange of a girder normally rests on top of a shore tower, the top flange of a girder normally hangs from a holding crane. Photos of a holding crane clamping onto the top flange of a steel I-girder are shown in Figure 4.3. In the photo on the left, the large crane with the lattice boom and with the spreader bar was used to lift the girder into place. The holding crane is the smaller crane in the photo on the left. The holding crane uses a single lifting clamp to apply a specified upward force to support the girder so that the lifting crane can be released to pick up the adjacent girder. The photo on the right side of Figure 4.3 is a close up showing the holding crane attached to the top flange. Holding cranes provide little restraint to the girder from translating in directions orthogonal to the cable. Therefore, structural analysis should be performed to make sure that the girder does not translate a significant amount when the lifting crane is released.



Figure 4.3: Holding Crane and its Attachment to the Top Flange of a Girder

Unlike shore towers, holding cranes do not typically require as large of a space around the bridge for extended periods of time. Therefore, they can be useful in situations where girders cross existing roadways, bodies of water, or other obstacles. Holding cranes also require less preparation before use and can be used for shorter periods of time. In addition, because of their mobility, the placement of holding cranes can be adjusted to meet last minute changes at the jobsite. Holding cranes, of course, also add cost to a project, both for the cost of the equipment and for the operator. The cost of a holding crane can escalate quickly if adversities arise and the holding crane is required for longer than initially estimated.

4.3 STUDY OBJECTIVES AND DESCRIPTION

As part of this research study, several issues related to the use and placement of shore towers and holding cranes were investigated using finite element analyses. The analysis methods and results are described below.

An objective of this analysis was to study the effect of shore tower and holding crane location on the safety and serviceability of the supported girder. An additional objective was to study the effect of varying the lifting load used for the holding crane. A final objective was to compare girder behavior and stability when the bottom flange is supported by a shore tower versus when the top flange is hung from a holding crane.

The analysis conducted in this study used the same ANSYS finite element model that was described in Chapter 3 for girder lifting simulations. Girders were modeled in three dimensions using shell elements for the flanges and web. All analyses were elastic, and considered both linear (first-order) and nonlinear (second-order) geometry. Further details of the model, along with information of validation of the model from field testing are described in Stith (2010).

4.3.1 Parameter Descriptions

The parameters investigated in the analyses dealing with shore towers and holding cranes were the flange width to girder depth ratio (b_f/D), the girder span length to girder depth ratio (L/D), radius of curvature of the girder (R), and the location of the shore

tower/holding crane along the length of the girder. Boundary conditions were also varied when considering the use of a shore tower. Both a small and large stiffness of the bracing connecting the top flange of the girder to the shore tower was considered. Lastly, the parameter considered when using a holding crane includes varying the upward load applied by the holding crane. Cross sectional variables used for this study are depicted in Figure 4.4.

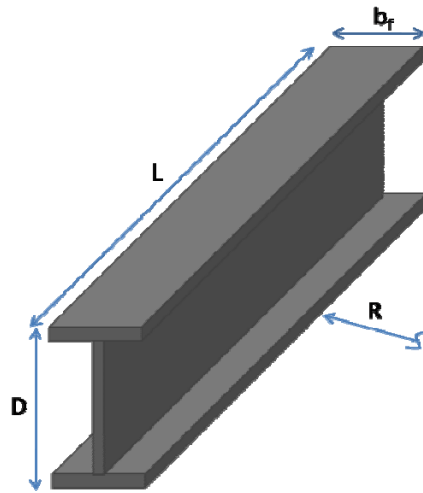


Figure 4.4: Girder Geometric Parameters

4.3.2 Parameter Ranges

The flange width to depth ratio recommended in the TxDOT Preferred Practices for Steel Bridge Design, Fabrication, and Erection is 1/3 (TxDOT 2007). AASHTO on the other hand allows a bridge design engineer to use a flange width to depth ratio as little as 1/6 as seen in Equation 6.10.2.2-2 of the AASHTO LRFD Bridge Specification (AASHTO 2008). In this study, the range of b_f/D ratios that were used was 1/3 to 1/6 to determine the behavior of the girders at the two recommended limits. For all parametric studies completed, the top and bottom flanges had the same dimensions.

The girder span to depth ratio was changed throughout the study to see if it had an effect on the optimal location of a shore tower. Additionally, the span to depth ratio was changed to determine if there was a significant effect on the stresses on the cross section for either the geometric linear or non-linear analysis. In trying to model realistic

dimensions that might occur in the field, the span to depth ratios that were considered are 26 and 37. These values were determined by examining available bridge plans.

For any given girder, the radius of curvature is the distance from the centerline of the girder cross section to the middle of the circular segment. For most bridges, arc lengths and tangent lines are used to describe the horizontal profile. The radius of curvatures that were considered in this study ranged from 500 feet to 10,000 feet (representing a straight girder). Most bridges constructed in Texas have a radius of curvatures greater than 800 feet.

To help determine the optimal location to place a temporary support (i.e. shore tower/holding crane), the temporary support position along the length of the girder was varied. The temporary support location typically varied as a ratio x/L where x is the distance from the start of the girder to the temporary support location and L is the length of the span. Figure 4.5 shows the parameter definitions for the location of the temporary supports.

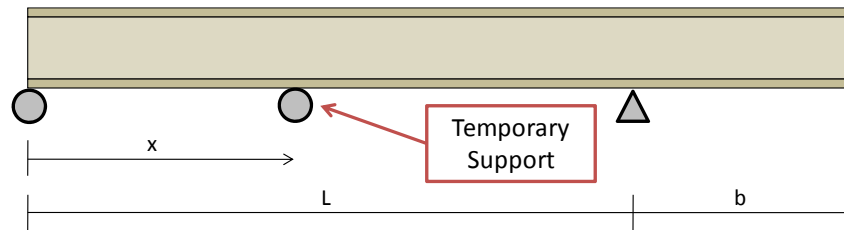


Figure 4.5: Temporary Support Location Parameter Definitions

The stiffness of the brace that connects the top flange of the girder to the shore tower was varied. At first, a very stiff spring was used as a lateral brace for the top flange, as illustrated in the right portion of Figure 4.6. The stiffness corresponded to a 10-inch long steel rod with a cross-sectional area of 0.5 in^2 . In some of the analyses, it was observed that the top flange of the girder at the location of the shore tower experienced a considerable movement and also experienced large warping stresses. As a comparison, a rigid lateral support was also used at the top flange in the model, as illustrated in the left portion of Figure 4.6.

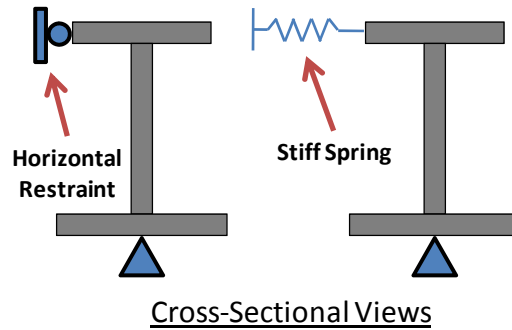


Figure 4.6: Top Flange Rotational Support Options Considered

For analyses of girders supported by a holding crane, the vertical load of the holding crane was varied substantially depending on the girder being considered in the parametric study. A vertical load of 20 kips to 50 kips at 5 kip intervals was typical for most early parametric studies. For later studies, the holding crane load was varied depending on the load that would be equivalent to the vertical reaction of a rigid support placed at the holding crane location. From this starting point, the holding crane load was varied $\pm 5\%$, $\pm 10\%$, and $\pm 20\%$ of the rigid support reaction.

4.4 RESULTS OF PARAMETRIC STUDIES

4.4.1 Shore Tower Location

An important aspect when using a shore tower is determining the location. The shore tower position can dramatically change the system behavior along with the vertical and horizontal reaction that will be induced to maintain the proper orientation of the girder web. Many factors determine where the shore tower should be placed including many non-structural factors such as site access. The life of a shore tower from erection to removal can be quite lengthy. Therefore, the site where the shore tower is to be constructed needs to be available for the entire duration of service. If there is a road passing underneath that needs to maintain traffic flow, placing a shore tower along the width of the roadway may not be acceptable. Additionally, the use of a shore tower may necessitate extra web stiffeners in the girder. The large concentrated load produced by the shore tower can cause local deformations associated with application of a

concentrated force to a girder, including flange local bending, web local yielding or crippling, and web sideway buckling. Consequently, it is often preferable to place the shore tower at a location on the girder where a stiffener is already located. Regardless if a shore tower is placed at a stiffener location or not, it is still necessary to conduct an analysis to assure local failure modes associated with concentrated forces do not occur.

A series of analyses were conducted to examine the response of different girders to different shore tower locations. In these analyses, the shore tower was assumed to permit no vertical deflection of the girder at the location of the shore tower. Based on analysis results, it is recommended that the shore tower be placed close to the location of maximum positive moment for any given span between two permanent supports. This location will approximately minimize the total deflections that are observed for a given span and will be close to the location that requires the shore tower to hold the minimum amount of load. In bridge erection, it is common for a contractor to lift a section of girder that creates a simply supported beam with a cantilever off on one of the sides as illustrated in Figure 4.7. For this case, the location of the maximum positive moment can be obtained from

Eq. 4.1 where L is the length of the simple span, b is the length of the cantilever, and $X_{M_{Max}}$ is the distance from the beginning of the simple span to the location of maximum positive moment. It should be noted that this equation, which can be derived from simple structural analysis, is only valid for uniform loading and was derived for a straight girder. The results from the equation are considered reasonable for curved girders with a radius of curvature larger than 300 feet.

$$X_{M_{Max}} = \frac{L}{2} \left(1 - \frac{b^2}{L^2} \right) \quad \text{Eq. 4.1}$$

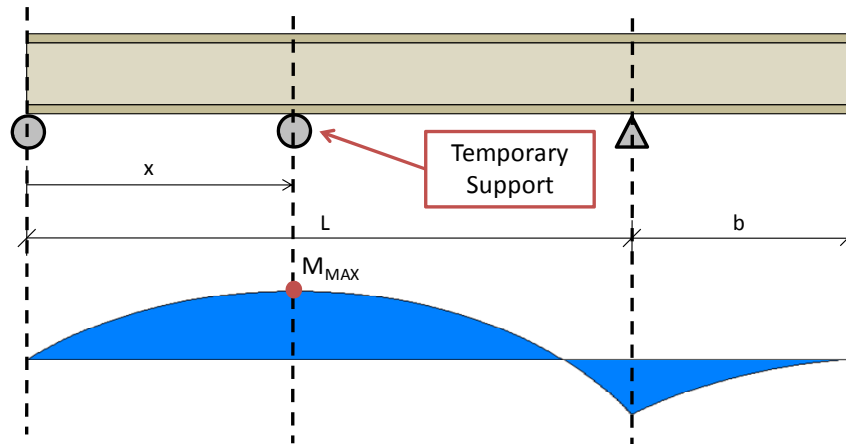


Figure 4.7: Location of Maximum Positive Moment; Simple Span with Cantilever

In Figure 4.8, a sample girder is shown with a span of 185 ft. and a cantilever on one side of 51 ft. The temporary support was varied ± 10 ft. and ± 20 ft. on either side of the location of maximum positive moment. The figure shows a plot of the girder reaction at the shore tower versus the normalized shore tower location (x/L). It can be seen that for this case, the lowest required vertical reaction for the shore tower coincides with the location of the maximum positive moment. Additionally, it can be seen that the shore tower reaction gradually increases as the shore tower position varies from the location of maximum positive moment.

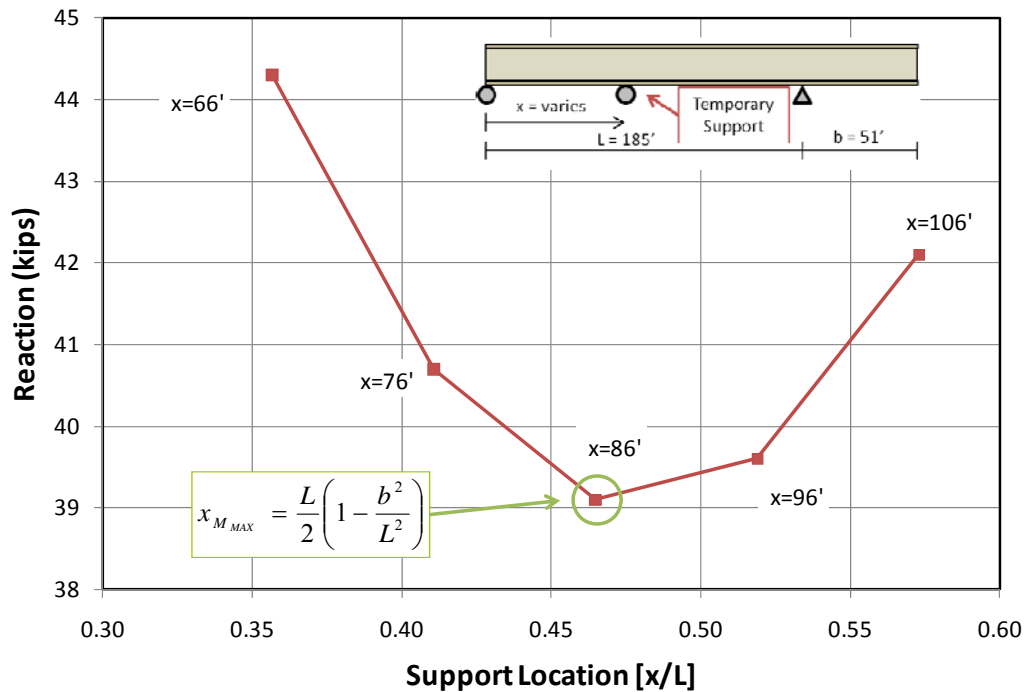


Figure 4.8: Vertical Reactions for Various Locations along a Girder [L =185' , b = 51']

In Figure 4.9, the out of plane displacements along the length of the sample girder shown in Figure 4.8 above are plotted for different shore tower positions. These displacements are based on first-order analyses. Although placing the shore tower at the maximum positive moment location in the simple span portion of the girder ($x_{M,Max} = 86$ ft.) will generally minimize the girder's displacements and necessary shore tower reaction, it may not always be the optimal position. Placing the shore tower at the maximum positive moment location in the simple span is a good starting point, but further analysis can determine whether or not there is a better place to put the shore tower depending on the individual girder stiffness and geometric properties. By placing the shore tower at 76 feet in the sample girder, the out-of-plane displacements along the simple span are actually lower at certain points along the girder than placing the shore tower at 86 feet. Yet, the displacements at the end of the girder are greater for the 76 foot location. In general, keeping the shore tower location within about $\pm 5\%$ of the

maximum positive moment location in the simple span will result in low displacements, a low vertical shore tower reaction, and reduce the second order effects.

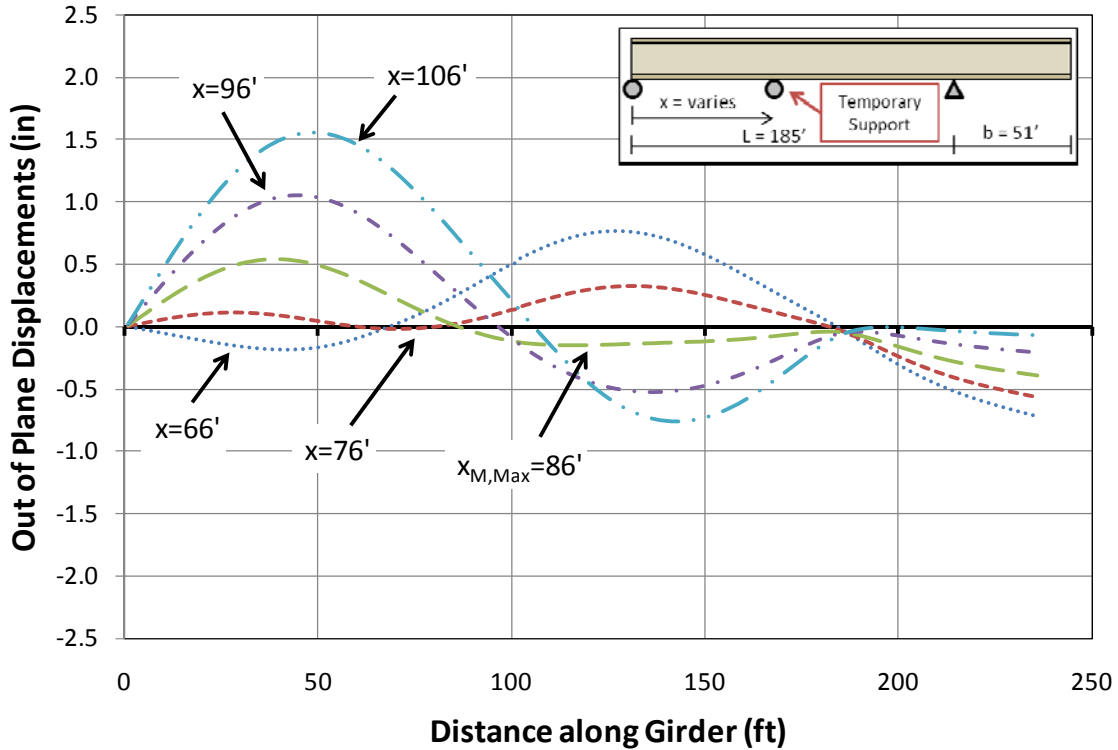


Figure 4.9: Top Flange Out-of-Plane Displacements for Various Shore Tower Positions

4.4.2 Holding Crane Location

The location of the holding crane affects the upward force that the crane must resist. Like shore towers, many non-structural criteria such as site access, construction methodology, and girder properties can affect the erector's ability to be able to place a holding crane in the optimal location. Yet, just like a shore tower, it is desirable to place a holding crane at the point of maximum positive moment between the two permanent supports. This location results in approximately the smallest value for the required crane load and will minimize both displacements and stresses on the girder cross section. Figure 4.10 shows first-order displacements for the same girder that was considered for the shore tower analysis shown in Figure 4.9 except that a holding crane was placed at

different locations instead of a shore tower. The holding crane force was set equal to the vertical reactions obtained from the shore tower analysis. It can be seen that by placing a holding crane at the location of maximum positive moment (86 ft.) the out-of-plane displacements are minimized along the length of the girder. Unlike shore towers, placing a holding crane at the location of maximum positive moment tends to give the lowest displacements and warping stresses of any location along the girder. Therefore, if possible it is recommended that holding cranes be placed at this location.

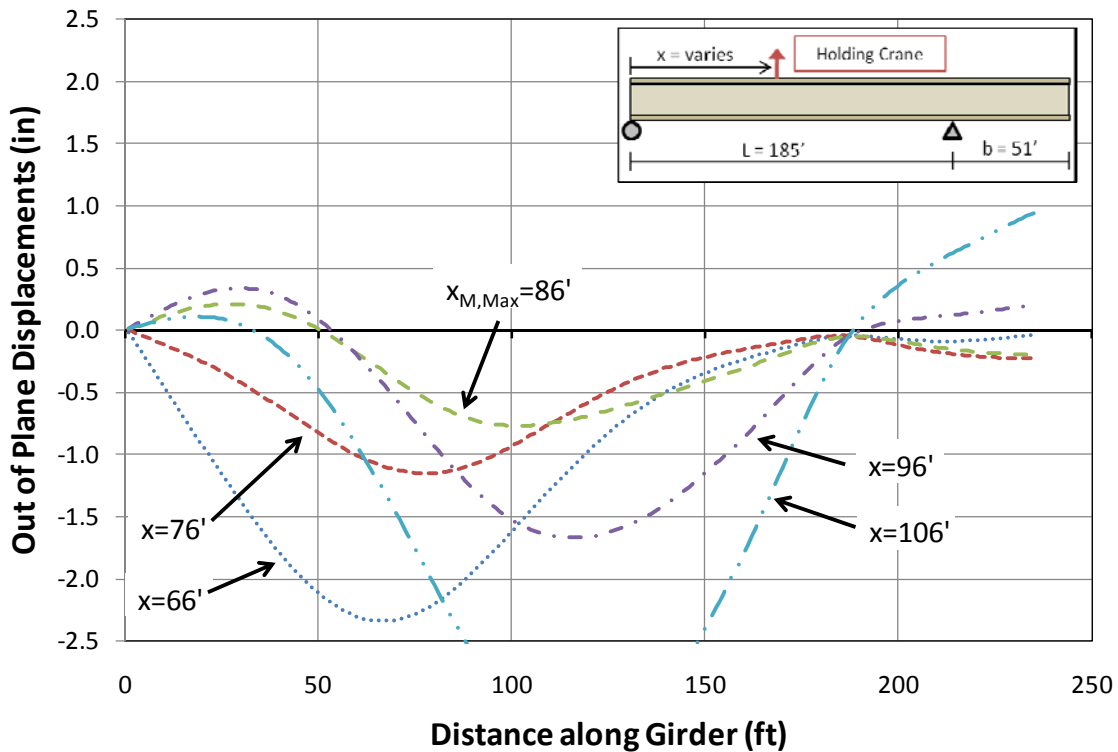


Figure 4.10: Top Flange Out-of-Plane Displacements for Various Holding Crane Locations

It should be noted that deviations in holding crane location on the order of $\pm 10\%$ may be acceptable assuming that the holding crane lifts with the optimal load. This concept is discussed more in the following section.

4.4.3 Holding Crane Lifting Load

Most modern cranes have the ability of measuring the magnitude of the lifting force in the crane. The load that the holding crane applies significantly affects the behavior of the girder being supported. It is recommended that the holding crane lift with a load that is equivalent to the reaction of a rigid support placed at the same location. This load allows the web of the girder to remain vertical and minimizes deformations helping with fit-up. Using a load in the holding crane that differs from this optimal load will not keep the girder's web vertical.

A geometrically linear analysis can be used to determine the reaction that would occur at a rigid support for a given location along the length of the girder. The difference in reactions for a first order analysis and second order analysis is small assuming the top flange of the girder is properly braced to prevent excessive rotations. It is important to model the horizontal curvature of the bridge when determining the reaction. Studies were conducted where the reaction at a given support was up to 10% higher if the curvature of the bridge was considered when compared to that of a straight bridge with the same properties. Accurately computing the reaction for a rigid support is crucial because small deviations from the optimal lifting load can result in large differences in out of plane deflections. Figure 4.11 shows three out of plane displacement plots of the same girder with different holding crane forces and a b_f/D ratio of about 1/3.5. By changing the holding crane force by only $\pm 5\%$, the maximum vertical displacements can increase by over an inch. For this particular case, the optimal load is 47.8 kips. In the field, the erector will often use the crane to lift up or lower the girder segment to assist in making the connection; however the optimum load provides a good starting point to expedite the erection.

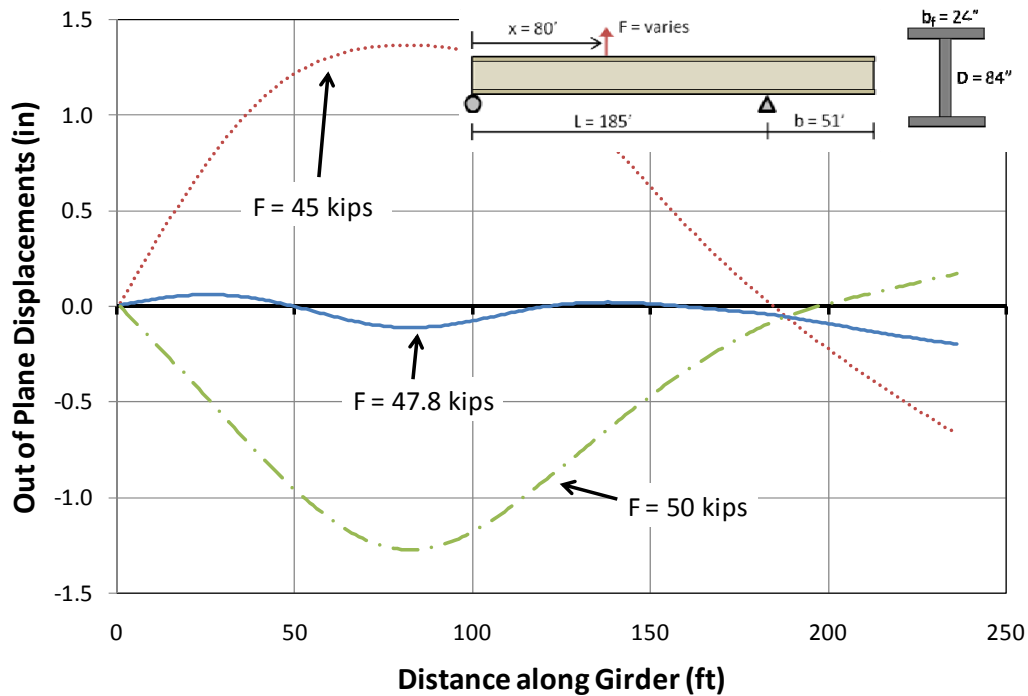


Figure 4.11: Out of Plane Deflections for Varying Crane Loads

As long as the optimal load is determined correctly and is used as the holding crane force, then the location of the holding crane becomes less important, although it is still desirable to place the holding crane close to the location of maximum positive moment. For the girder shown in Figure 4.12, the optimal place to put a holding crane is at 86 feet. As stated above, it is desirable to place the holding crane close to this location. If the holding crane were placed at 80 feet, the optimal lifting load is 36.5 kips. The b_f/D ratio for the girder in Figure 4.12 is $1/6$. This ratio was used to evaluate the girder slenderness at the AASHTO limit. Figure 4.13 shows the lateral displacements for the girder if it were held at 80 feet which is very close to the optimal holding crane location and with a force of 36.5 kips which is exactly what the optimal holding crane load is for the 80 foot location. This is the ideal case and shows the minimal girder deflections when using a holding crane for this specific case. Figure 4.14 shows the out of plane displacements down the length of the girder when close to the optimal lifting location but not using the optimal lifting load for the 80 foot location. It can be seen that even though

the holding crane is close to the optimal lifting location, with a lifting load just 3.5 kips higher than the desired load, the displacements are much larger than in Figure 4.13. Figure 4.15 shows the displacements along the girder when using the optimal lifting load but for a lifting location of 100 feet which is relatively far away from the optimal lifting location. Even though the lifting location is relatively far away from the optimal lifting location, the displacements along the length of the girder are not as severe as seen in Figure 4.14. Therefore, it can be concluded that the holding crane location can be varied more from the optimal value than the holding crane load. Maintaining the correct holding crane load is more critical for minimizing girder deformations.

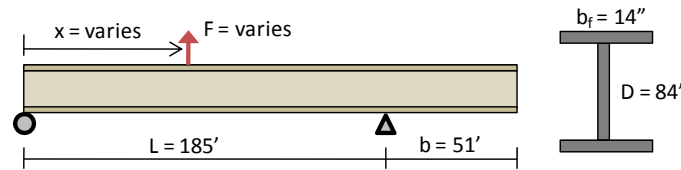


Figure 4.12: Geometry Used for Figure 5.18, Figure 5.19, and Figure 5.20

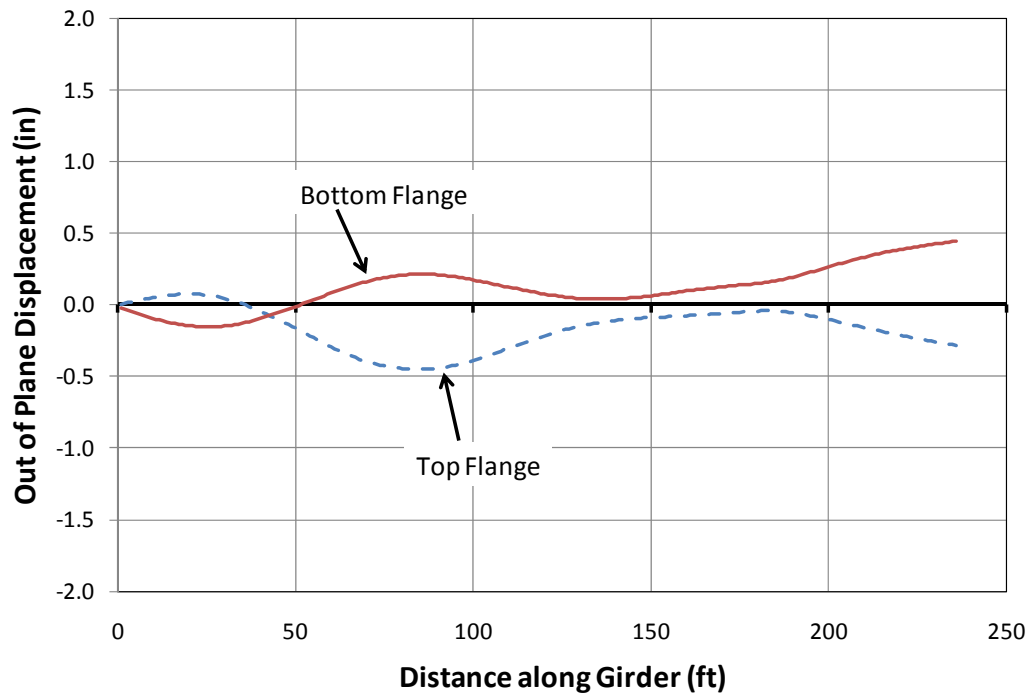


Figure 4.13: Optimal Load (36.5 kips) and Optimal Location (80 feet)

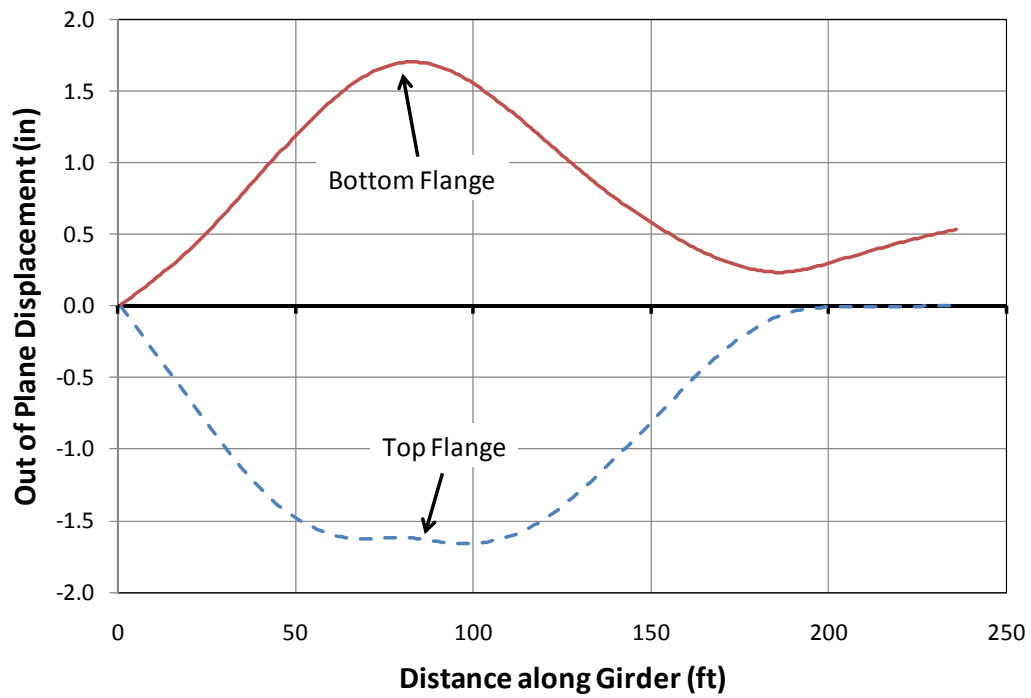


Figure 4.14: Non-Optimal Load (40 kips) and Optimal Location (80 feet)

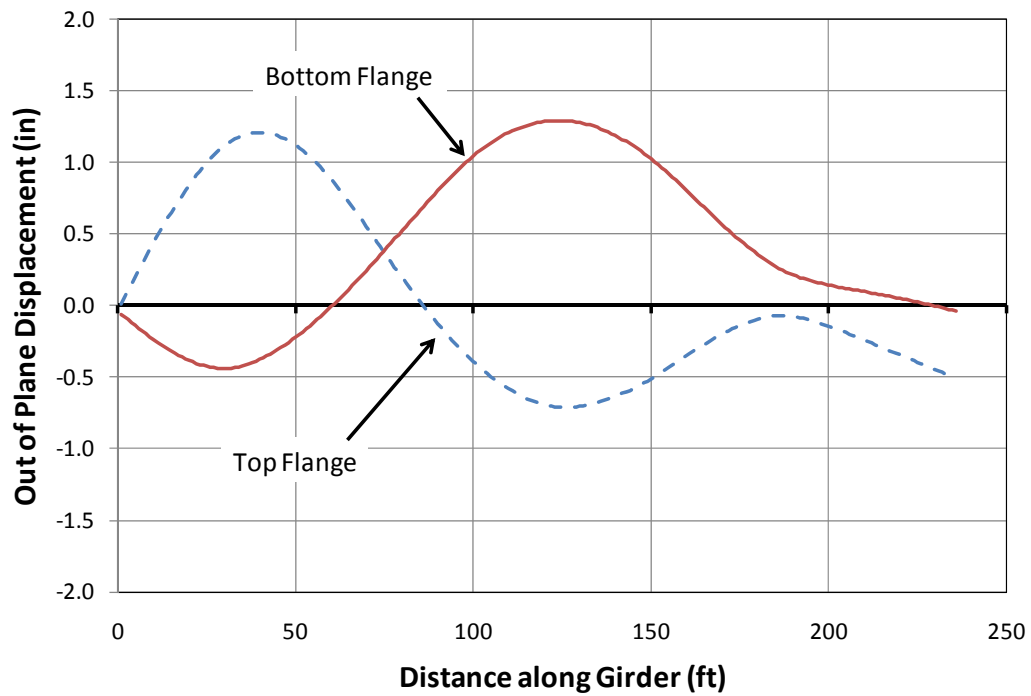


Figure 4.15: Optimal Load (37.6 kips) and Non-Optimal Location (100 feet)

4.5 LOAD HEIGHT EFFECTS

4.5.1 Shore Towers

Shore towers support a girder on the bottom flange. This is below the girder's center of gravity. Therefore, if the girder is not vertical and is not braced against rotation, the self weight will cause a disturbing moment that will tend to destabilize the girder. Figure 4.16 shows the disturbing moment that is created by the girder self weight when the girder is supported from below. Note that the effect of the self weight shown in Figure 4.16 depends on how the bottom flange is supported. If the bottom flange is supported at a single point in the middle of the flange (directly below the web), or is supported by a bearing with high rotational flexibility, then the girder will rotate about the middle of the flange as demonstrated by the left diagram in Figure 4.16. For this case, the self weight will generate a destabilizing moment for any initial rotation of the girder. However, if the bottom flange of the girder is supported over its full width by a stiff support as demonstrated by the center and right diagrams in Figure 4.16, then the girder will rotate about the edge of the bearing pad. For this case, the self weight will generate a restoring moment as seen in the center diagram until the girder has a sufficient rotation so that the center of gravity is located outside of the bearing pad as shown by the right diagram in Figure 4.16. For the analyses conducted herein, it was assumed that the girder will tip about mid-width of the flange, as this represent the worst case for stability.

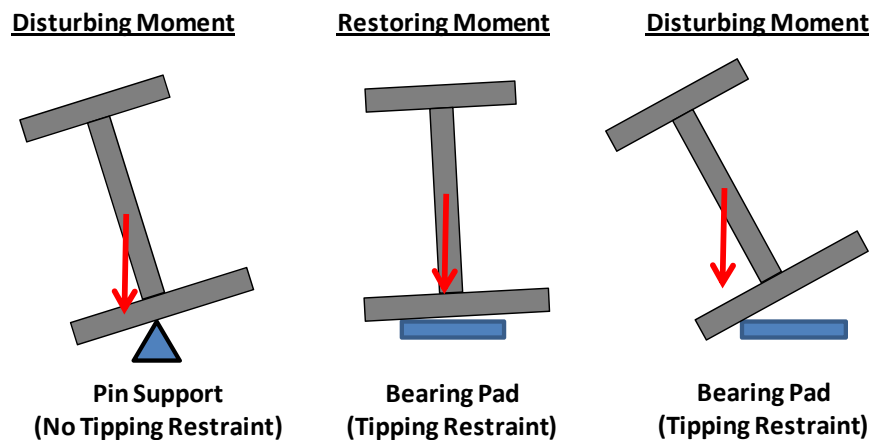


Figure 4.16: Disturbing Force Caused by a Lack of Bracing on the Top Flange

Because the disturbing force is only present after the girder has rotated due to its own self weight, it can only be detected by a second-order analysis that includes geometric, non-linear effects. A number of analyses were conducted using both first-order and second order analysis. When comparing results, the bending stresses were generally very similar for first- and second-order analyses. However, the warping stresses and out-of-plane displacements were typically significantly different. This effect can be seen in Figure 4.17 where the lateral displacements are graphed down the length of the girder for both the first-order and second-order analyses.

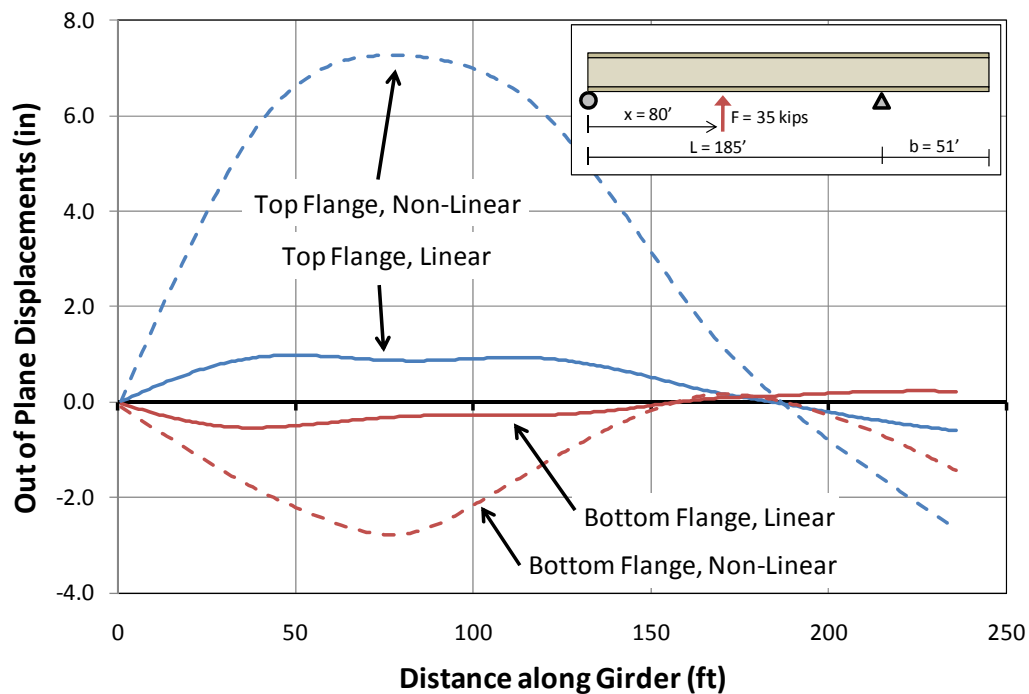


Figure 4.17: Linear and Non-Linear Displacements along a Girder for a Girder with a Disturbing Force

The large lateral deflections predicted by the nonlinear analysis emphasize the destabilizing effect of the girder self weight when the girder is supported at the bottom flange. As noted above, this analysis assumed the most severe condition in which the girder is supported at the middle of the flange by a pin support that offers no tipping restraint. Tipping restraint, if present, reduces the second-order lateral displacements.

These lateral displacements can also be minimized, of course, by bracing the girder against rotation at the location of the shore tower. Taking advantage of tipping restraint requires a detailed second-order analysis that accurately models the bottom flange support conditions. Providing bracing for the girder at the shore tower precludes the need for such an analysis and therefore may be the more straightforward and certain approach for assuring girder stability.

4.5.2 Holding Cranes

Holding cranes generally support a girder on the top flange and the girder essentially hangs from the support. The support is therefore above the girder's center of gravity. Unlike shore towers, holding cranes do not have the ability to brace the system in the translational directions orthogonal to the lifting load or in any of the rotational directions. As the girder begins to rotate, the holding crane force creates a restoring moment that opposes the rotation, as illustrated in Figure 4.18.

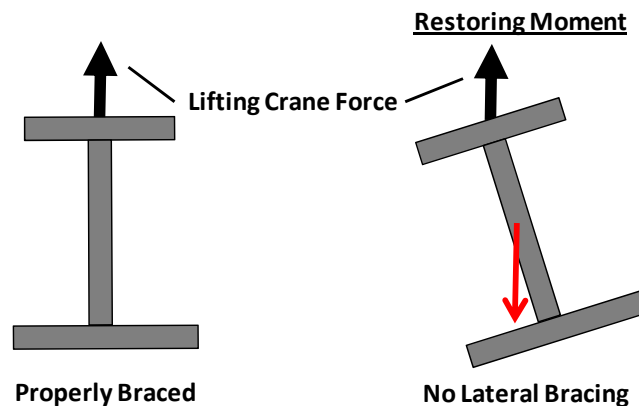


Figure 4.18: Restoring Force Caused by Lack of Bracing

Because the restoring force is only present after the girder has rotated, a second-order analysis is needed to account for this effect. As was the case with the shore tower, comparing first- and second-order analyses of girders supported by a holding crane showed little difference in the predicted bending stresses. However, there were large differences in the warping stresses and out-of-plane displacements predicted by the first-order versus second-order analyses. This effect is demonstrated in Figure 4.19 where the

out-of-plane displacements are plotted along the length of a girder for both a linear (first-order) and non-linear (second-order) analysis. Note that the out-of-plane displacements for the second-order analysis are smaller than for the first-order analysis. This demonstrates the stabilizing effect of supporting the girder from above.

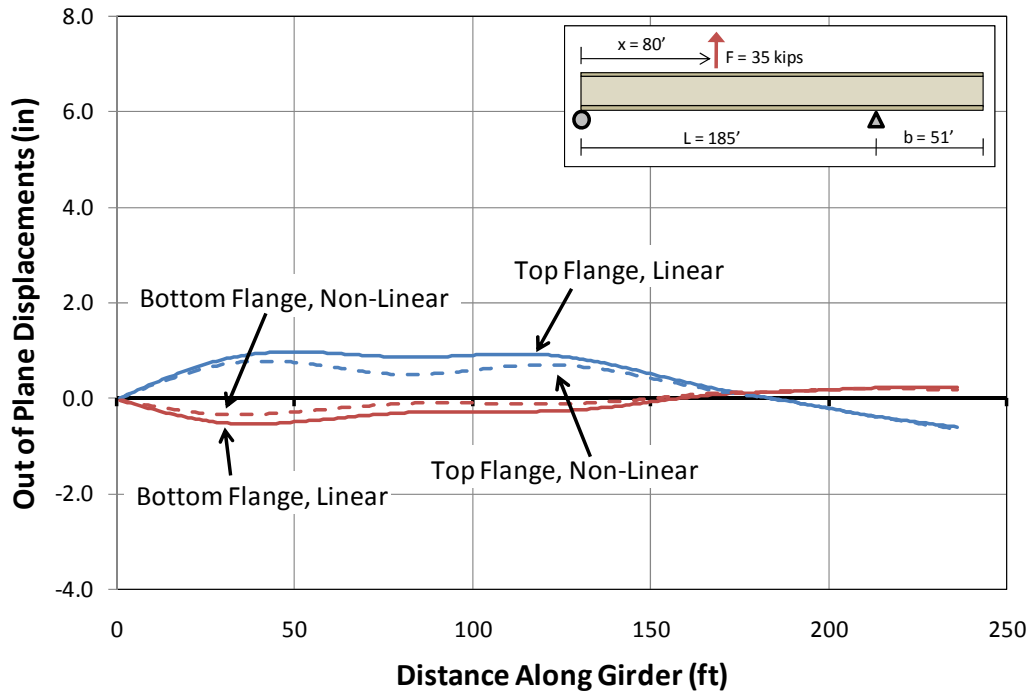


Figure 4.19: Displacements along a Girder Supported by a Holding Crane based on Linear versus Nonlinear Geometry Analysis

As noted above, the restoring and disturbing effects that are generated as a result of the girder support conditions can only be calculated using a second-order, geometric non-linear analysis. Therefore the linear analysis done on both the top flange and bottom flange loadings should be the same for both the shore tower and holding crane because both were loaded with a 35 kip load. In Figure 4.20 and Figure 4.21, the out-of-plane displacement results shown for the shore tower and holding crane analyses are amplified. It is clear from these plots that the first-order displacements are identical for the two cases. It is also again clear that the second-order displacements are smaller than the first-order displacements for the holding crane, in sharp contrast to the shore tower.

Supporting a girder by a holding crane therefore provides an intrinsic advantage over a shore tower in regard to girder stability.

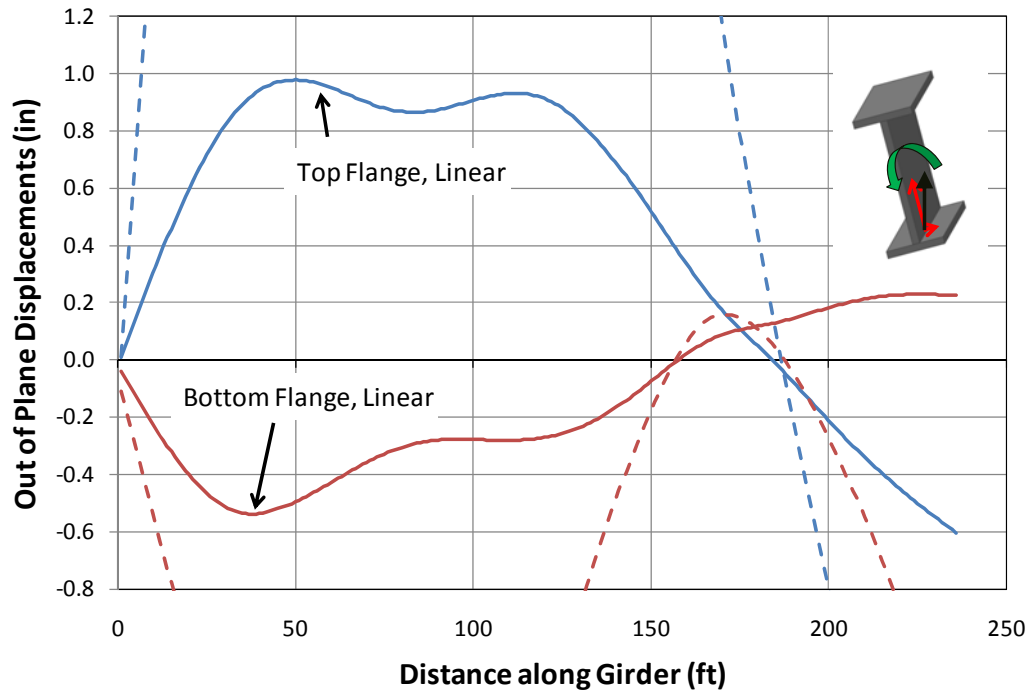


Figure 4.20: Displacements along a Girder Supported by a Shore Tower based on Linear versus Nonlinear Geometry Analysis - Amplified Displacement Scale

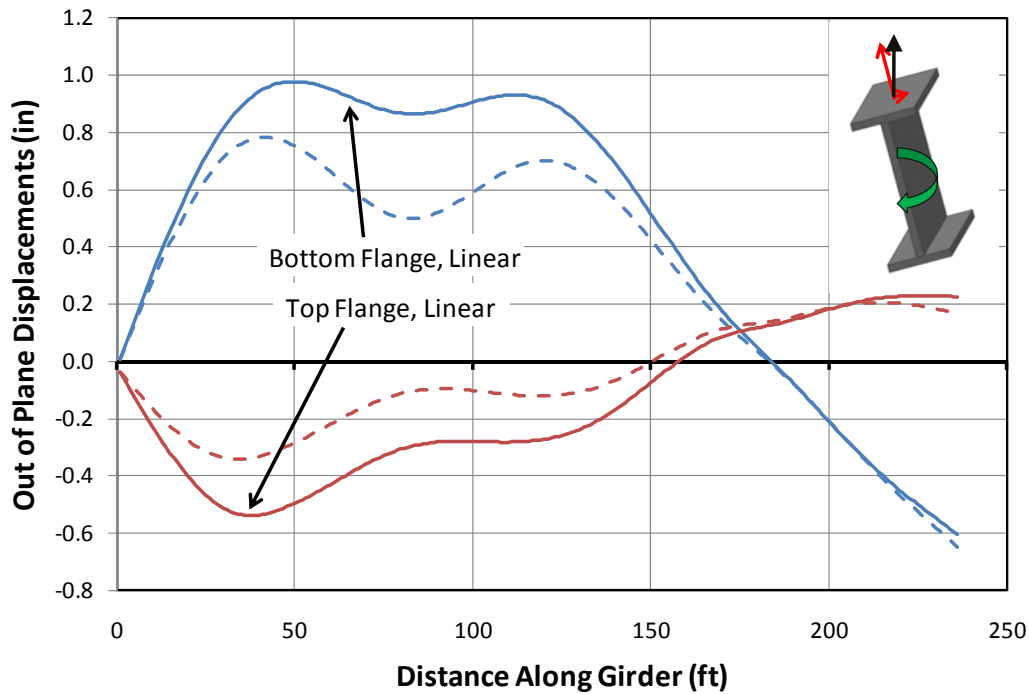


Figure 4.21: Displacements along a Girder Supported by a Holding Crane based on Linear versus Nonlinear Geometry Analysis - Amplified Displacement Scale

4.6 CRITICAL STAGES DURING CONSTRUCTION

From a stability perspective, the most critical stage in a bridge's life is typically during erection and during casting of the concrete bridge deck. During erection, the bridge is usually only partially braced. Therefore, shore towers and holding cranes are commonly required to safely erect the bridge. All erection stages should be analyzed without temporary supports to determine if excessive deformations or stresses occur and if a temporary support is required.

One of the more critical stages during construction is when a single girder segment has been lifted for a particular cross section along the length of the bridge as seen in Figure 4.22.



Figure 4.22: Single Girder Segment Lifted for a Particular Cross Section

Because there are no adjacent girder segments in place, there is no bracing along the length of the single segment. As a result, the unbraced length of the single girder segment is significantly longer than the rest of the bridge which is usually the critical stage for girder stability. Once the second girder is erected and some of the cross frames are connected, the two girder system is much more stable compared to the single girder system. Even with the added stability, each erection stages should be checked to determine how long the holding crane is necessary. Figure 4.23 shows a bridge system with a temporary support located at 80 feet from the left end. Lateral deflections are plotted for the one, two, three, and four girder systems. It can be seen that after the second girder is erected, the bridge's lateral deflections are small, which is an indication that the system is stable. Therefore, this shows the flexibility of a single girder system and the importance of checking the single girder system for stability. It should also be noted that the stability of the system without a temporary support should be analyzed before assuming the girder system is stable after the second girder is erected.

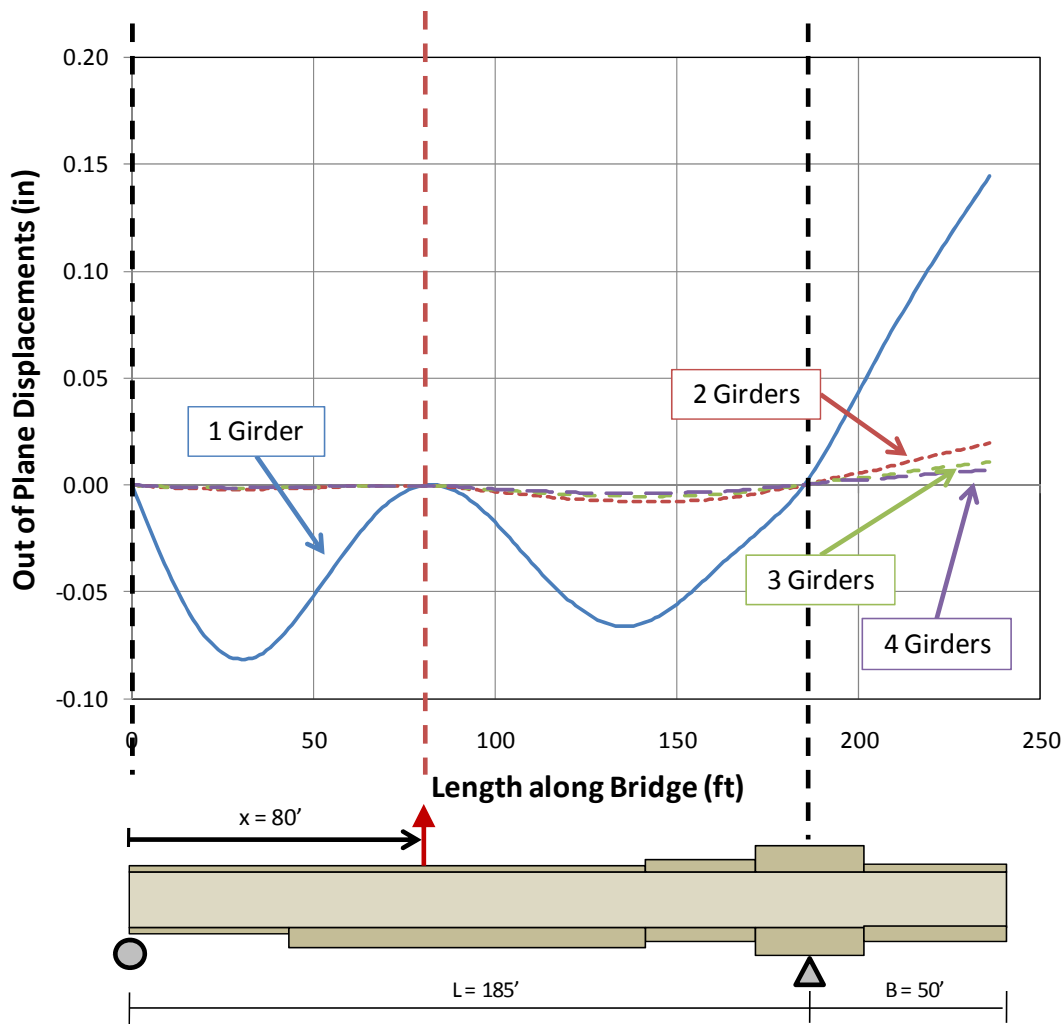


Figure 4.23: One, Two, Three, and Four Girder Erected Systems – Temporary Support at 80'

Another critical stage during construction occurs during the first concrete placement stage on a span. When the concrete is initially poured on a span, the concrete is essentially a fluid that acts as a large dead load on the system and provides no restraint. Once the concrete begins to cure, the top flange of the girder gains significant lateral and torsional bracing. In some irregular systems, the concrete pour can be subdivided and spaced out over multiple days so that the bracing effect of the concrete can be used to assist in stabilizing the girder system. However, care should be taken in these cases to consider the impact of the partially composite stiffness on the girder deflections to ensure

good ride quality in the finished bridge. The program UT Bridge has the ability to model the contributions of early age concrete.

4.7 CONCLUSIONS

The stability of partially erected bridges can be difficult to assess because of the limited presence of bracing and uncertainty in support conditions. Because of the lack of appropriate analytical tools, erection engineers often rely heavily on experience and on rules-of-thumb when developing an erection plan for a bridge. Guidelines and tools based on research are needed to help both contractors and design engineers better understand the behavior of curved I-girder bridges in the partially constructed state.

Common practices that are used for additional support and bracing during the partially constructed state include temporary shore towers and holding cranes. Although shore towers are desirable because they prevent translation of the girder in two directions, it is important to make sure that the top flange of the girder is properly braced to prevent undesirable twist of the cross sections. Additionally, shore towers can be difficult to use because they require their own engineering to ensure that they can withstand the load of the bridge and require adequate space below the bridge to be placed on. In areas of heavy traffic, care must be taken to protect the shore tower from potential vehicle impact that could jeopardize the safety of the partially erected bridge. In many cases, holding cranes can sometimes be more desirable due to their ability to be used only when needed and the ability to minimize time over obstacles such as busy roads or water.

This chapter described a series of parametric finite element studies on issues related to the use of shore towers and holding cranes. Many geometric parameters were varied as well as the stiffness of the top flange bracing used for the shore towers and the load parameters used for the holding cranes. Based on analyses of both the shore towers and the holding cranes, it suggested that they are placed close to the position of maximum positive moment. When using a 3-D finite element analysis software package, this position can often occur at the location of the highest stresses. Placing a shore tower at the position of highest moment allows the shore tower to be designed for close to the minimum amount of load and will minimize the girder bending/warping stresses as well

as the girder displacements. When using a holding crane, it is recommended to lift with a value equal to the reaction of a rigid vertical support at the same position. This will keep the web of the cross section vertical and will minimize the second order effects that occur due to twisting of the cross section. It is important to keep the load in a holding crane very close to the reaction of a rigid support placed at the same position because a small deviation from this load can significantly increase both the warping/bending stresses as well as increase the deflections of the girder. As long as the proper lifting load is used for a given location of the holding crane, the location of the holding crane can vary somewhat from the location of maximum moment without causing large changes in the bending/warping stresses and the displacements.

Due to load height effects associated with shore towers and holding cranes, it is important to consider second-order effects when conducting an analysis. Because shore towers are supported on the bottom flange, as the girder cross section rotates, the girder self weight can cause a disturbing moment that will tend to destabilize the girder at the support location. This can be prevented if the top flange of the girder is properly braced against rotation at the location of the shore tower. Holding cranes, on the contrary, typically support the girder from above at the top flange. As a result, as the girder cross section rotates, the girder self weight causes a restoring moment that tends to stabilize the girder at the location of the holding crane support. With a holding crane, the predicted displacements will typically be smaller than for the case with a second-order analysis.

Some of the most critical stages of construction occur when a single girder section is lifted or during the first concrete placement on a given span. Both of these stages are critical due to the minimal amount of bracing. Therefore, it is typically desirable to use a shore tower or holding crane on partially erected girders to temporarily brace the system until additional bracing can be provided to the system. In general though, it is good practice to check stability of a system anytime support conditions or bracing is changed or large additional loads are applied to the system.

CHAPTER 5

Conclusions and Recommendations

5.1 INTRODUCTION

The research reported in this thesis was conducted as part of TxDOT Research Project 0-5574 on *Curved Plate Girder Design for Safe and Economical Construction*. This project focused on a number of issues involved in assessing the safety and serviceability of curved steel I-girder bridges during construction. More specifically, this project considered structural safety and serviceability during three critical stages of construction: girder lifting, erection sequencing, and concrete deck placement.

The overall scope of research in TxDOT Project 0-5574 included:

- Two field monitoring studies.
- Parametric studies focused on developing a simple methodology to predict the buckling capacity of prismatic and non prismatic girders during lifting. These studies included eigenvalue buckling analyses as well as nonlinear geometric analyses.
- Parametric studies focused on developing lifting location guidelines for prismatic girders to prevent excessive displacements and rotations during lifting.
- A nationwide survey of erectors and contractors to establish industry standards and preferred practices.
- Parametric studies focused on determining when temporary supports are necessary during erection sequencing.
- Development of two analysis tools: UT Lift and UT Bridge.

This thesis focused on the parametric study on girder lifting using nonlinear geometric analyses as well as the parametric study looking at the stability of partially constructed bridges and the necessity and behavior of temporary support systems. In addition to the parametric studies, this thesis also provided the reader with a literature

review of work done in recent years as well as a comprehensive summary of work previously done on this curved girder project. The following sections provide a summary of the key conclusions from both of the parametric studies

5.2 NON-LINEAR ANALYSIS OF LIFTING OF CURVED STEEL I-GIRDERS

- Eigenvalue buckling analyses can provide an accurate prediction of instability for a straight girder during lifting. For curved girders, on the other hand, eigenvalue buckling analysis is less useful. The eigenvalue provides a general indication of the load to cause instability of a curved girder. However, by the time the load corresponding to the eigenvalue is reached for a curved girder, very large lateral deflections and rotations may have already occurred. The eigenvalue, by itself, may not be a reliable indicator of the potential for strength or serviceability problems during lifting of curved I-girders.
- As an alternative to eigenvalue buckling analyses, computing the rotations of a curved girder during lifting can provide an improved approach for assuring safety and serviceability. Based on a nationwide survey of bridge erectors, a rotation limit of 1.5 degrees at the end of the girder is suggested to avoid problems with connecting the lifted girder to previously erected portions of the bridge. The analyses conducted herein suggest that this limit will generally be reached before the eigenvalue is reached for curved girders.
- It is recommended that in planning a lift of a curved girder that will not result in safety or serviceability problems, engineers should limit girder rotations to approximately 1.5 degrees and also check the eigenvalue. For girders with any significant curvature, the rotation limit is likely to control. However, for girders with only slight curvature, the eigenvalue is likely to provide a useful prediction of instability.
- For curved girders with a flange width to depth ratio (b_f/d) close to the current AASHTO limit of $1/6$, it may not be possible to lift these girders in

a manner that will limit end rotations to 1.5 degrees, due to the low lateral and torsional stiffness of these girders. Consequently, designing girders with b_f/d near 1/6 can result in significant problems during lifting, and should be approached with great caution. With very slender girders, improved stability during girder lifting can be obtained by using two separate cranes with two lifting bars.

5.3 PARTIALLY CONSTRUCTED BRIDGES

- To add additional support for partially constructed bridges, erectors often use temporary supports such as holding cranes and shore towers.
- It is recommended that both shore towers and holding cranes be placed at location of maximum positive moment in the girder. Placing a temporary support at this location minimizes the amount of load that a shore tower needs to be designed for as well as minimizing the lifting load required of the holding crane. In addition, this location minimizes both the bending and warping stresses as well as the displacements of the girder.
- It is important to lift with a load in a holding crane that is close to the reaction that would develop in a rigid support placed at the same location. Lifting with loads only slightly different than this value can cause displacements and stresses to increase at a greater rate than placing the holding crane away from the location of maximum moment.
- There are load height effects that are associated with temporary supports. When using a shore tower, if the top flange is not properly braced against rotation, a disturbing moment can form causing additional second-order rotations and stresses on the cross section. Holding cranes on the other hand typically support the girder on the top flange and create a restoring moment on the cross section which reduces both the stresses and displacements. Therefore it is typically conservative to neglect second-order effects in cases with holding cranes.

- Without considering a second-order analysis, the computed displacements and stresses will be similar for both shore towers and holding cranes.

APPENDIX A

Parametric Study Summary for the Lifting of Curved Steel I-Girders

As described in Chapter 3, an extensive parametric study was conducted to study the non-linear behavior of horizontally curved steel I-girders during lifting. In this study, two support points were utilized to represent a girder being lifted with two cranes or with one crane and a spreader bar. In order to complete the study, many finite element models were created in ANSYS 11.0 (2007) and a non-linear geometric analysis was conducted to determine displacements, stresses, and rotations. This appendix supplements Chapter 3 and provides a summary of the various analysis results to support the observations and conclusions in Chapter 3. The parameters in bold under the *Parameters and Range* section in each study signify that the range has been changed in comparison to the previous study.

A.1 PARAMETRIC STUDY SUMMARY

The following summary and results are organized in order in which they were completed. It should be noted that each study has some similar characteristics, which are described in the study summaries below. The parameters that were varied and kept constant are also noted.

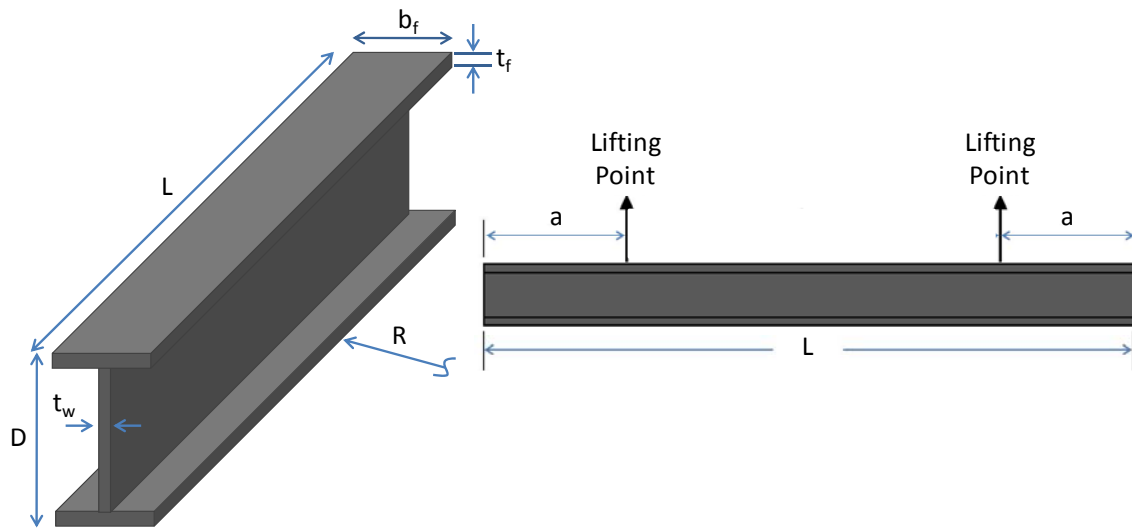


Figure A.1: Parameter Definitions

A.1.1 Study One

- Prismatic Girder: $b_f/D = 0.15 - 0.33$: $a/L = 0.15 - 0.34$: $R = 500' - 8000'$

A.1.1.1 Summary

For the first study, the slenderness ratio (b_f/D), lifting location (a/L), and the radius of curvature (R) are varied. The out of plane displacements for the top of the girder are monitored at the end of the girder and at mid-span. The eigenvalues are also recorded.

A.1.1.2 Parameters and Range

- Varied:
 - $b_f/D = 0.15$ ($\sim 1/6$) : $1/4$: $1/3$
 - $t_f = 0.5''$: $0.75''$: $1''$
 - $a/L = 0.15$: 0.21 : 0.34
 - $R = 500'$: $1000'$: $8000'$ (\sim straight)
- Constant:
 - $L = 125'$

- $D = 60''$
- $t_w = 0.5$

A.1.1.3 Results

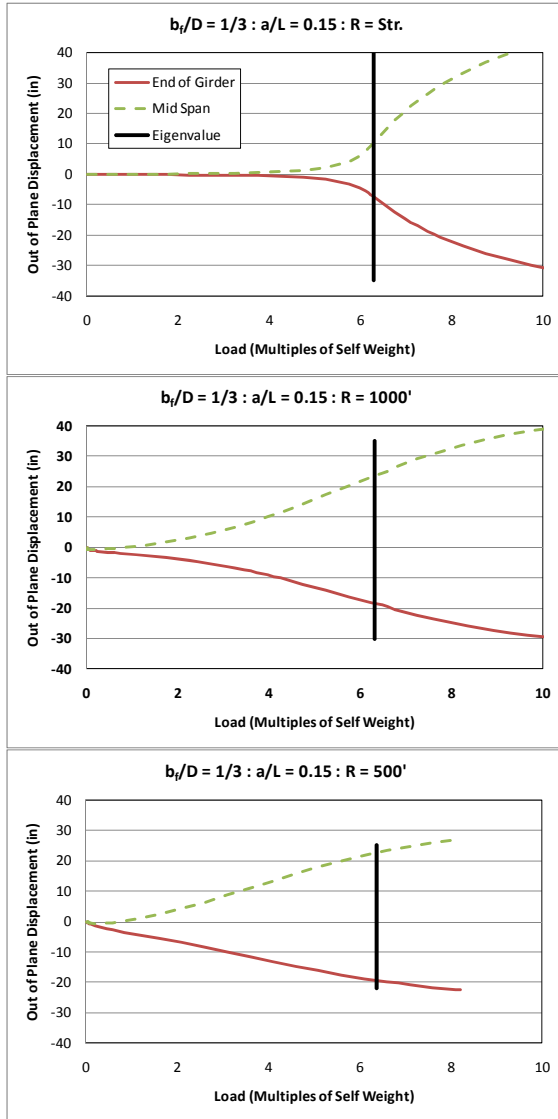


Figure A.2: $b_f/D = 1/3 : a/L = 0.15$:

$R = \text{Varies}$

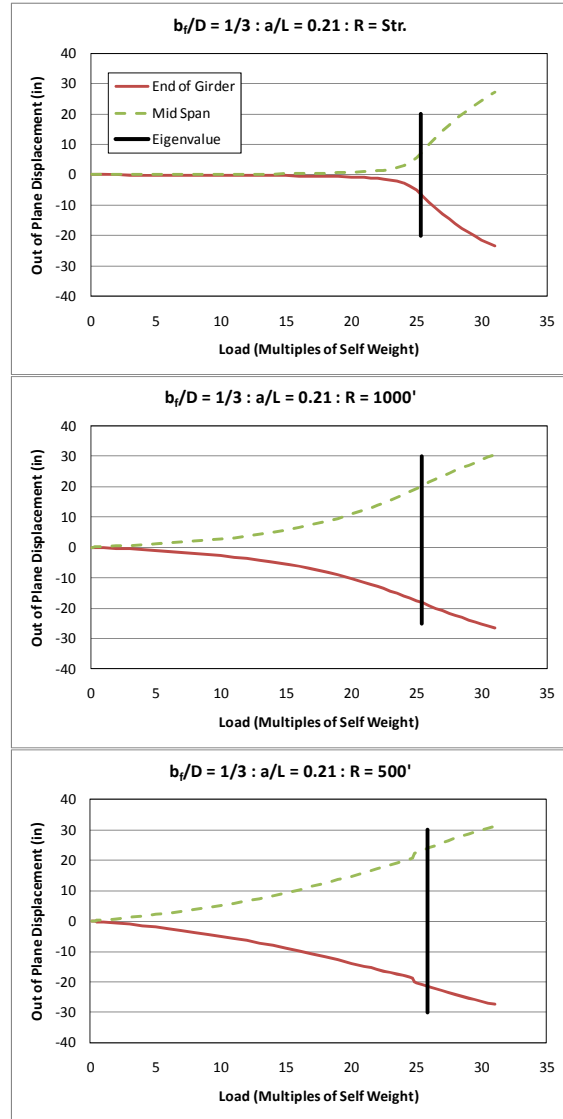


Figure A.3: $b_f/D = 1/3 : a/L = 0.21$:

$R = \text{Varies}$

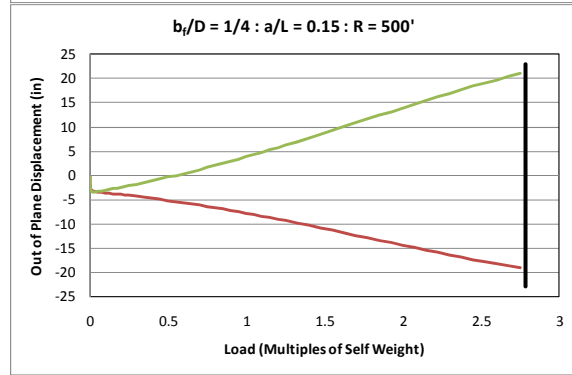
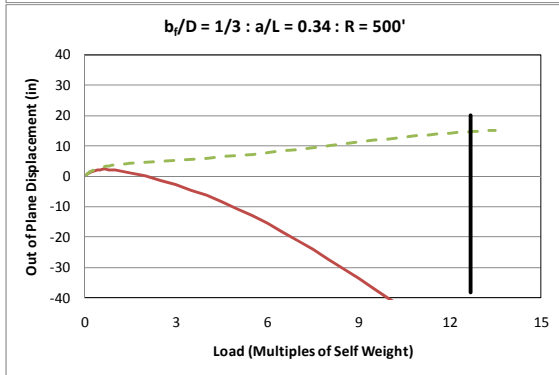
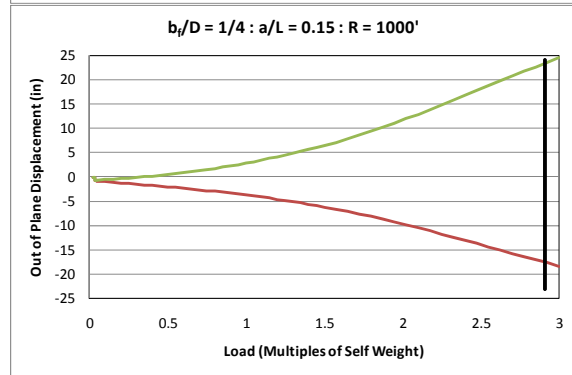
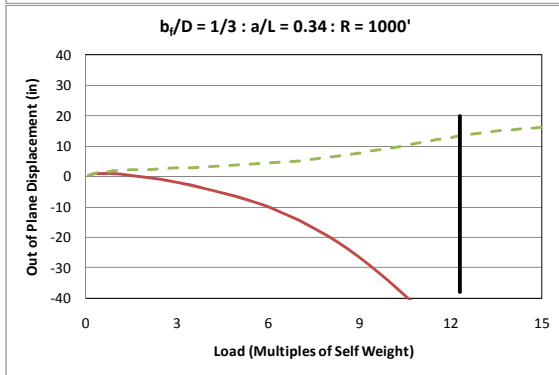
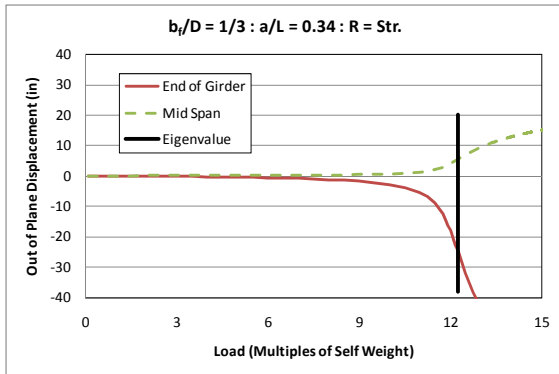


Figure A.4: $b_f/D = 1/3 : a/L = 0.34 :$

R = Varies

Figure A.5: $b_f/D = 1/4 : a/L = 0.15 :$

R = Varies

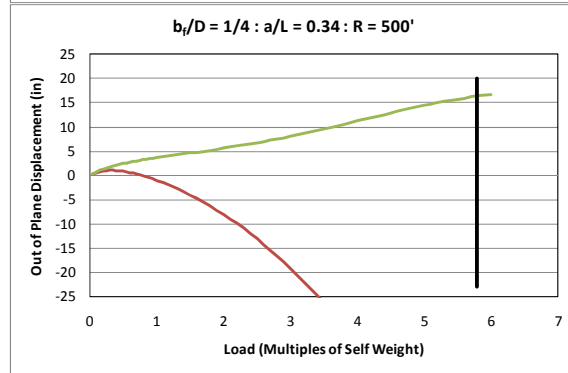
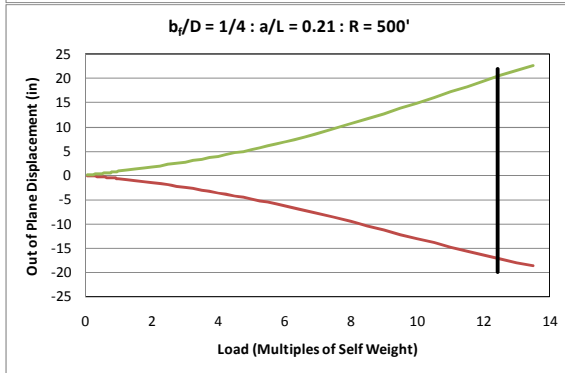
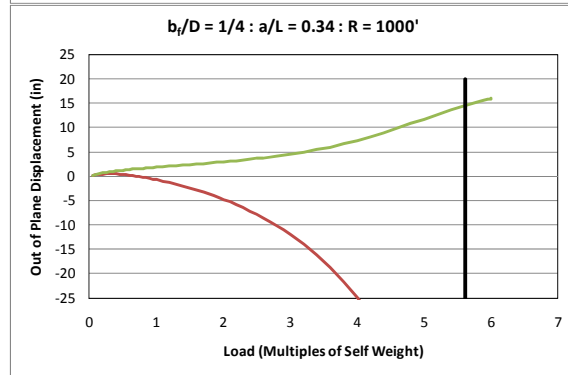
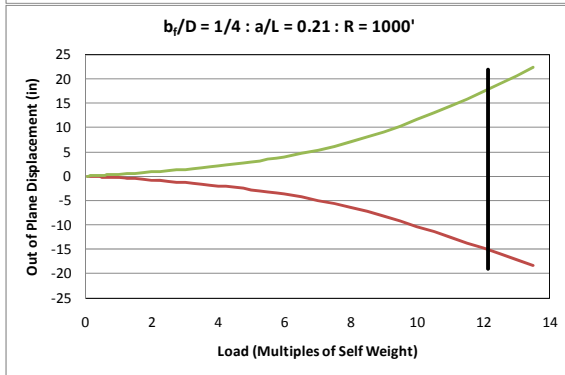
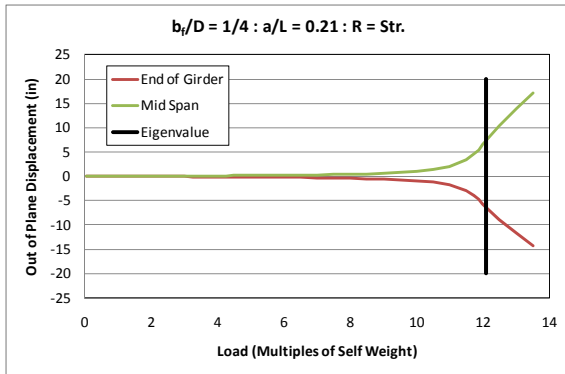


Figure A.6: $b_f/D = 1/4 : a/L = 0.21:$

R = Varies

Figure A.7: $b_f/D = 1/4 : a/L = 0.34:$

R = Varies

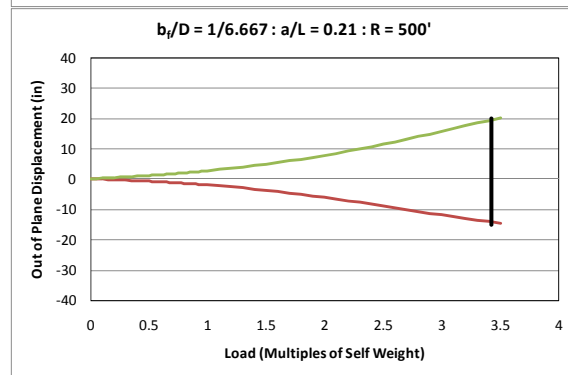
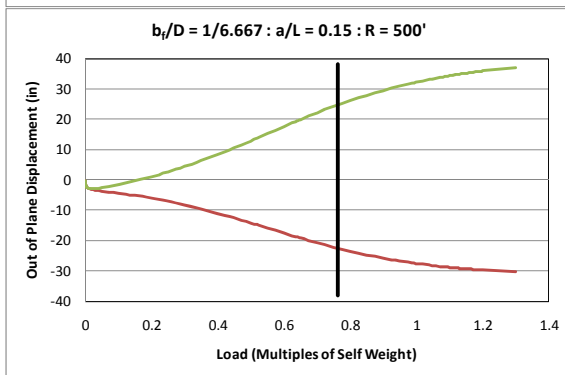
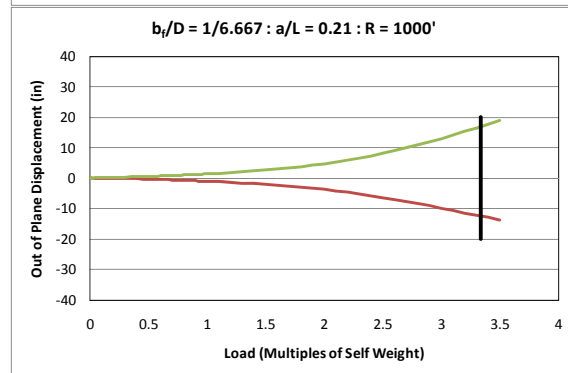
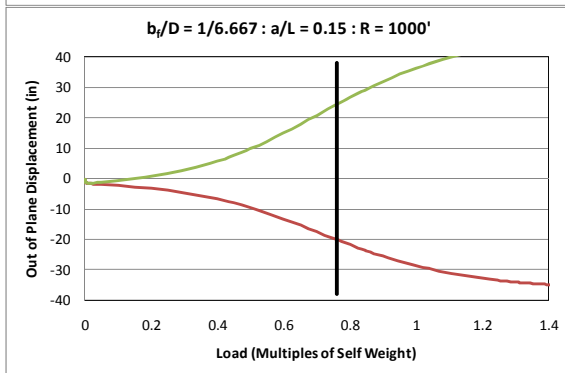
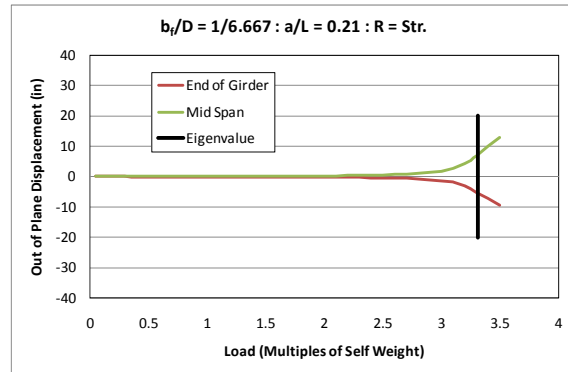


Figure A.8: $b_f/D = 1/6.667 : a/L = 0.15 :$

R = Varies

Figure A.9: $b_f/D = 1/6.667 : a/L = 0.21 :$

R = Varies

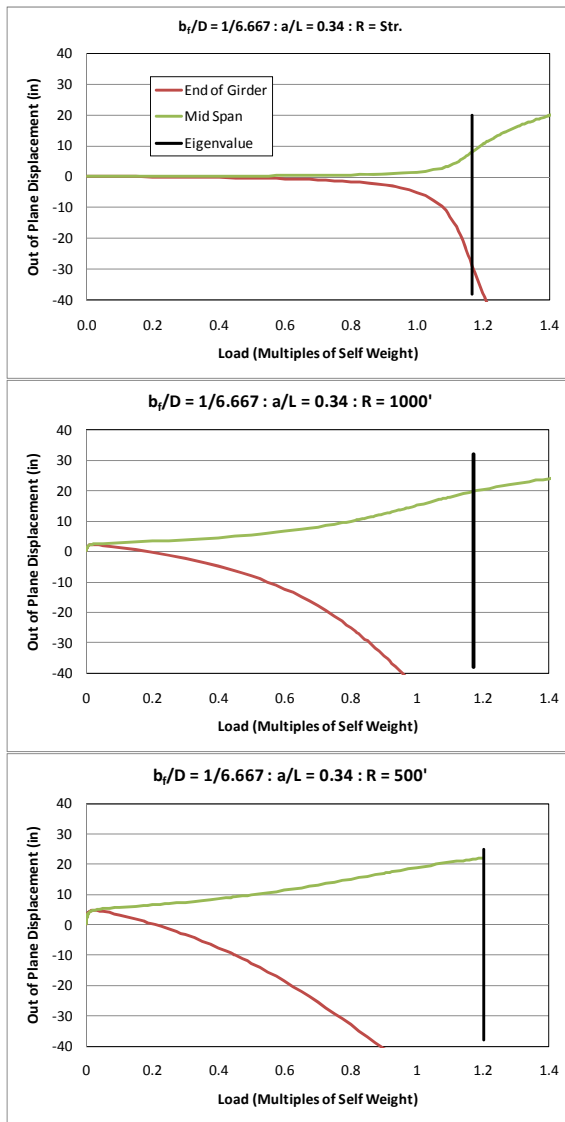


Figure A.10: $b_f/D = 1/6.667 : a/L = 0.34:$

R = Varies

A.1.2 Study Two

- Prismatic Girder: $b_f/D = 0.15 - 0.33 : a/L = 0.2 - 0.3 : R = 500' - 8000'$

A.1.2.1 Summary

In the second study, the a/L range is decreased compared to that of the first study. The top and bottom flange is monitored at the midspan and at the end of the girder for out of plane displacements and rotations instead of just at the top flange. The eigenvalue is also recorded as well as the yield limit (load resulting in an in-plane stress of 50 ksi). Timoshenko's lateral torsional buckling load limit is determined (using $L_b = L$ and $C_b = 1$) as well as the rotational load limit (load resulting in a rotation of 4 degrees or 0.6981 rad, set arbitrarily).

A.1.2.2 Parameters and Range

- Varied:
 - $b_f/D = 0.15$ ($\sim 1/6$) : $1/4$: $1/3$
 - $t_f = 0.5''$: $0.75''$: $1''$
 - $a/L = \mathbf{0.20 : 0.25 : 0.30}$
 - $R = 500'$: $1000'$: $8000'$ (\sim straight)
- Constant:
 - $L = 125'$
 - $D = 60''$
 - $t_w = 0.5$

A.1.2.3 Results

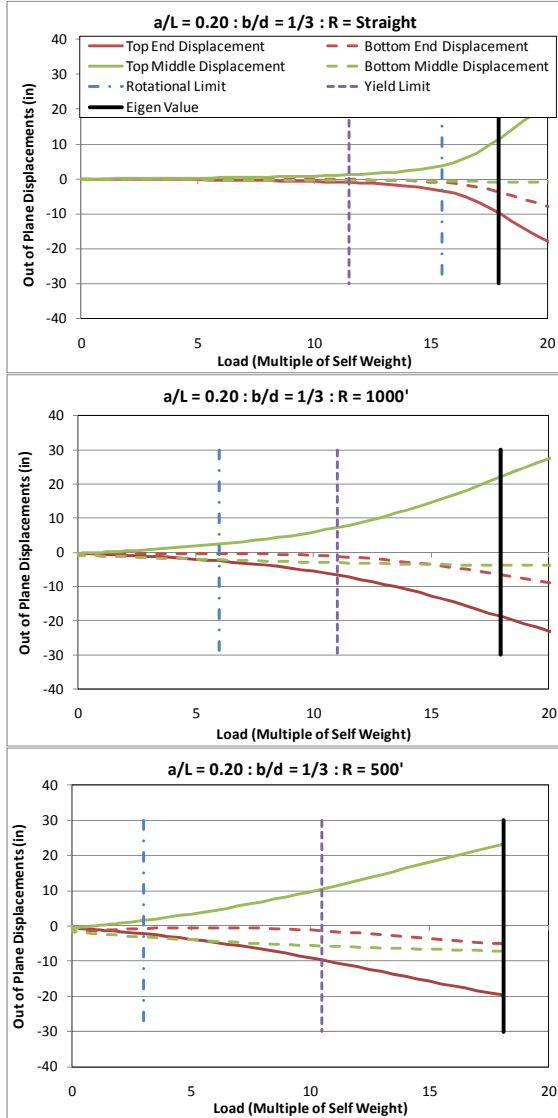


Figure A.11: $b_f/D = 1/3 : a/L = 0.20:$

$R = \text{Varies}$

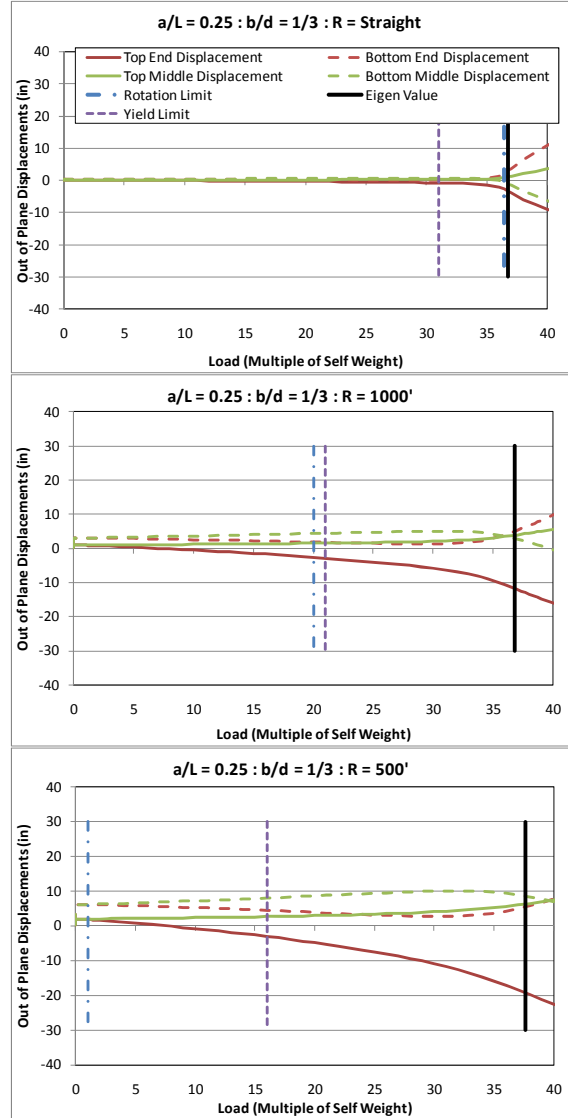


Figure A.12: $b_f/D = 1/3 : a/L = 0.25:$

$R = \text{Varies}$

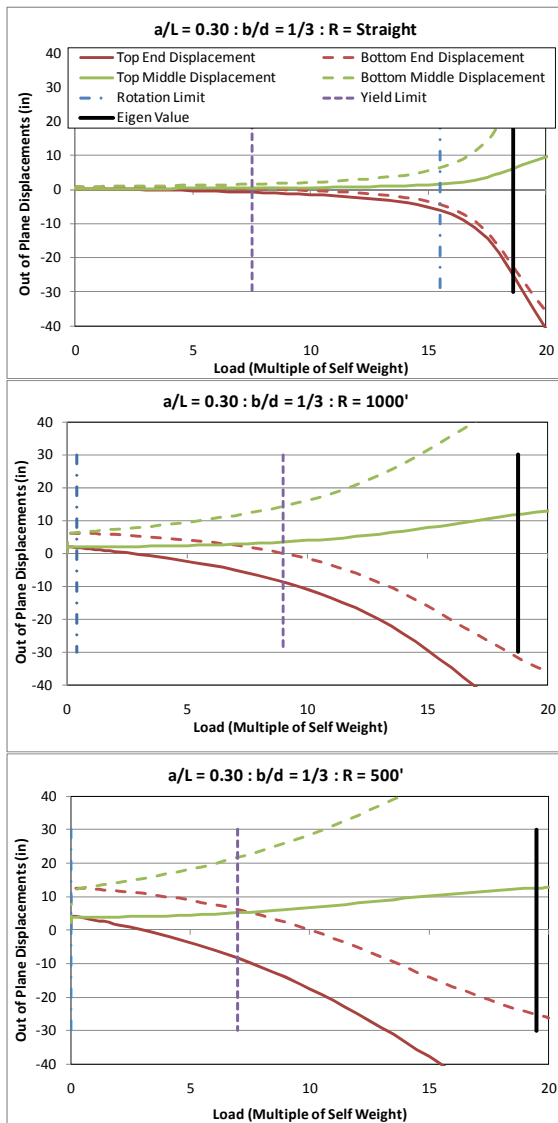


Figure A.13: $b/d = 1/3 : a/L = 0.30:$

R = Varies

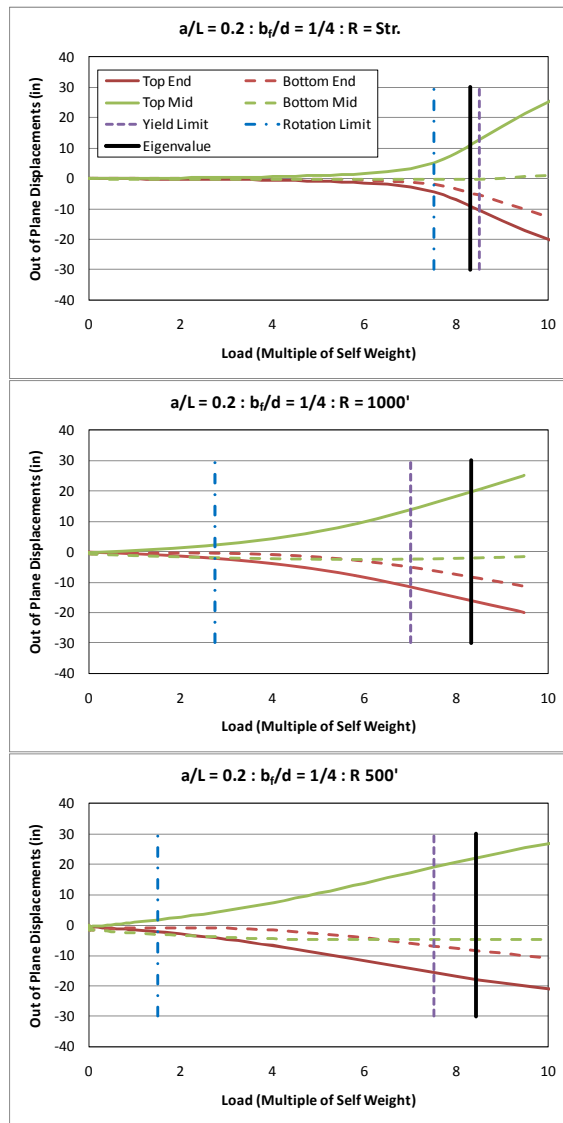


Figure A.14: $b/d = 1/4 : a/L = 0.20:$

R = Varies

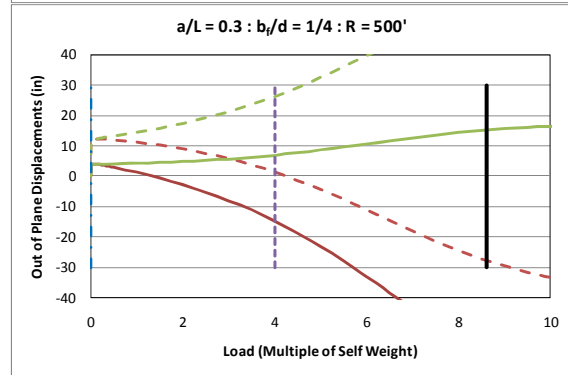
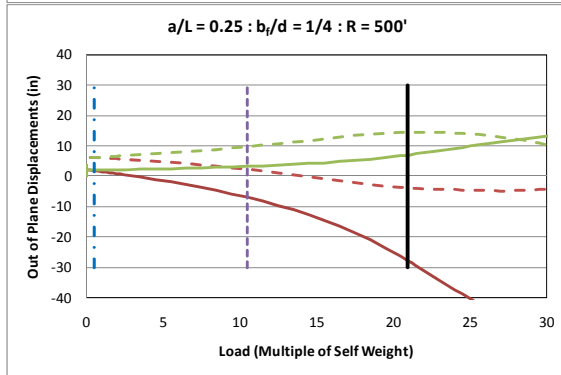
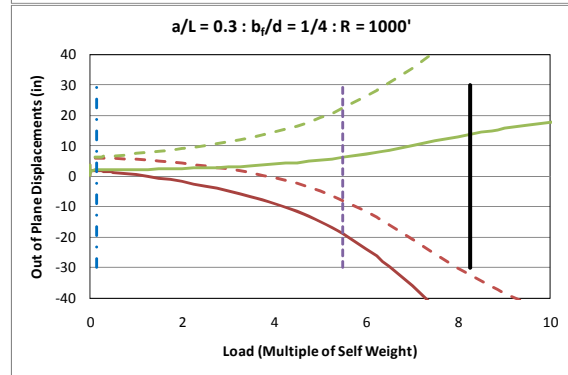
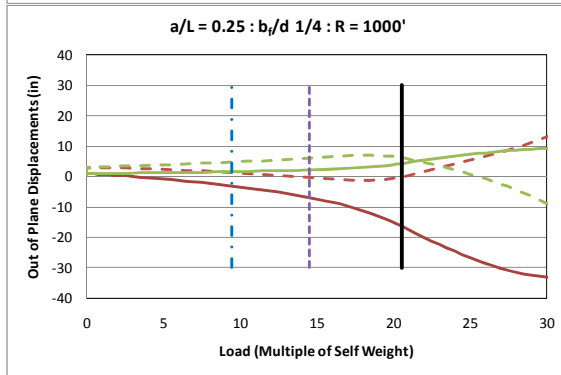
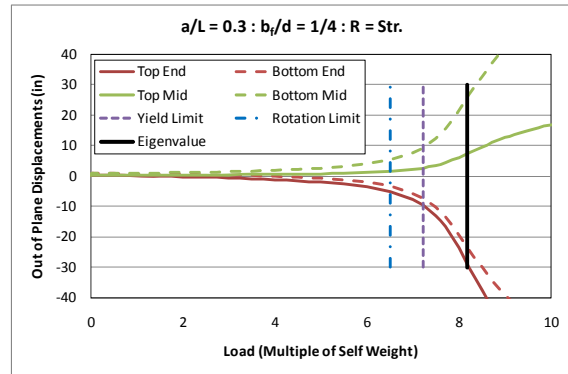
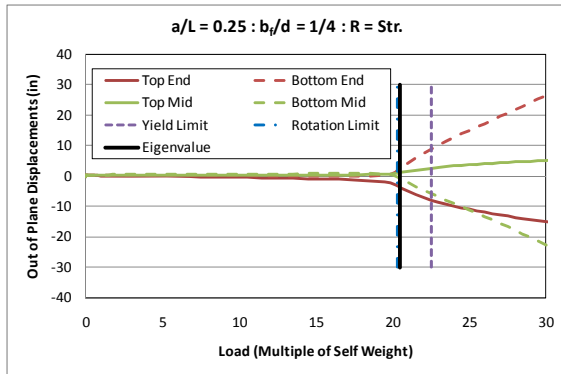


Figure A.15: $b_i/D = 1/4 : a/L = 0.25:$

R = Varies

Figure A.16: $b_i/D = 1/4 : a/L = 0.30:$

R = Varies

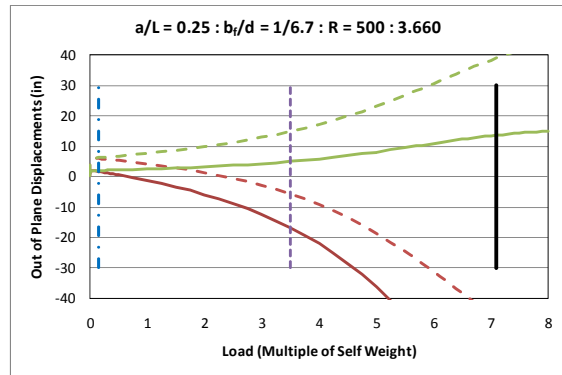
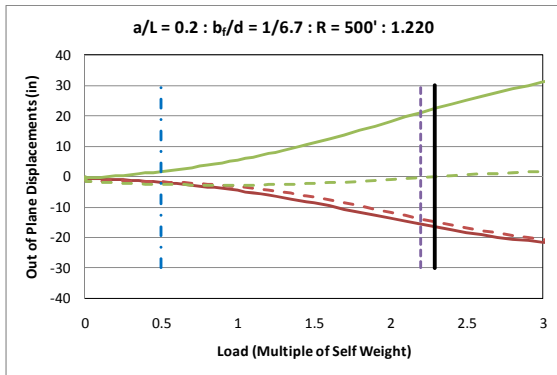
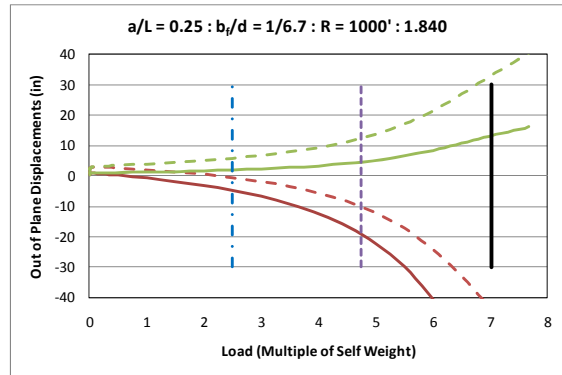
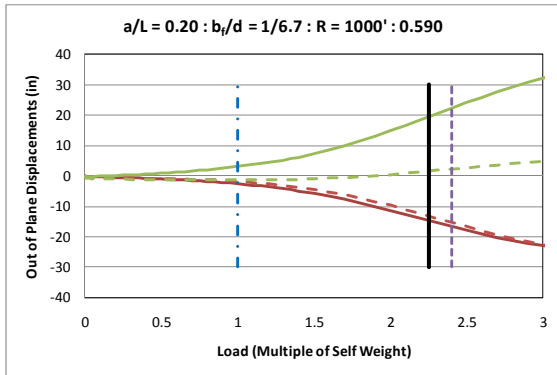
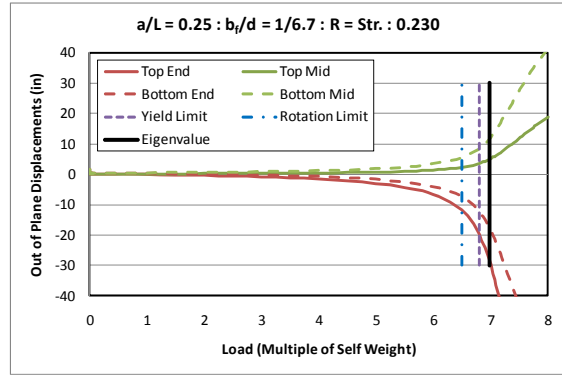
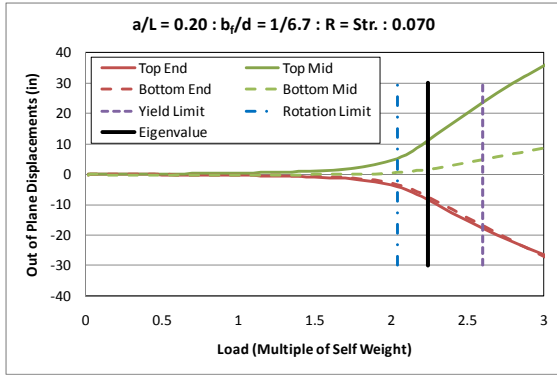


Figure A.17: $b_f/D = 1/6.7$: $a/L = 0.20$:

R = Varies

Figure A.18: $b_f/D = 1/6.7$: $a/L = 0.25$:

R = Varies

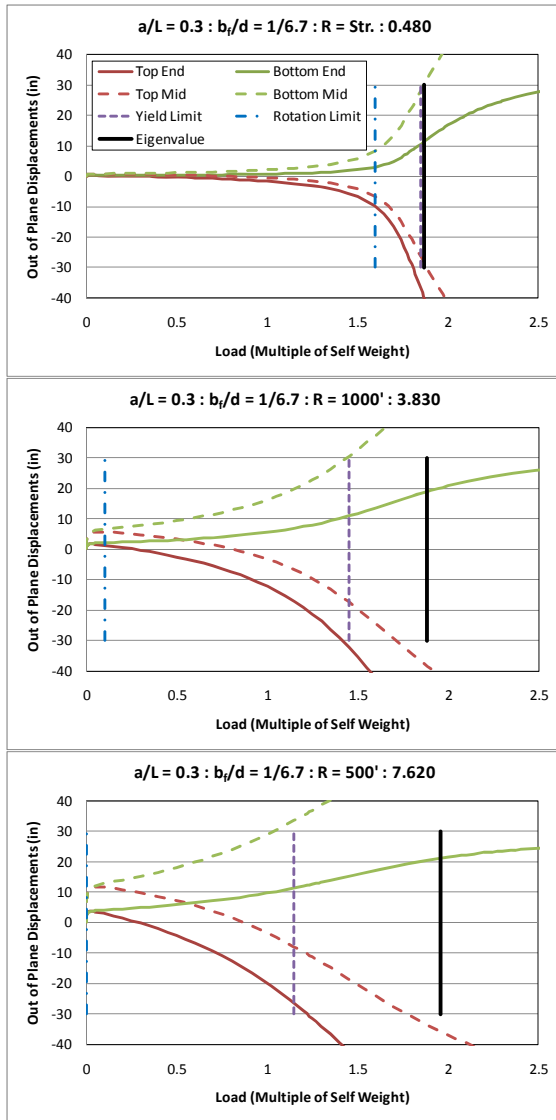


Figure A.19: $b_f/D = 1/6.7$: $a/L = 0.30$:

R = Varies

A.1.3 Study Three

- Prismatic Girder: $b_f/D = 0.167 - 0.25$: $a/L = 0.2 - 0.25$: $R = 500' - 8000'$

A.1.3.1 Summary

In the third study, the a/L range is once again reduced. In addition, the slenderness ratio, b_f/D range is also reduced leaving out the case where $b_f/D = 1/3$. The out of plane displacements and rotations are once again monitored at the ends and at the middle, yet only at 0.1 times self weight (representing the rigid body rotation of the system) and at 1.5 times self weight (representing the total rotation of the system). The 1st and 2nd eigenvalues are also recorded.

A.1.3.2 Parameters and Range

- Varied:
 - $b_f/D = 1/6 : 1/5 : 1/4$
 - $t_f = 0.5'' : 0.625'' : 0.75''$
 - $a/L = 0.20 : 0.21 : 0.23 : 0.25$
 - $R = 500' : 1000' : 8000'$ (~straight)
 - $L = 80' : 125'$
- Constant:
 - $D = 60''$
 - $t_w = 0.5$

A.1.3.3 Results

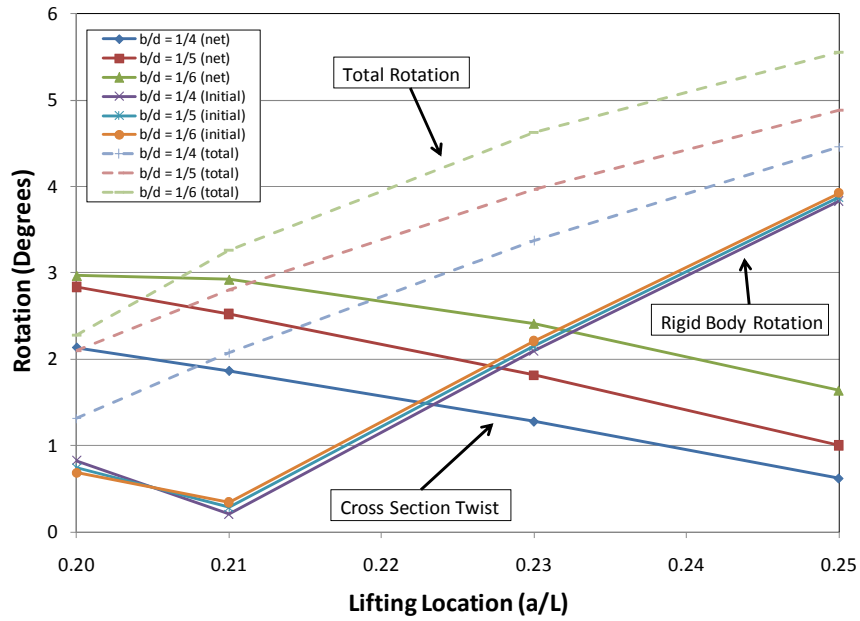


Figure A.20: Rotations : $L = 125'$: $R = 500'$

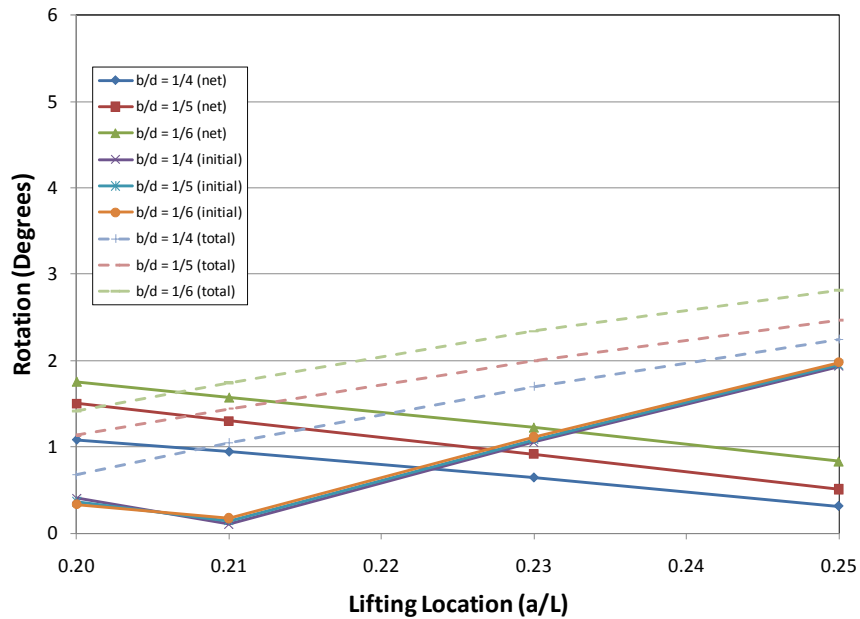


Figure A.21: Rotations : $L = 125'$: $R = 1000'$

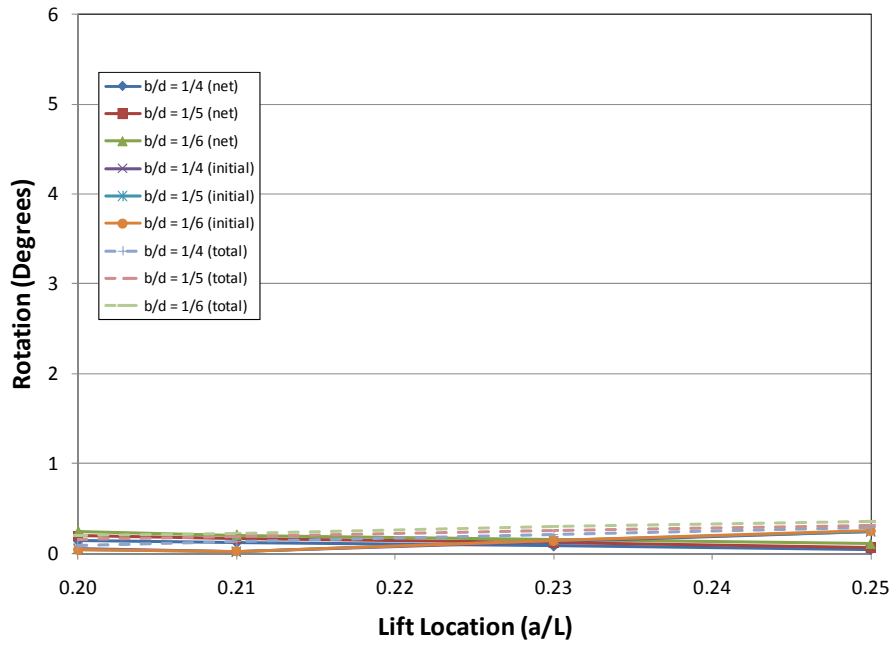


Figure A.22: Rotations : $L = 125'$: $R = 8000'$ (~Str)

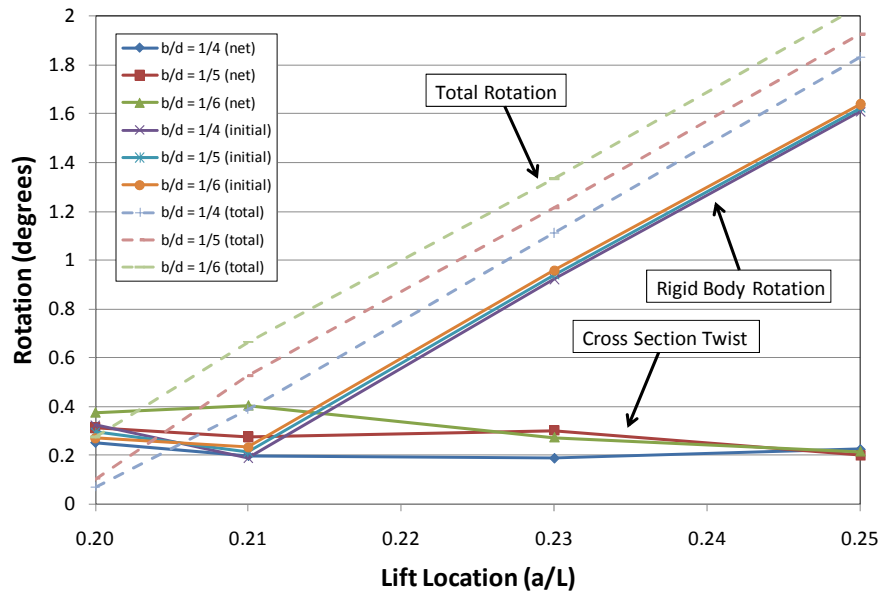


Figure A.23: Rotations : $L = 80'$: $R = 500'$

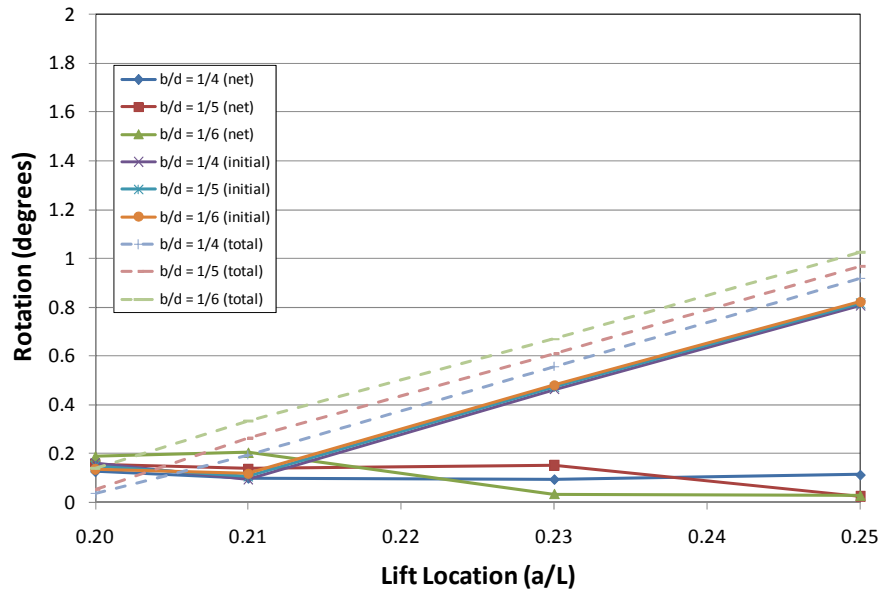


Figure A.24: Rotations : $L = 80'$: $R = 1000'$

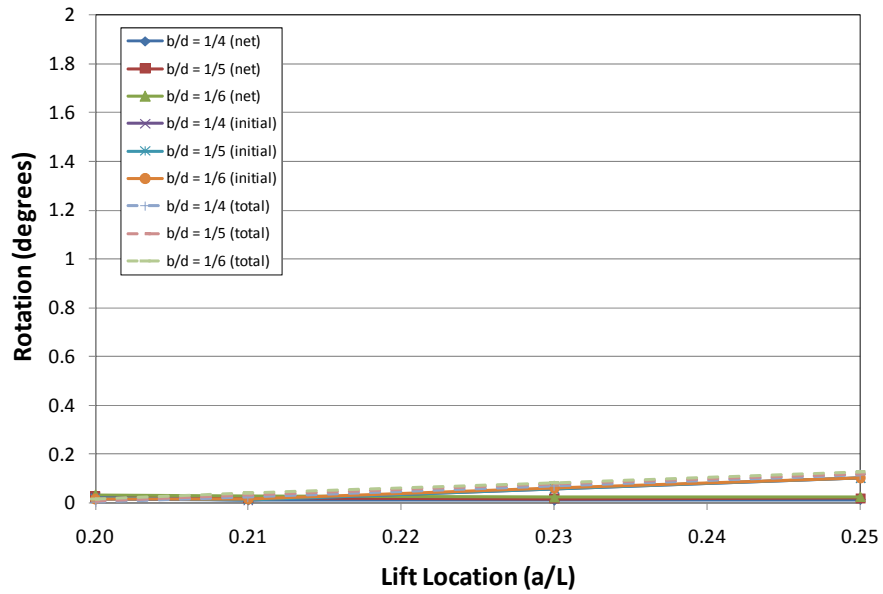


Figure A.25: Rotations : $L = 80'$: $R = 8000'$ (~Str)

A.1.4 Study Four

- Prismatic Girder: $b_f/D = 0.167 - 0.25$: $a/L = 0.2 - 0.25$: $R = 500$: $D = 60'' - 96''$

A.1.4.1 Summary

In the fourth study, the slenderness ratio and the lifting locations are kept the same as in the third study, yet the radius of curvature is kept constant at 500' and the depth is now varied. The out of plane displacements and the rotations are now monitored at 0.1 times self weight, 1.0 times self weight, and 1.5 times self weight. In addition, the longitudinal stresses at the top and bottom flange tips in the middle of the girder and at the end of the girder and monitored to determine the bending and warping stresses in the flanges.

A.1.4.2 Parameters and Range

- Varied:
 - $b_f/D = 1/6 : 1/5 : 1/4$
 - $t_f = 0.5'' : 0.625'' : 0.75''$
 - $a/L = 0.20 : 0.21 : 0.23 : 0.25$
 - **$D = 60'' : 96''$**
- Constant:
 - **$L = 125'$**
 - **$R = 500'$**
 - $t_w = 0.5$

A.1.4.3 Results

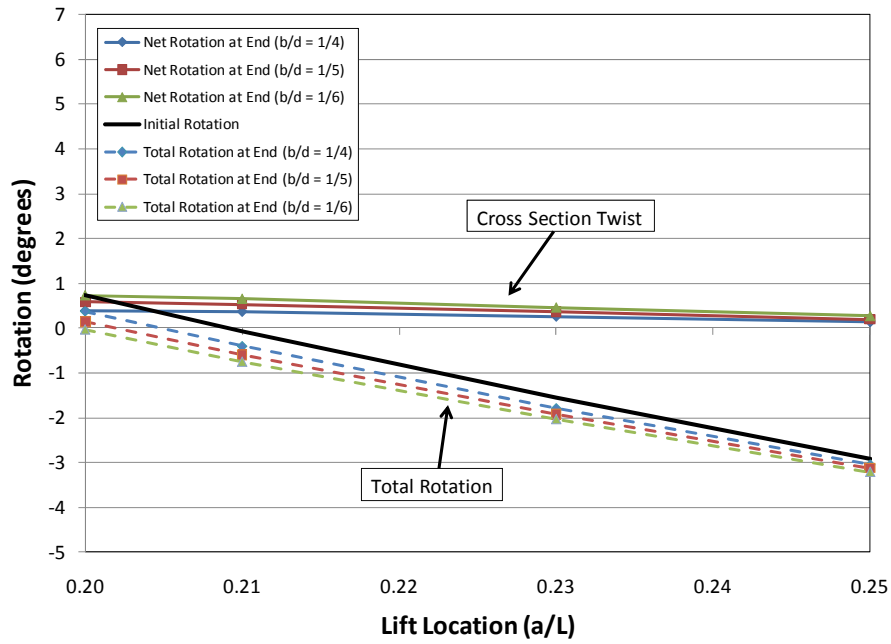


Figure A.26: End Rotations : R = 500' : D = 96"

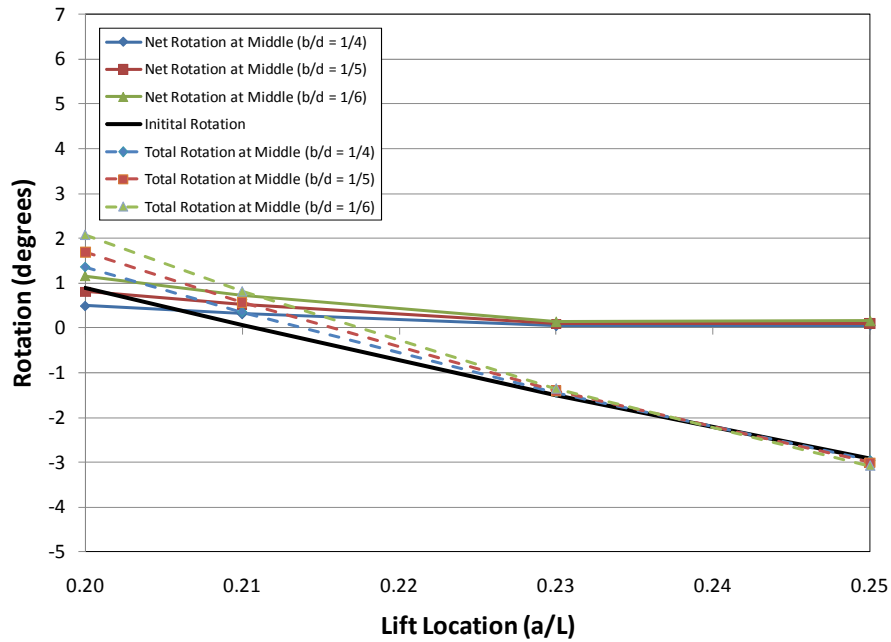


Figure A.27: Middle Rotations : R = 500' : D = 96"

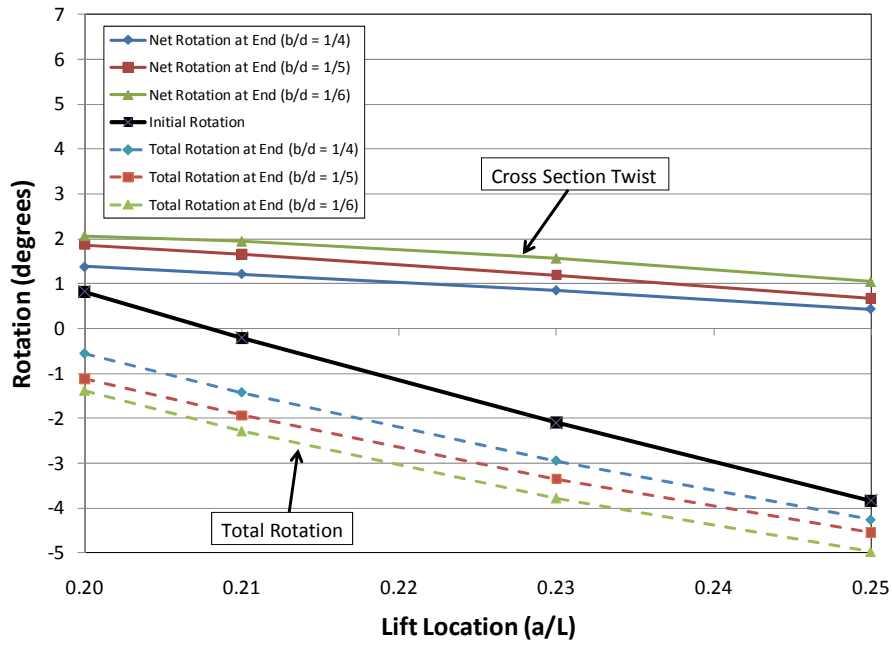


Figure A.28: End Rotations : $R = 500'$: $D = 60''$

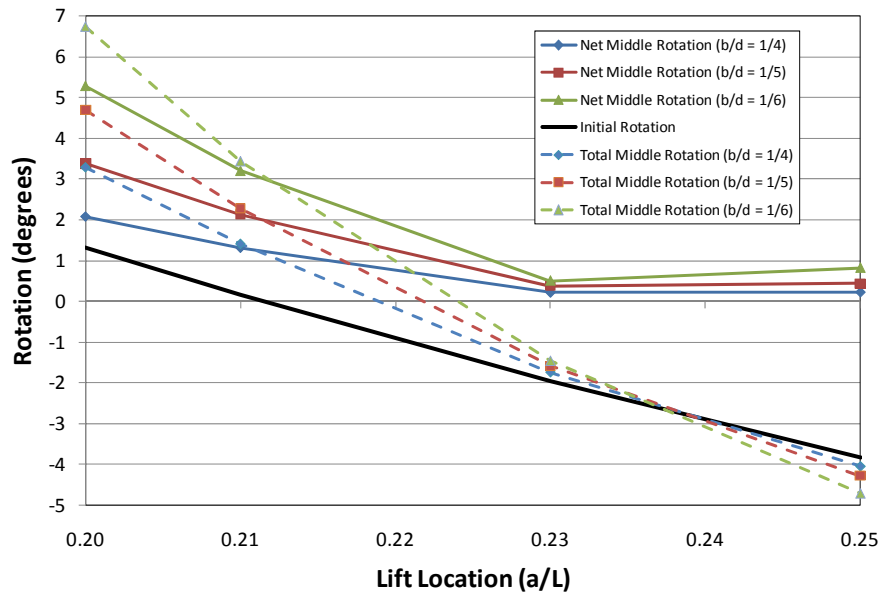


Figure A.29: Middle Rotations : $R = 500'$: $D = 60''$

A.1.5 Study Five

- Prismatic Girder: $b_f/D = 0.167 - 0.25$: $a/L = 0.2 - 0.25$: $R = 500 - 2500'$

A.1.5.1 Summary

In the fifth study, the accuracy of the eigenvalue to predict a serviceability limit state was determined. In order to do this, the rotations at the end of the girder are monitored as the load on the girder increases in multiples of the girder's self weight. The load in terms of girder self weight is recorded when the end of the girder rotates 1.5 degrees. This is done for the same slenderness ratio and lifting location range as the previous study. The radius of curvature is varied for a given length and the depth is kept constant.

A.1.5.2 Parameters and Range

- Varied:
 - $b_f/D = 1/6 : 1/5 : 1/4$
 - $t_f = 0.5'' : 0.625'' : 0.75''$
 - $a/L = 0.20 : 0.21 : 0.23 : 0.25$
 - **$R = 1000' : 1500' : 1800' : 2000' : 2500'$**
- Constant:
 - $L = 125'$
 - **$D = 60'$**
 - $t_w = 0.5$

A.1.5.3 Results

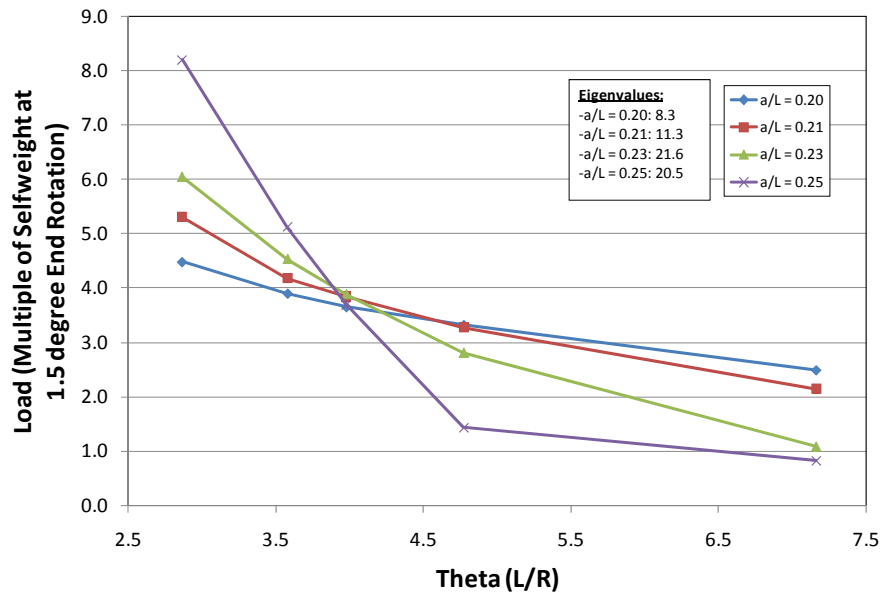


Figure A.30: Load to Reach Serviceability Limit vs. Interior Angle, Θ ($b_f/D = 1/4$)

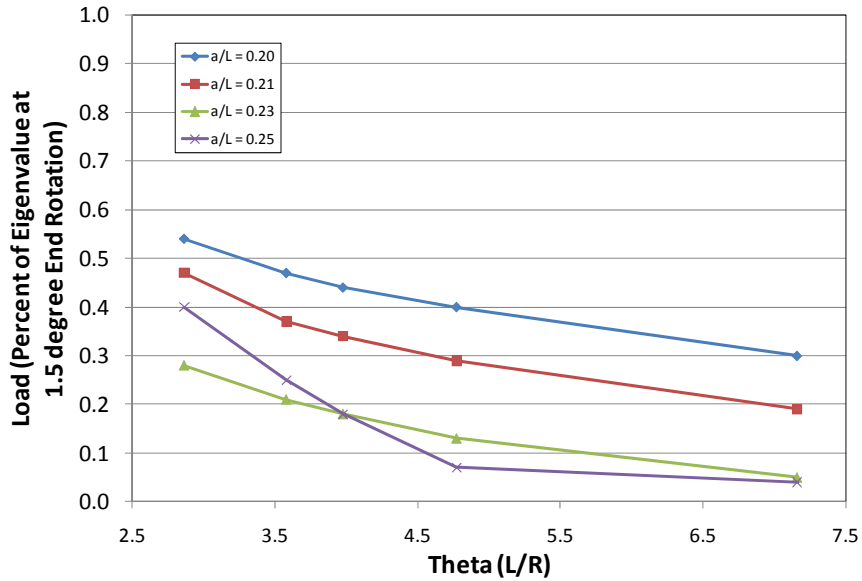


Figure A.31: Load to Reach Serviceability Limit vs. Interior Angle, Θ ($b_f/D = 1/4$)

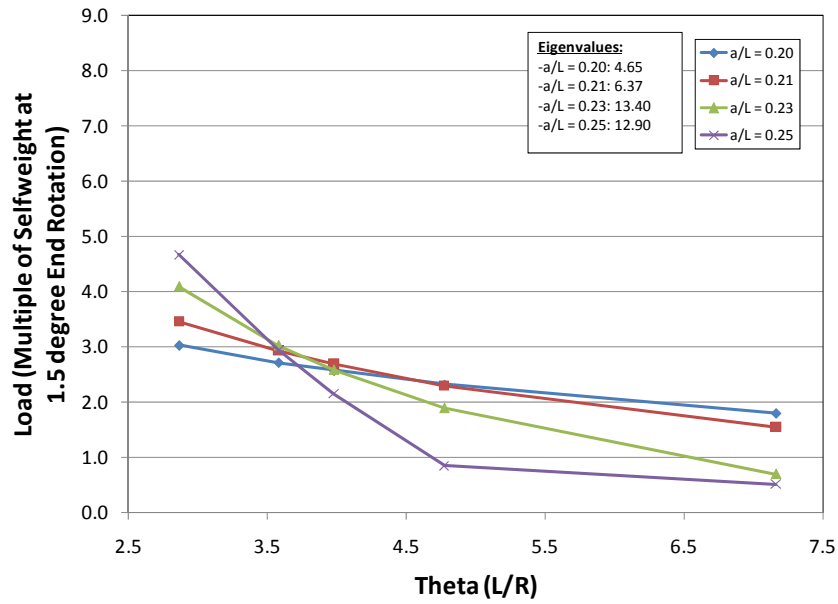


Figure A.32: Load to Reach Serviceability Limit vs. Interior Angle, Θ ($b_f/D = 1/5$)

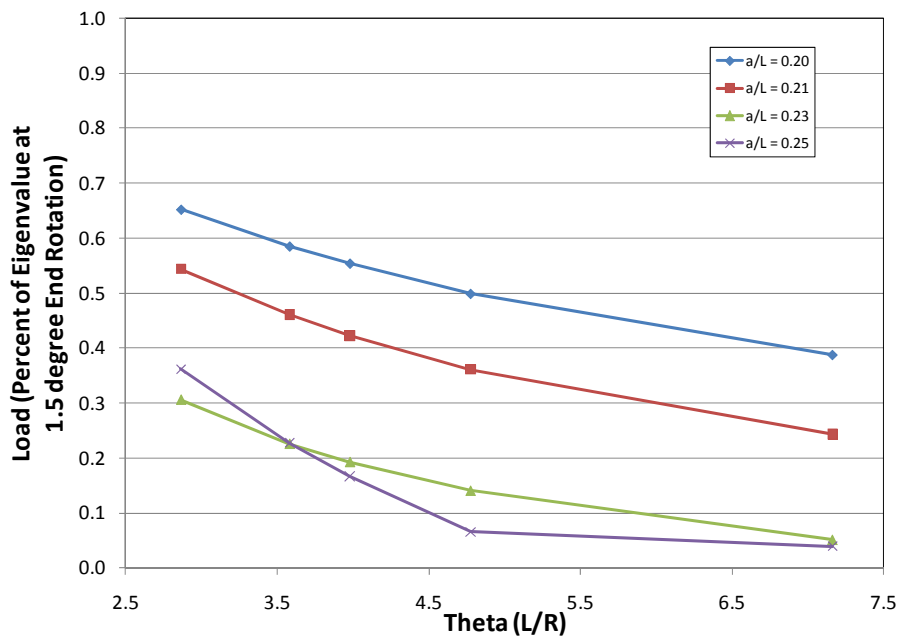


Figure A.33: Load to Reach Serviceability Limit vs. Interior Angle, Θ ($b_f/D = 1/5$)

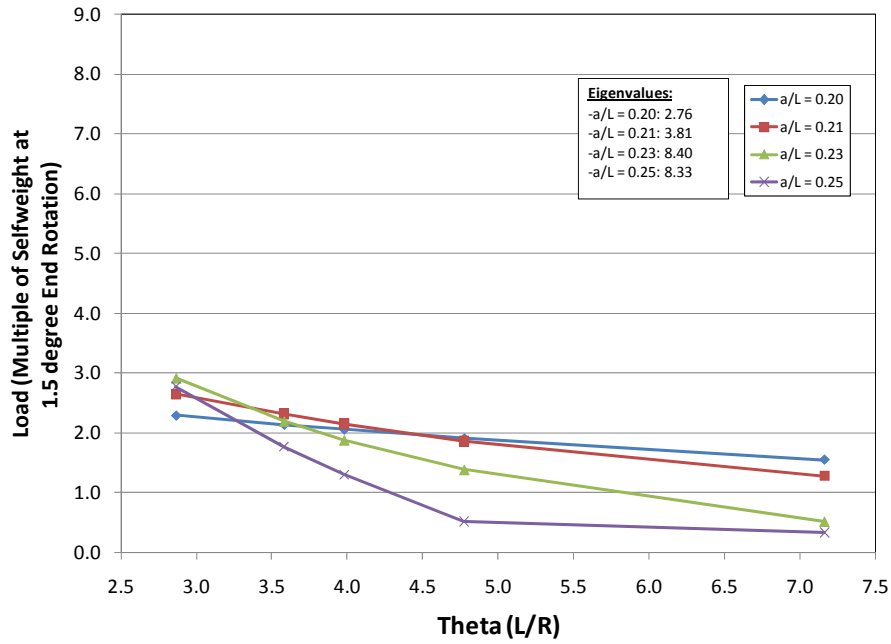


Figure A.34: Load to Reach Serviceability Limit vs. Interior Angle, Θ ($b_f/D = 1/6$)

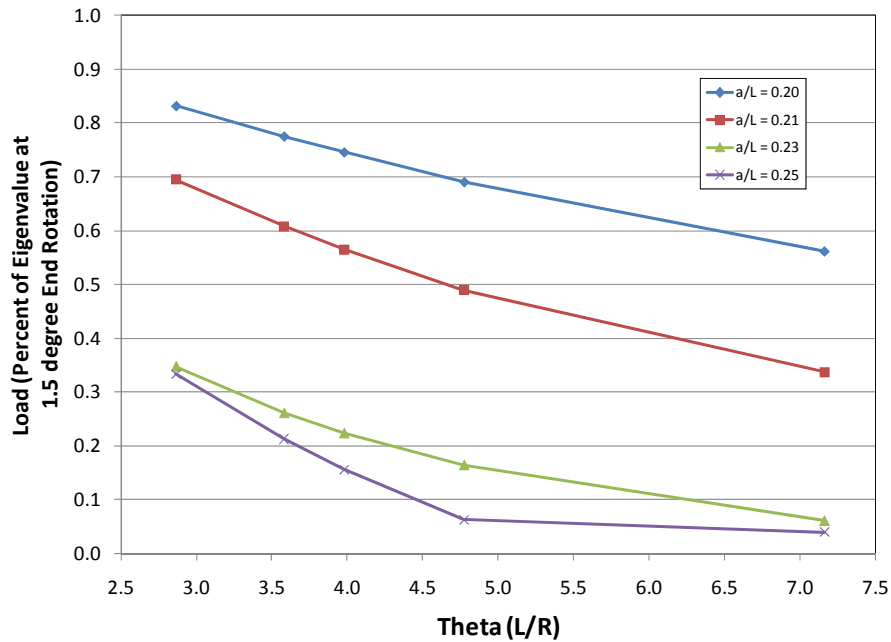


Figure A.35: Load to Reach Serviceability Limit vs. Interior Angle, Θ ($b_f/D = 1/6$)

A.1.6 Study Six

- Prismatic Girder: $b_f/D = 0.167 - 0.25$: $a/L = 0.2 - 0.25$: $R = 1800'$: $L = 90' - 225'$

A.1.6.1 Summary

In the sixth study, the accuracy of the eigenvalue to predict a serviceability limit is once again investigated. The rotations at the end of the girder are monitored as the load on the girder increases in multiples of the girder's self weight. The load in terms of girder self weight is recorded when the end of the girder rotates 1.5 degrees. This is done for the same slenderness ratio and lifting location range as the previous study. The radius of curvature is kept constant this time and the lengths are varied for a constant depth.

A.1.6.2 Parameters and Range

- Varied:
 - $b_f/D = 1/6 : 1/4$
 - $t_f = 0.5'' : 0.625'' : 0.75''$
 - $a/L = 0.20 : 0.21 : 0.23 : 0.25$
 - $L = 90' : 112.5' : 125' : 150' : 225'$
- Constant:
 - $D = 60'$
 - $R = 1800'$
 - $t_w = 0.5$

A.1.6.3 Results

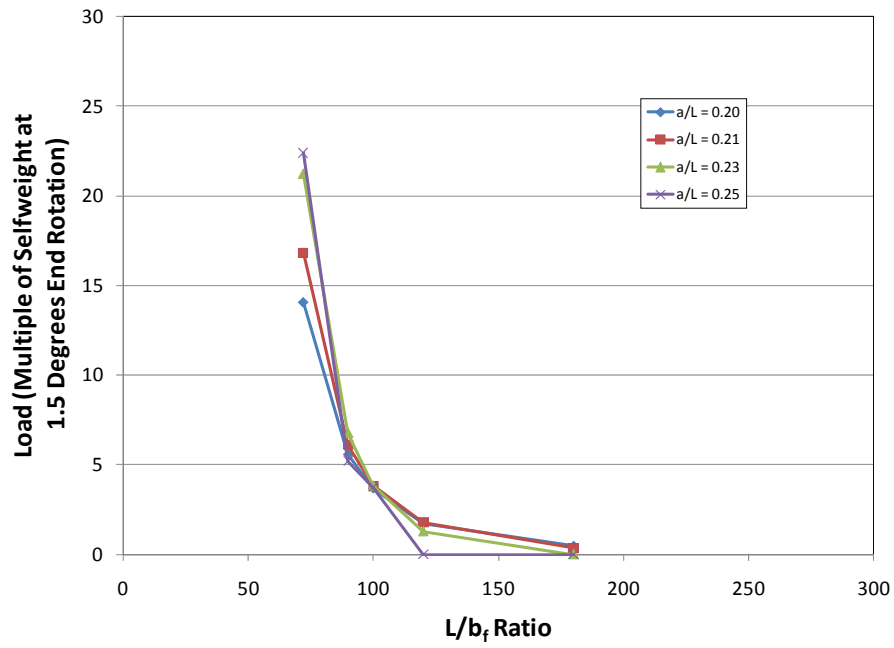


Figure A.36: Serviceability Limits – $b_f/D = 1/4 : D = 60'' : b = 15'' : R = 1800'$

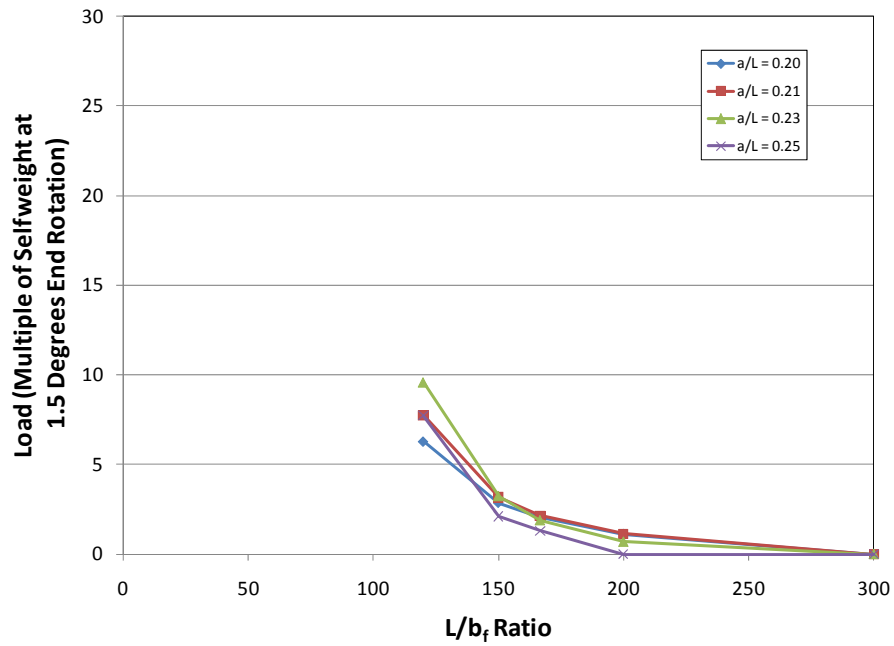


Figure A.37: Serviceability Limits – $b_f/D = 1/6 : D = 60'' : b = 9'' : R = 1800'$

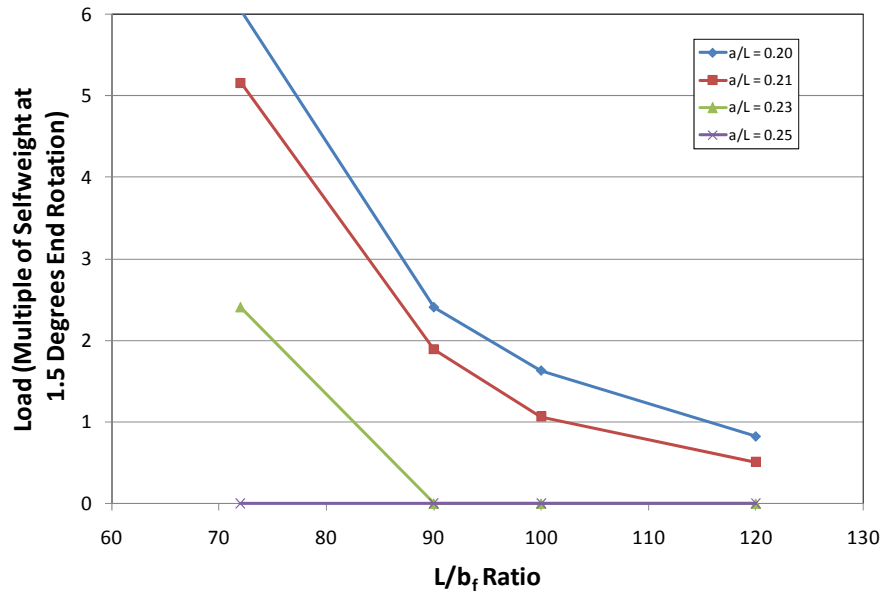


Figure A.38: Serviceability Limits – $b_f/D = 1/4$: $D = 60''$: $b = 15''$: $R = 500'$

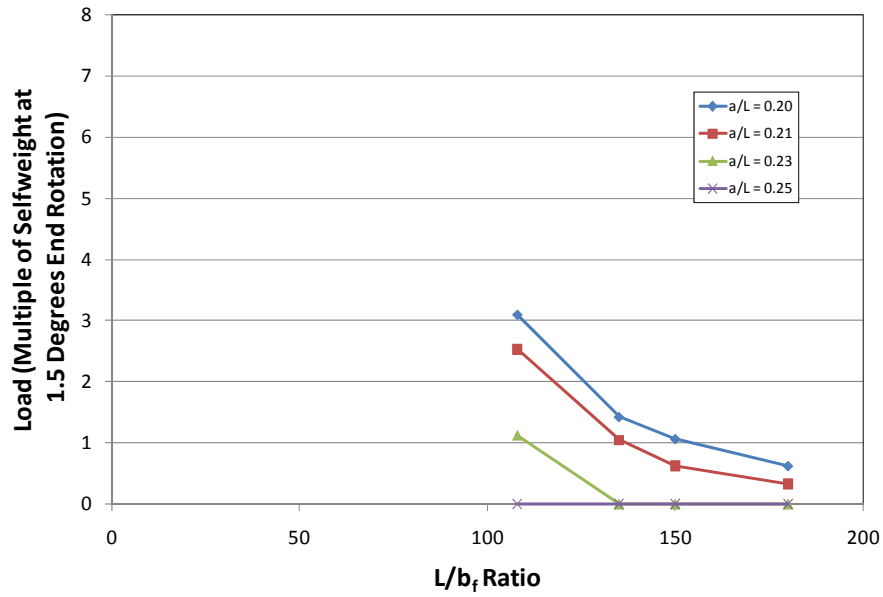


Figure A.39: Serviceability Limits – $b_f/D = 1/6$: $D = 60''$: $b = 10''$: $R = 500'$

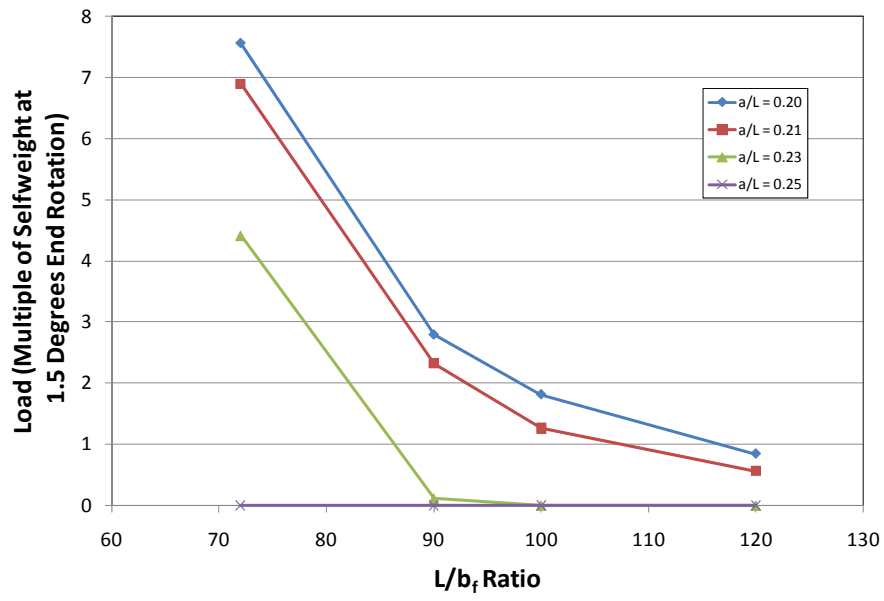


Figure A.40: Serviceability Limits – $b_f/D = 1/6$: $D = 90''$: $b = 15''$: $R = 500'$

APPENDIX B

Parametric Study Summary for Partially Constructed Bridges during Erection

As described in Chapter 4, an extensive parametric study was conducted to study the behavior of partially constructed horizontally curved steel I-girder bridges during erection sequencing and concrete placement. In this study, it was important to determine optimal locations to place shore towers and temporary holding cranes as well as the lifting force that should be used in a temporary lifting crane. In order to complete the study, many finite element models were created in ANSYS 11.0 (2007) and both linear and non-linear analyses was conducted monitoring displacements, stresses, and rotations. This appendix supplements the information in Chapter 4 and provides a summary of the various partially constructed scenarios studied. The parameters in bold under the *Parameters and Range* section in each study signify that the range has been changed in comparison to the previous study.

B.1 PARAMETRIC STUDY SUMMARY

The following summary and results are organized in the order in which they were completed. It should be noted that each study has some similar characteristics, which are described in the study summaries below. The parameters that were varied and kept constant are noted.

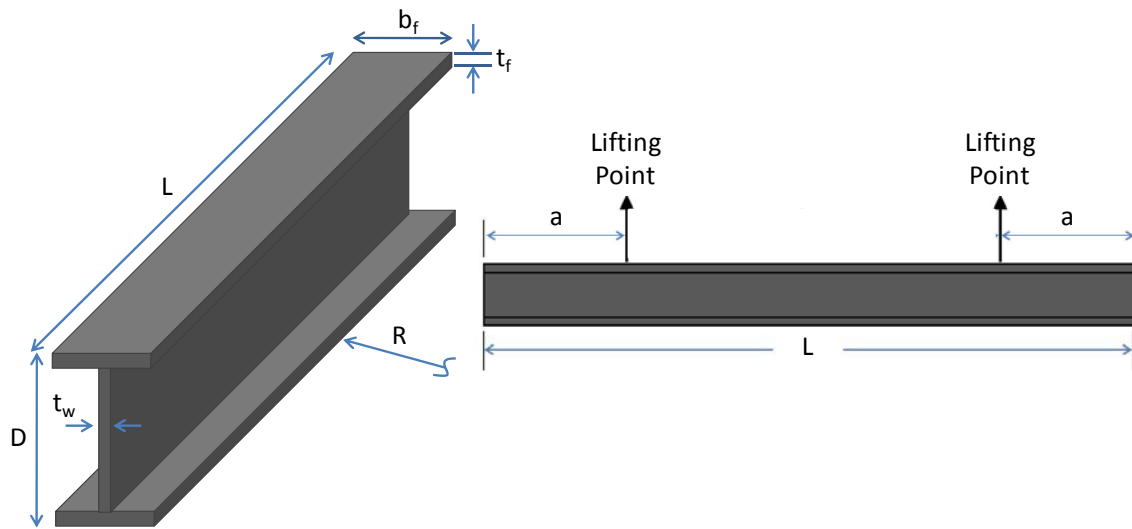


Figure B.1: Parameter Definitions

B.1.1 Study One

- Shore tower location varied

B.1.1.1 Summary

For the first study, an actual bridge design was used to determine the optimal place to place a temporary shore tower. Shore towers were placed along the girder to determine where stresses and displacements were lowest. The supports are simulated as resting on elastomeric bearing pads with 11 kips/in shear stiffness. A stiff lateral spring is placed at the top flange of the girder at supports to prevent rotation. Both linear and non-linear stresses and displacements are recorded.

B.1.1.2 Parameters and Range

- $b_f/D \sim 1/3.5$: $R = 1200'$: $L = 236'$: $D = 84''$: $b_f = 24''$
- Permanent supports located at 0 ft and 185 ft with the shore tower varied at distances of ~ 20 ft.

B.1.1.3 Results

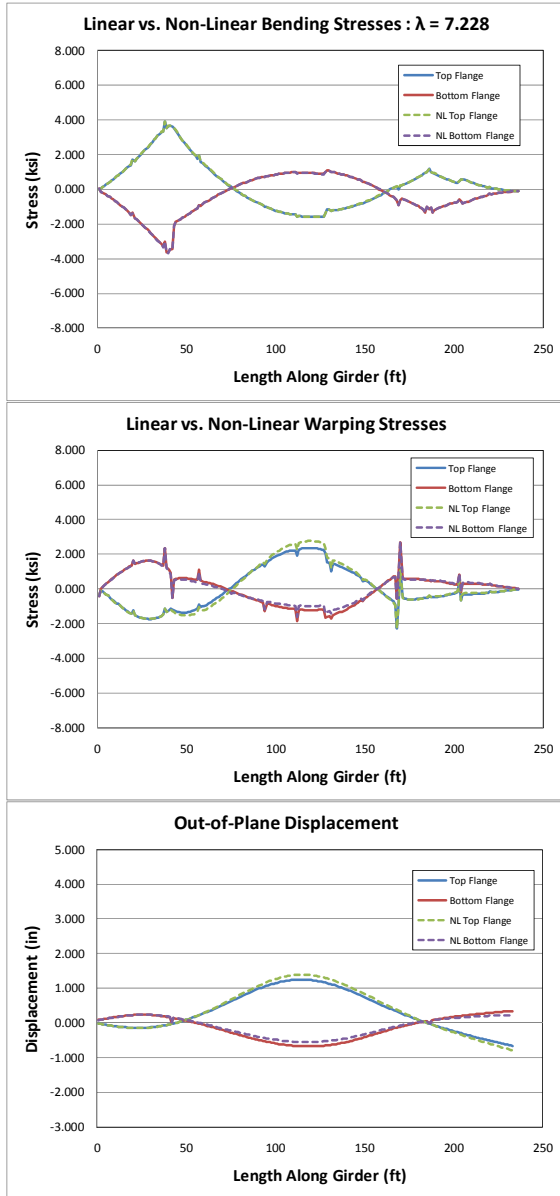


Figure B.2: Shore Tower at 40 ft

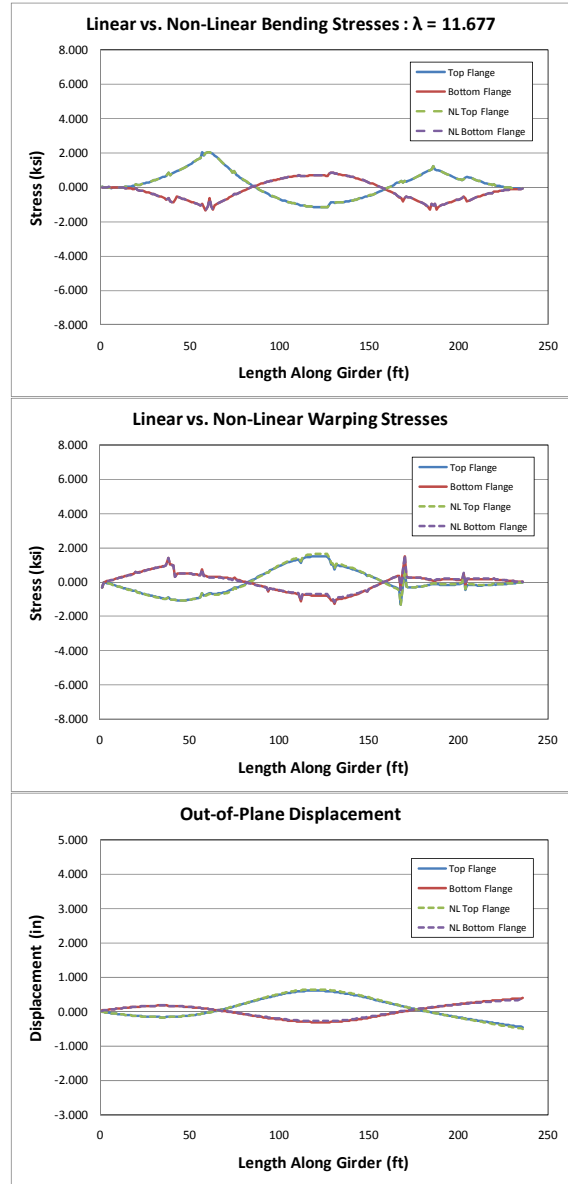


Figure B.3: Shore Tower at 60 ft

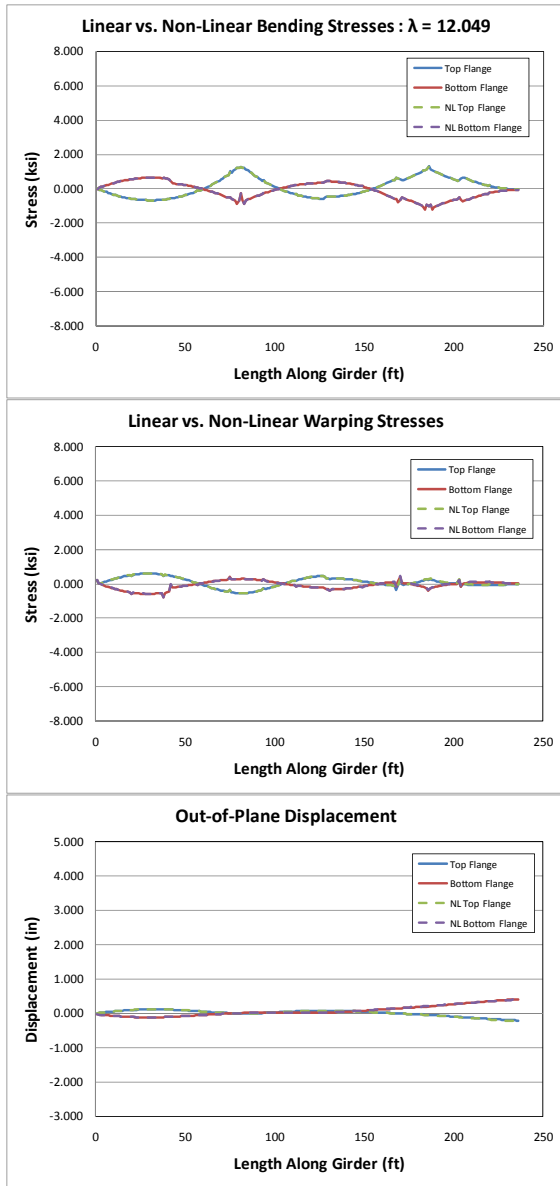


Figure B.4: Shore Tower at 80 ft

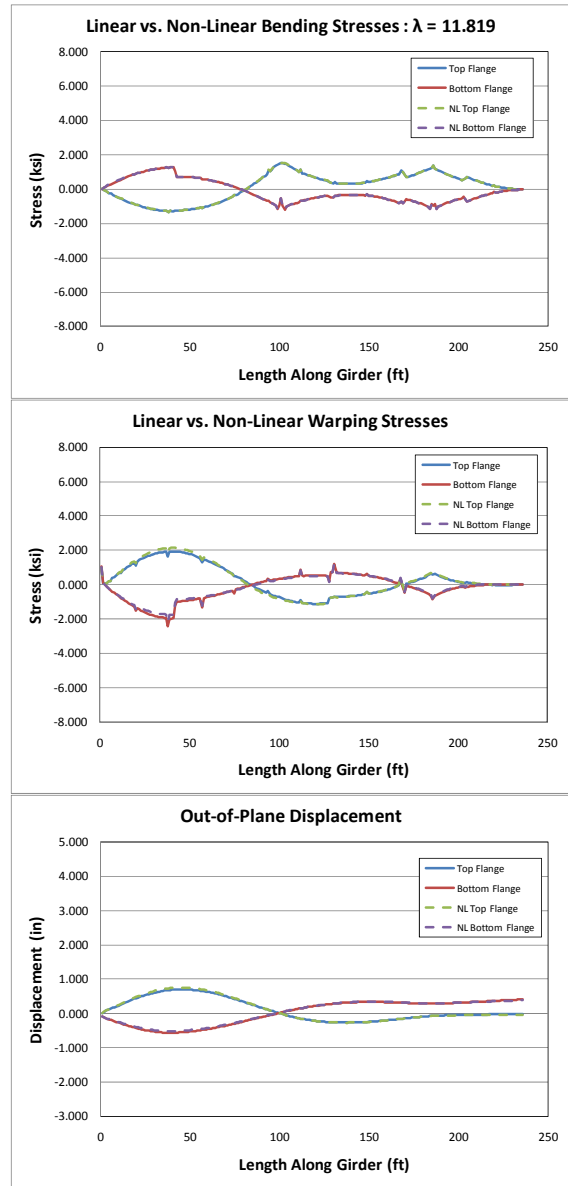


Figure B.5: Shore Tower at 100 ft

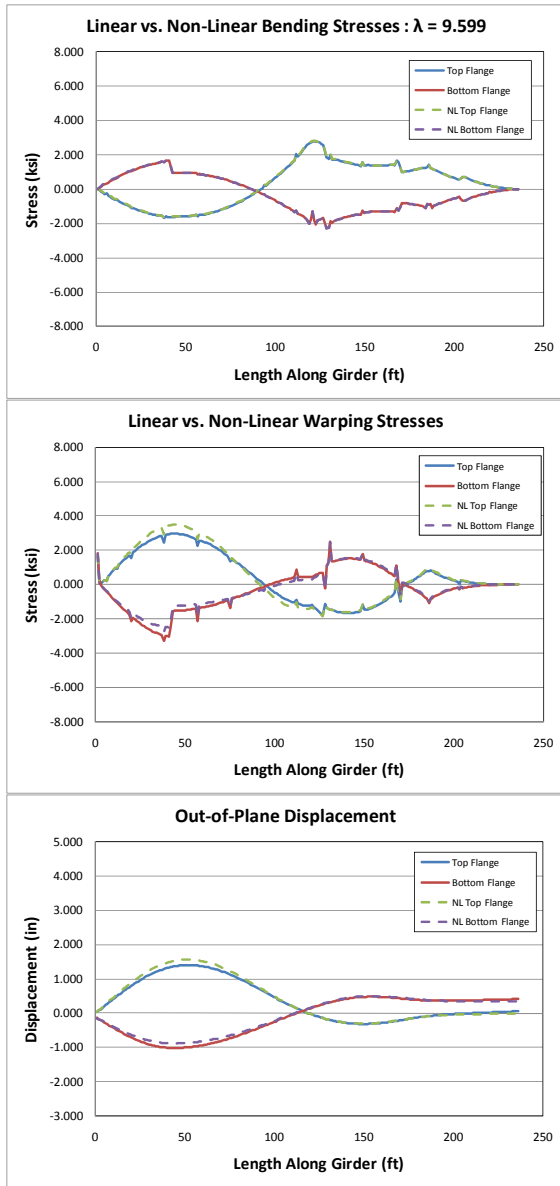


Figure B.6: Shore Tower at 120 ft

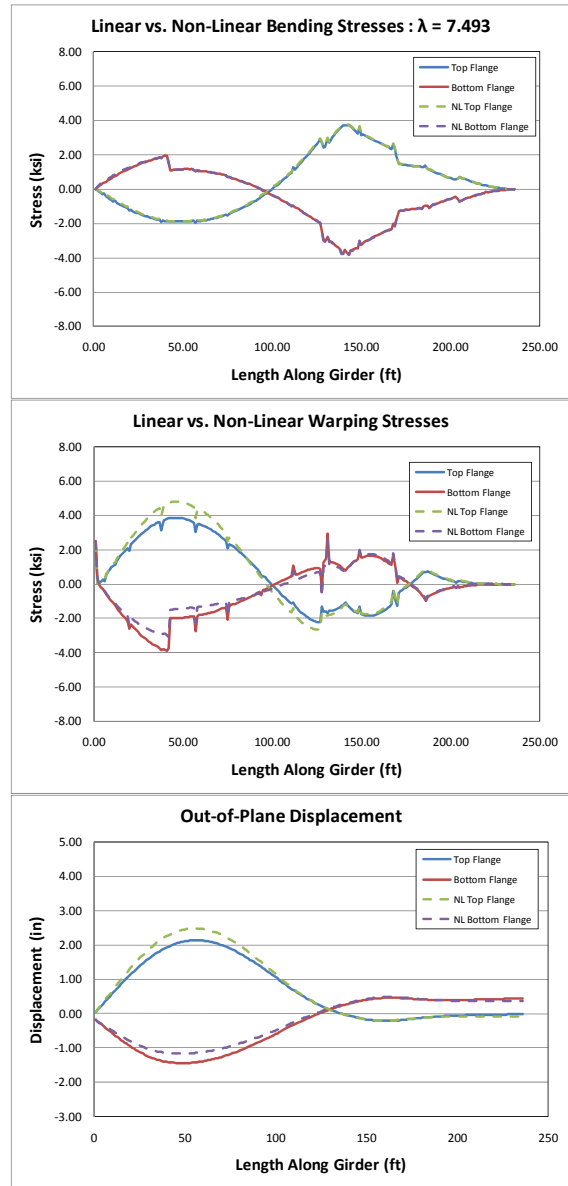


Figure B.7: Shore Tower at 140 ft

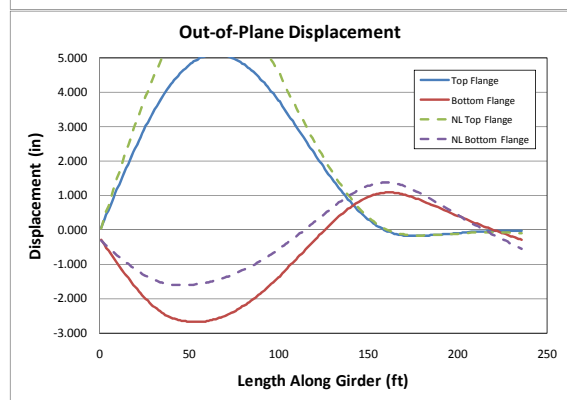
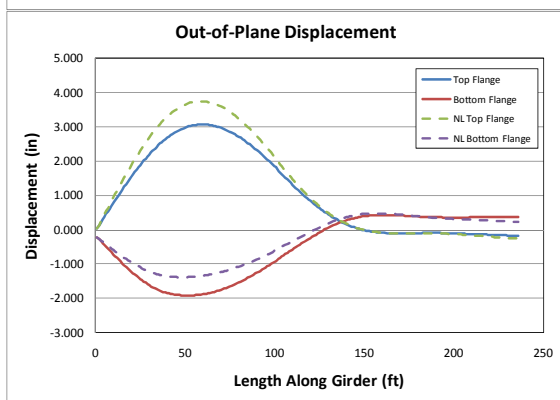
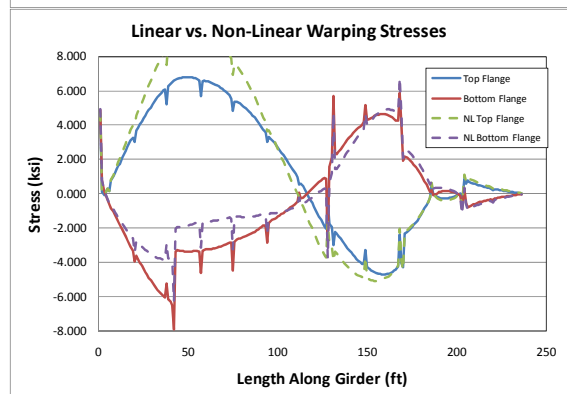
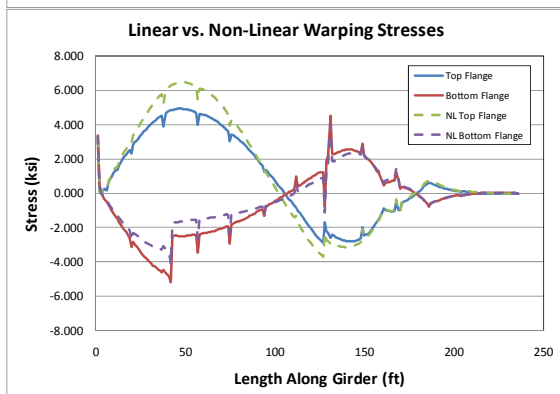
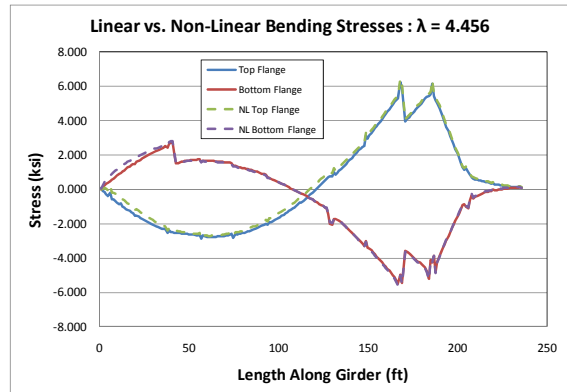
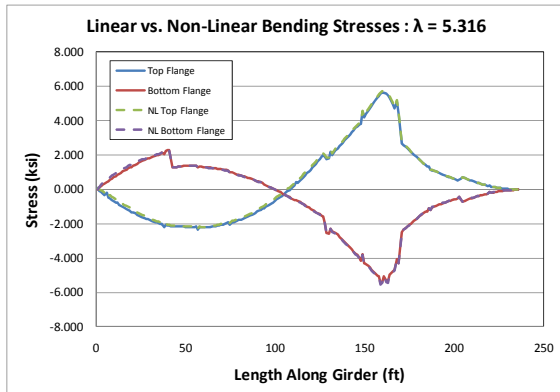


Figure B.8: Shore Tower at 160 ft

Figure B.9: Shore Tower at 205 ft

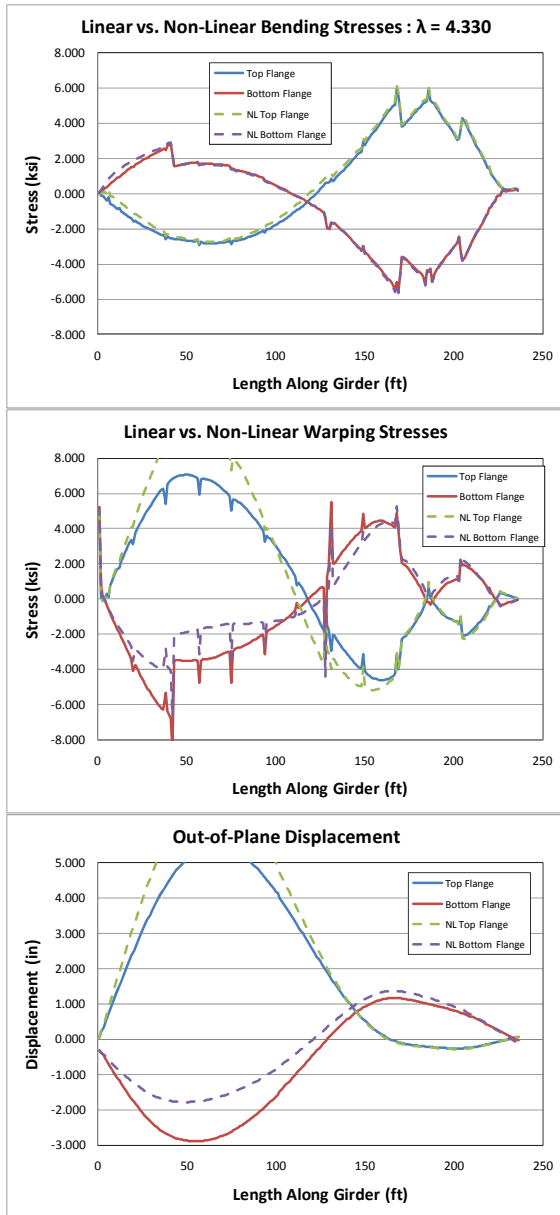


Figure B.10: Shore Tower at 225 ft

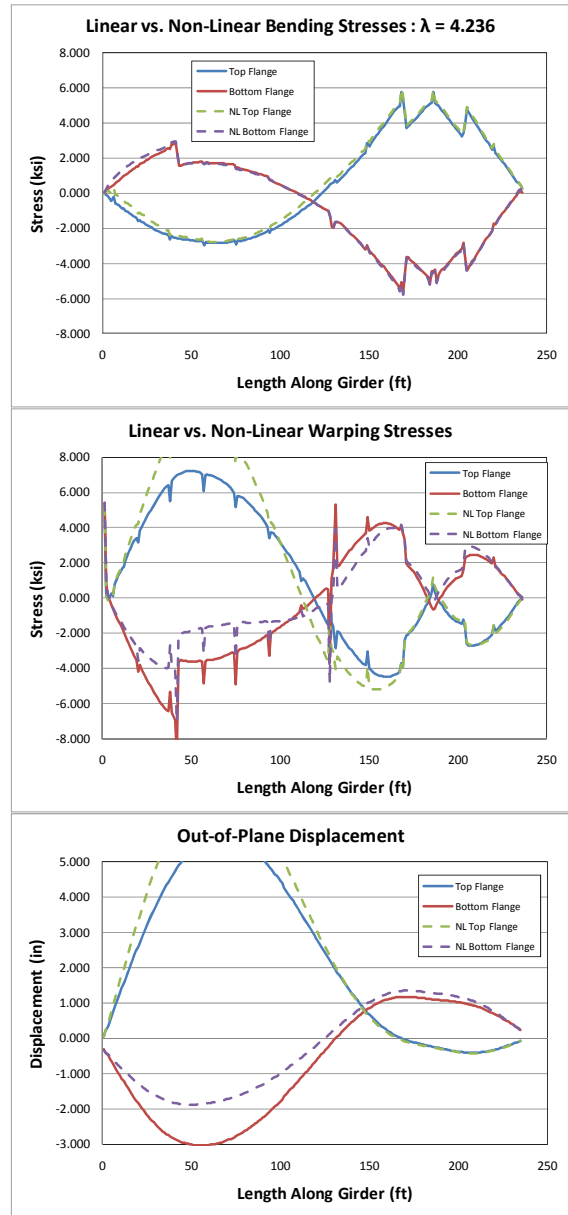


Figure B.11: Shore Tower at 245 ft

B.1.2 Study Two

- Holding crane location fixed : holding crane load varied

B.1.2.1 Summary

For the second study, the same bridge as used in Study 1 was used again to determine the optimal load to place in a temporary holding crane. The holding crane location was fixed at 80 ft which corresponded to the optimal shore tower location per study 1. Holding crane forces were changed to determine when stresses and displacements were lowest. The holding crane is modeling by placing a vertical force in the middle of the top flange. Both linear and non-linear stresses and displacements are recorded.

B.1.2.2 Parameters and Range

- $b_f/D \sim 1/3.5$: $R = 1200'$: $L = 236'$: $D = 84''$: $b_f = 24''$
- Permanent supports located at 0 ft and 185 ft
- **Holding crane location fixed at $x = 80$ ft**
- **Holding crane force varied from 20 kips to 60 kips at 5 kip intervals with an additional load of 47.8 kips used (vertical reaction in the shore tower placed at 80 ft per study 1).**

B.1.2.3 Results

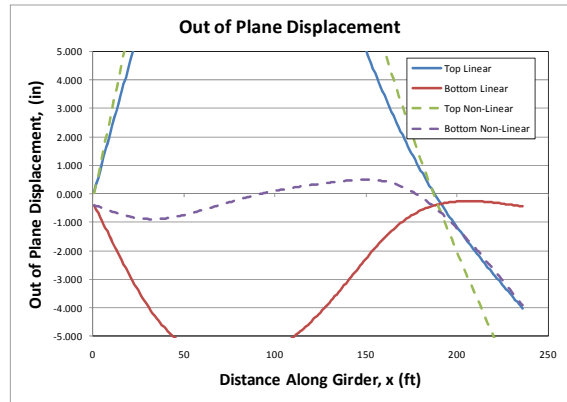
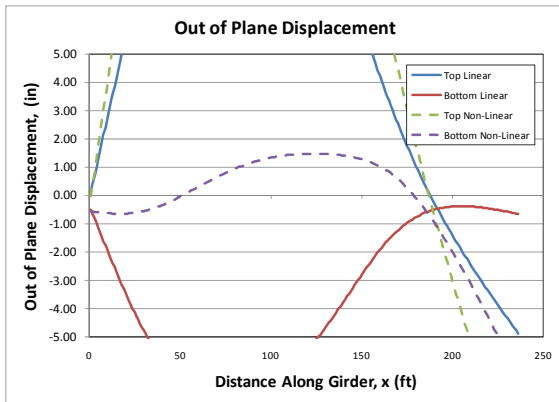
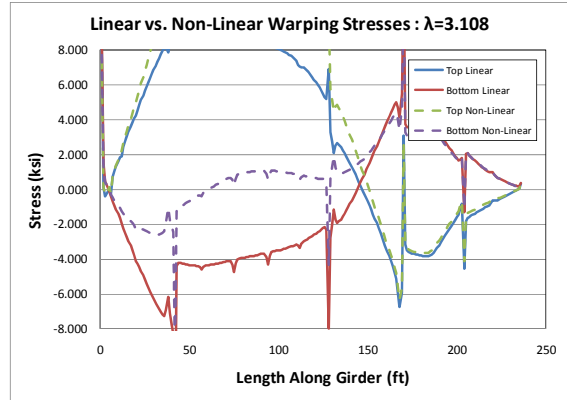
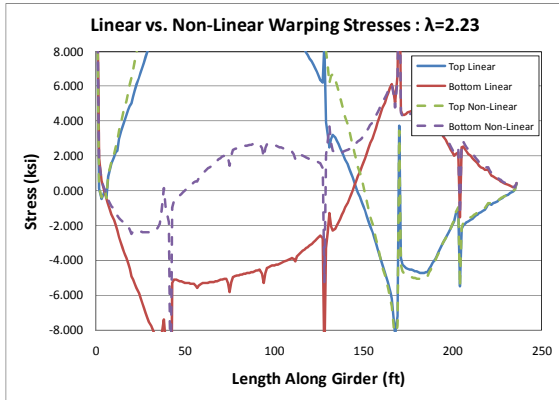
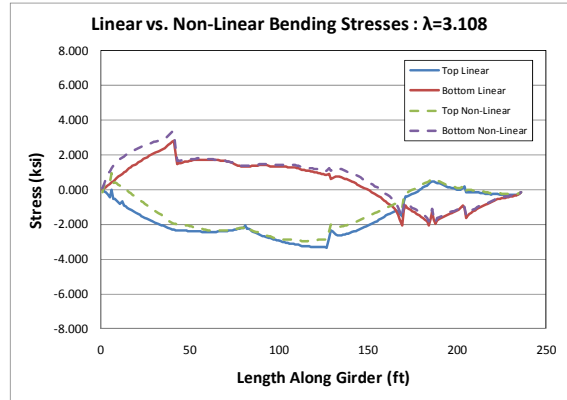
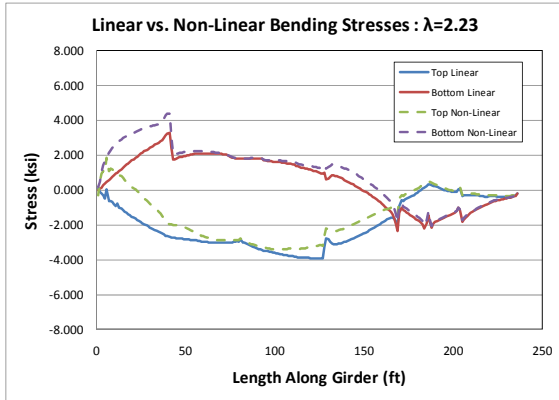


Figure B.12: Holding Crane with 20 kip Vertical Force

Figure B.13: Holding Crane with 25 kip Vertical Force

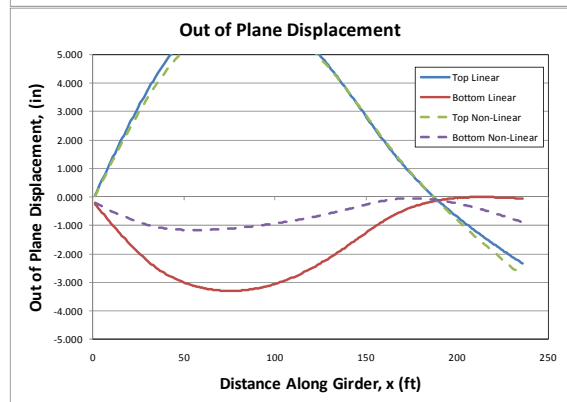
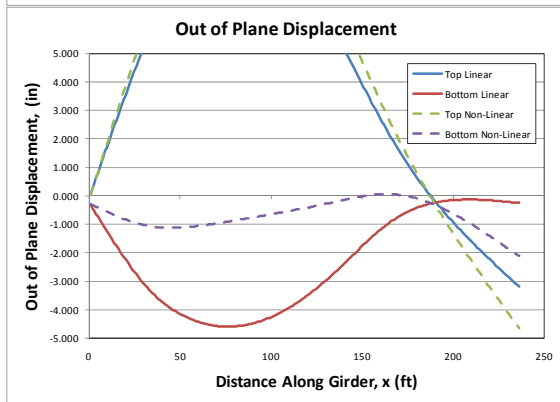
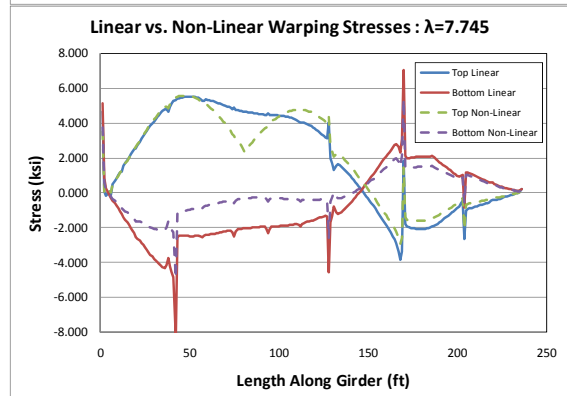
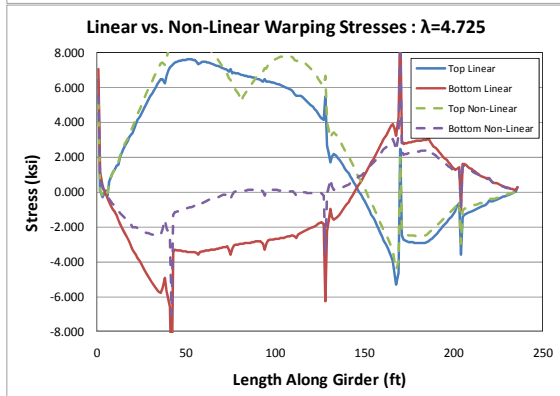
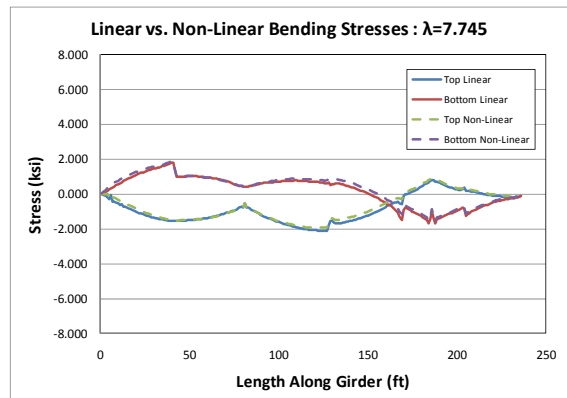
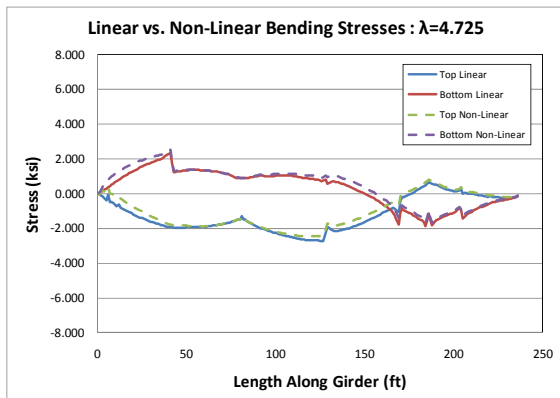


Figure B.14: Holding Crane with 30 kip Vertical Force

Figure B.15: Holding Crane with 35 kip Vertical Force

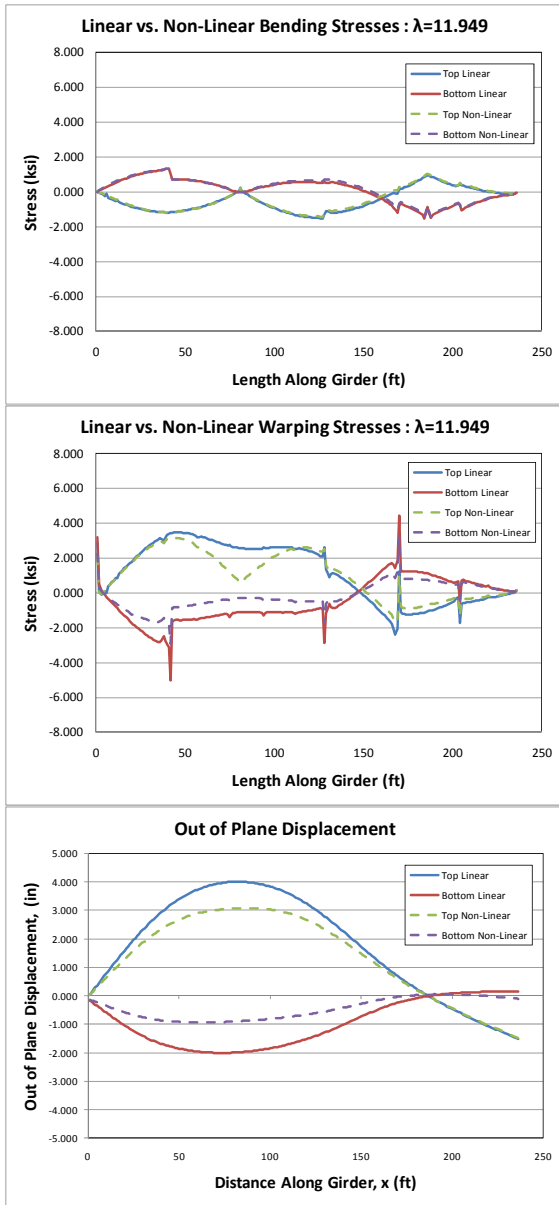


Figure B.16: Holding Crane with 40 kip Vertical Force

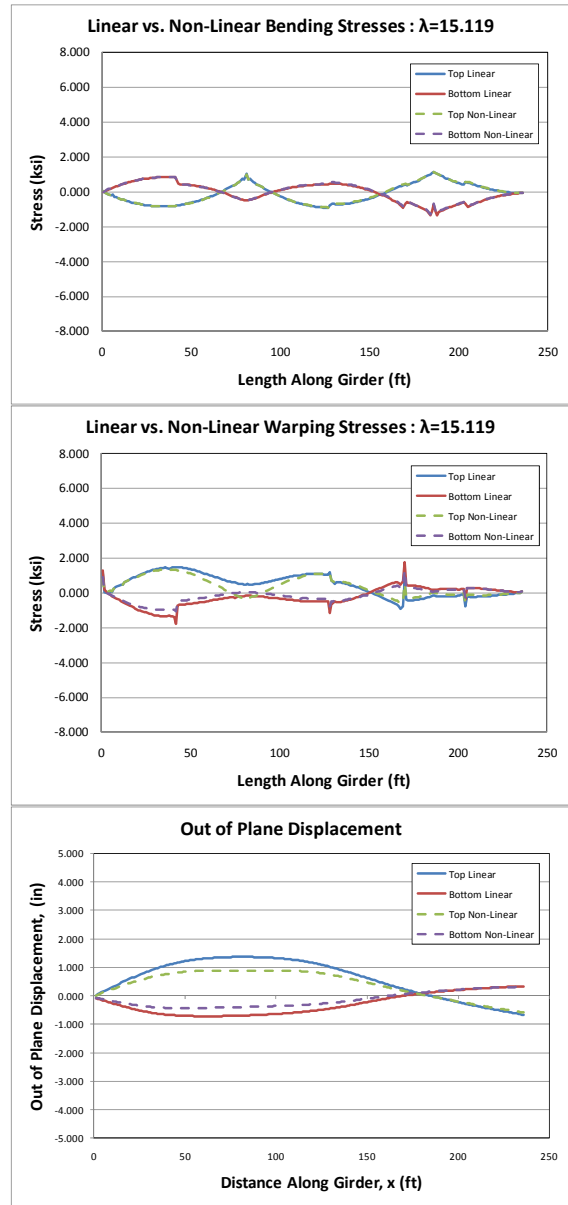


Figure B.17: Holding Crane with 45 kip Vertical Force

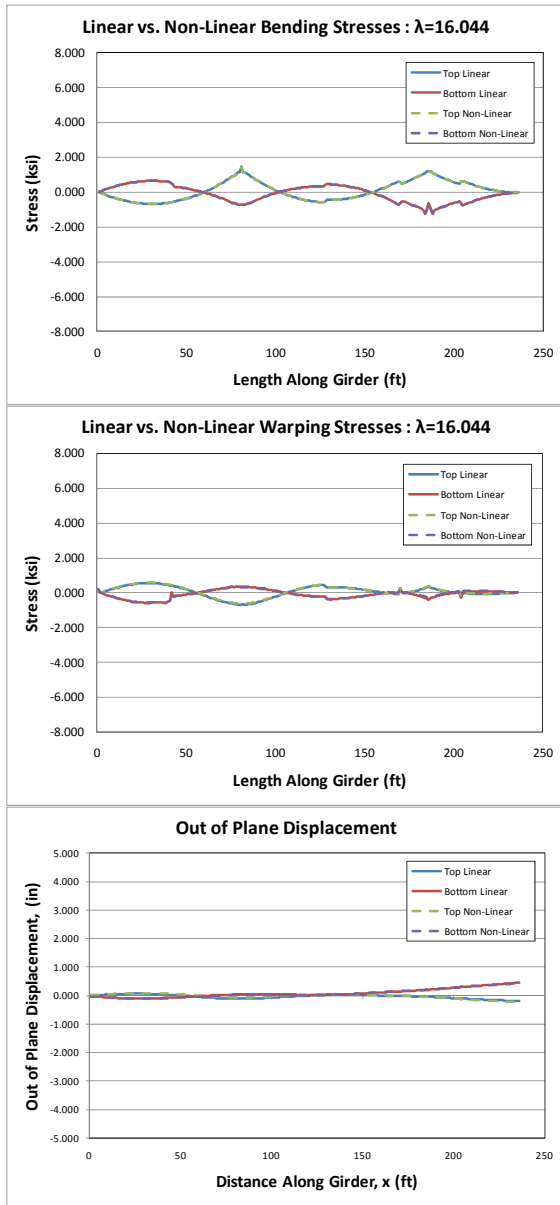


Figure B.18: Holding Crane with 47.8 kip Vertical Force

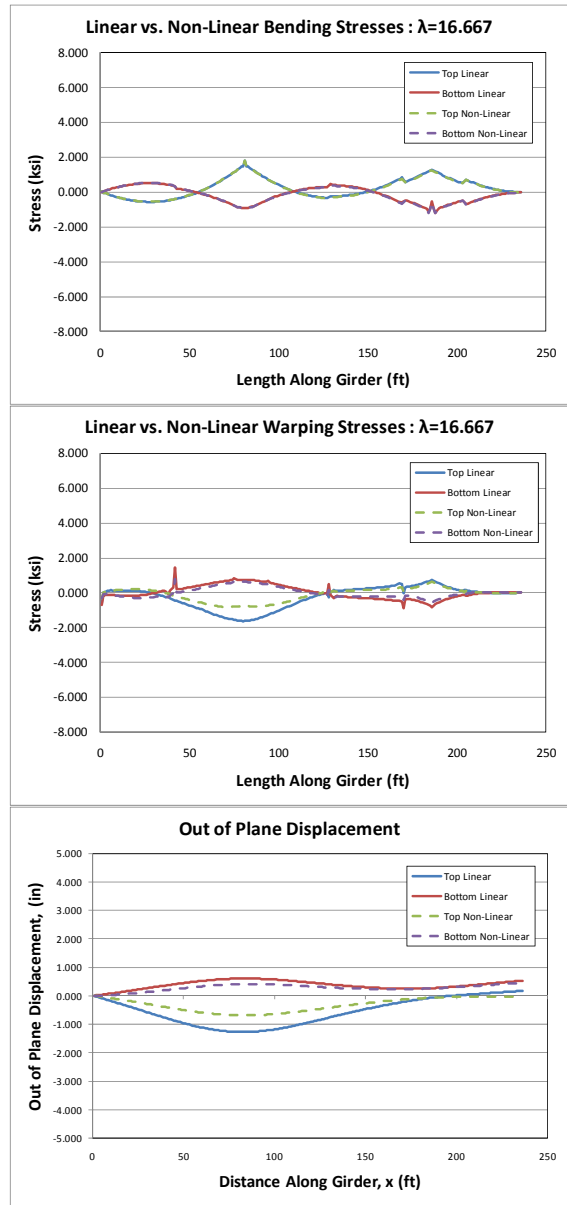


Figure B.19: Holding Crane with 50 kip Vertical Force

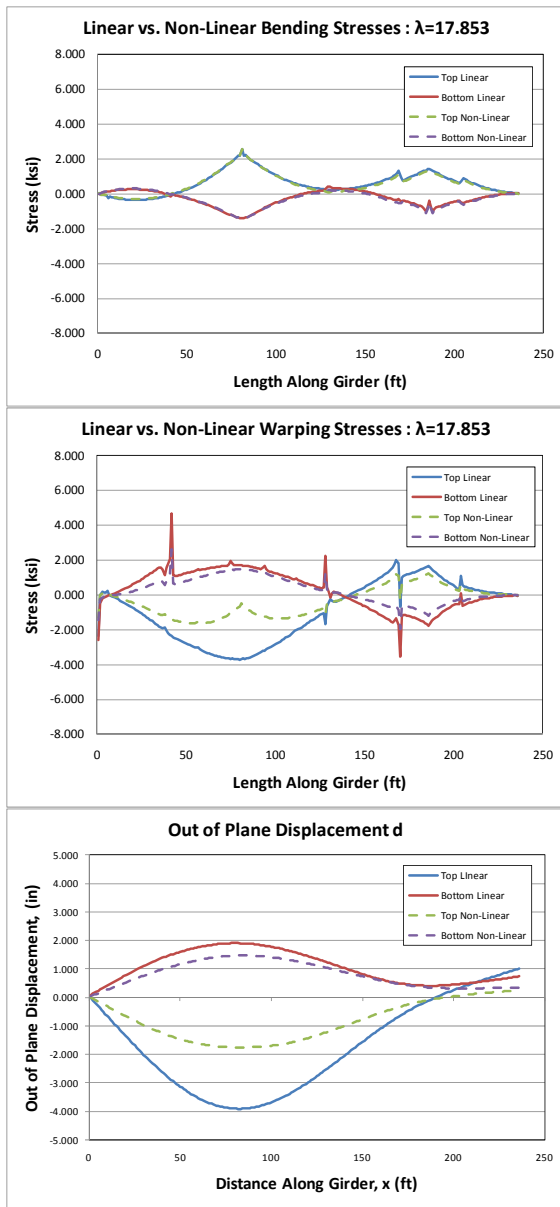


Figure B.20: Holding Crane with 55 kip Vertical Force

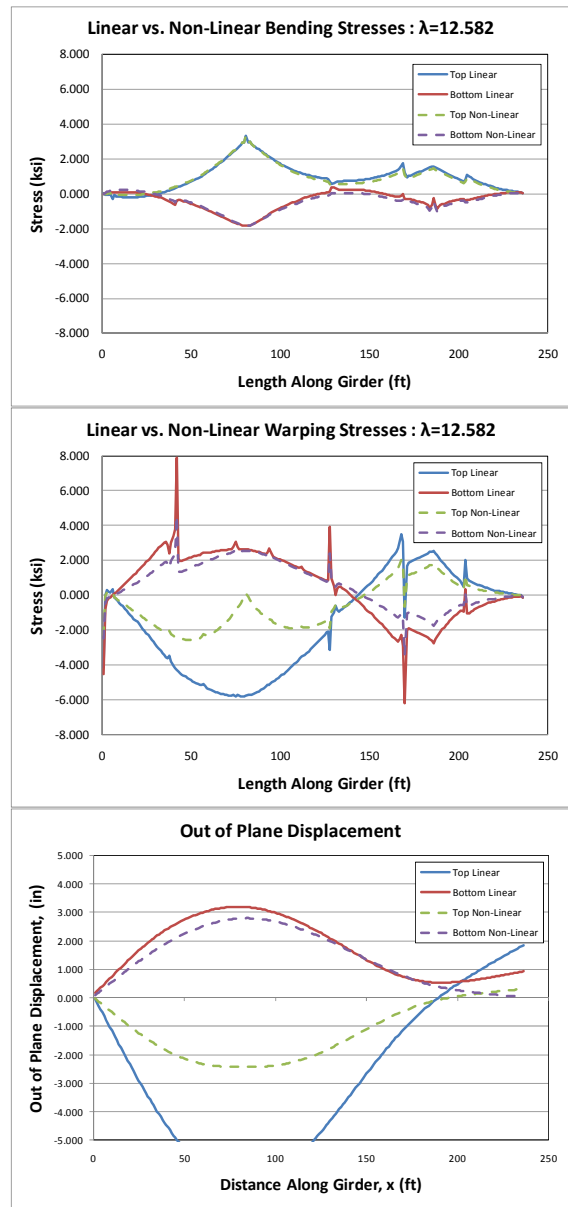


Figure B.21: Holding Crane with 60 kip Vertical Force

B.1.3 Study Three

B.1.3.1 Summary

For the third study, different cantilever ratios and beam lengths were used to see if it affected the results from the previous studies. The three cases that were looked at are as follows where b is the cantilever length, L is the simple span length, and L_{total} is the total propped cantilever length.

- Case 1: $L_{total} = 217$ ft ; $b/L_{total} = 0.15$
- Case 2: $L_{total} = 236$ ft ; $b/L_{total} = 0.22$
- Case 3: $L_{total} = 264$ ft ; $b/L_{total} = 0.30$

For each case, the holding crane was placed at the optimal lift location which corresponds to the location of maximum positive moment. For a propped cantilever beam with a uniformly distributed load such as that of a prismatic girder with only self weight applied, this location can be determined from Eq. 4.1. Analyses were also completed for holding crane locations equal to +/- 10% and +/- 20% of the optimal lift location. The ideal lifting force was used for each holding crane location. The ideal lifting load is equal to the vertical reaction that a shore tower is required to resist if modeled by a rigid support placed at the same location as the holding crane.

B.1.3.2 Parameters and Range

- $b_f/D = 1/6$: $R = 1200'$: $L = \text{varies}$: $D = 84''$: $b_f = 14''$
- Permanent supports located at 0 ft and 185 ft
- **Holding crane location: varies**
- **Holding crane force equal to vertical reaction in a shore tower modeled as a rigid support at the same location**

0.15 Cantilever		
Temporary Support Location (ft)	Support Location (% L+a)	Reaction (kips)
70	0.32	49.5
80	0.37	46
90	0.41	44.7
100	0.46	45.7
110	0.51	48.8

Table B.1: Case 1 Temporary Support Location and Corresponding Reaction

0.22 Cantilever		
Temporary Support Location (ft)	Support Location (% L+a)	Reaction (kips)
66	0.28	44.3
76	0.32	40.7
86	0.36	39.1
96	0.41	39.6
106	0.45	42.1

Table B.2: Case 2 Temporary Support Location and Corresponding Reaction

0.30 Cantilever		
Temporary Support Location (ft)	Support Location (% L+a)	Reaction (kips)
56	0.21	32.5
66	0.25	28.4
76	0.29	26.3
86	0.33	25.9
96	0.36	27.3

Table B.3: Case 3 Temporary Support Location and Corresponding Reaction

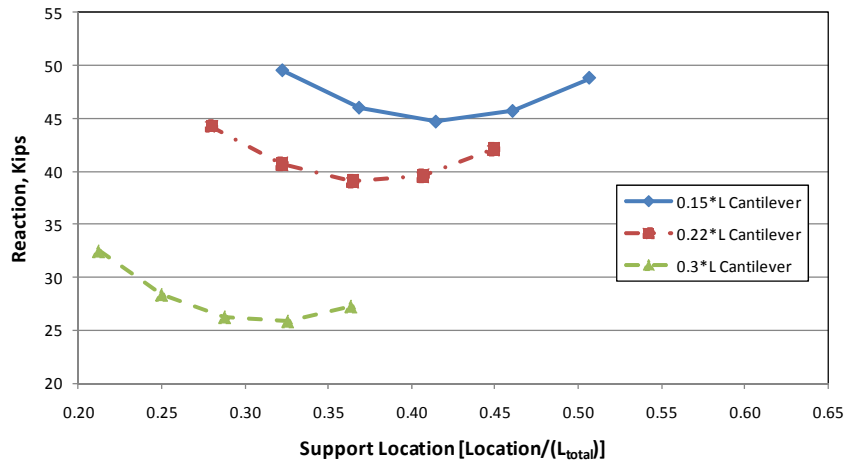


Figure B.22: Shore Tower Reaction vs. Location [% L_{total}]

B.1.3.3 Results

B.1.3.3.1 Case 1

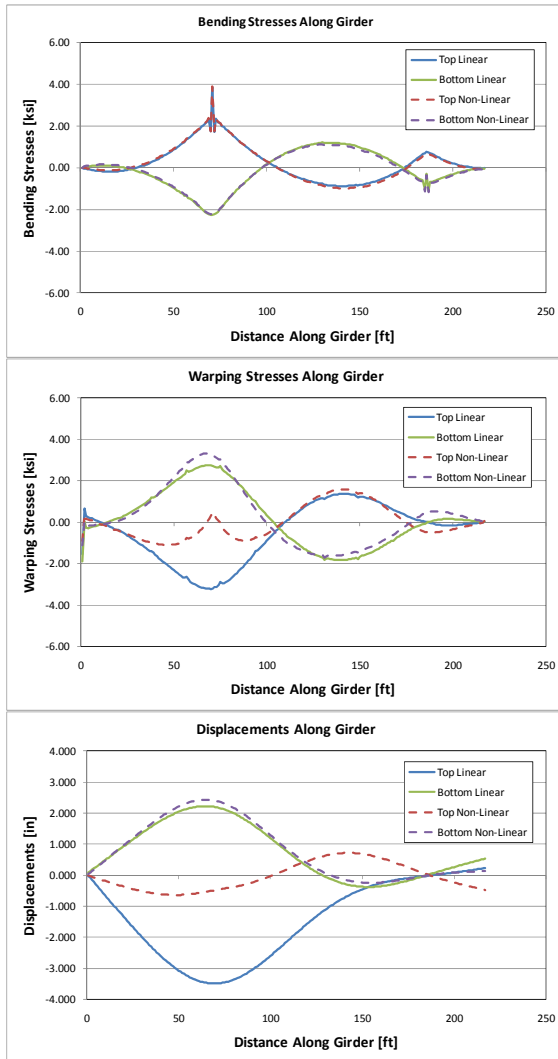


Figure B.23: Case 1: $x = 70$ ft : $F = 49.5$ kips : 0.15 Cantilever

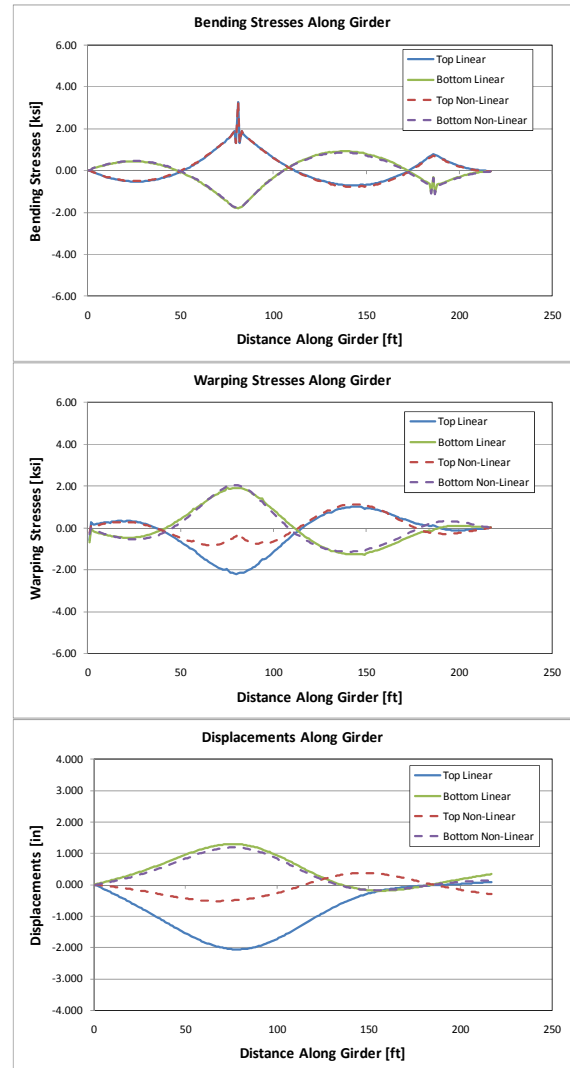


Figure B.24: Case 1: $x = 80$ ft : $F = 46.0$ kips : 0.15 Cantilever

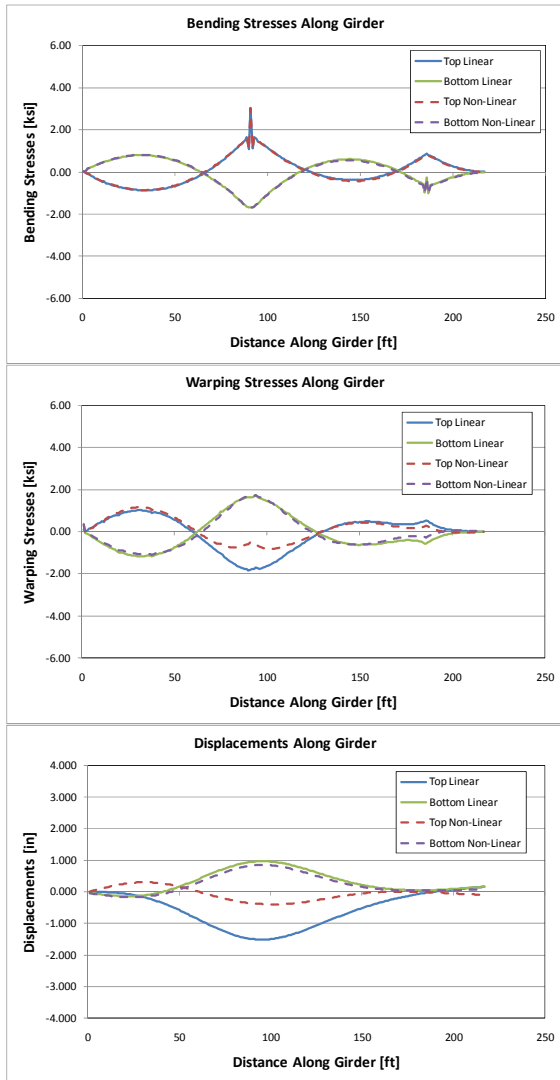


Figure B.25: Case 1: $x = 90$ ft : $F = 44.7$ kips : 0.15 Cantilever

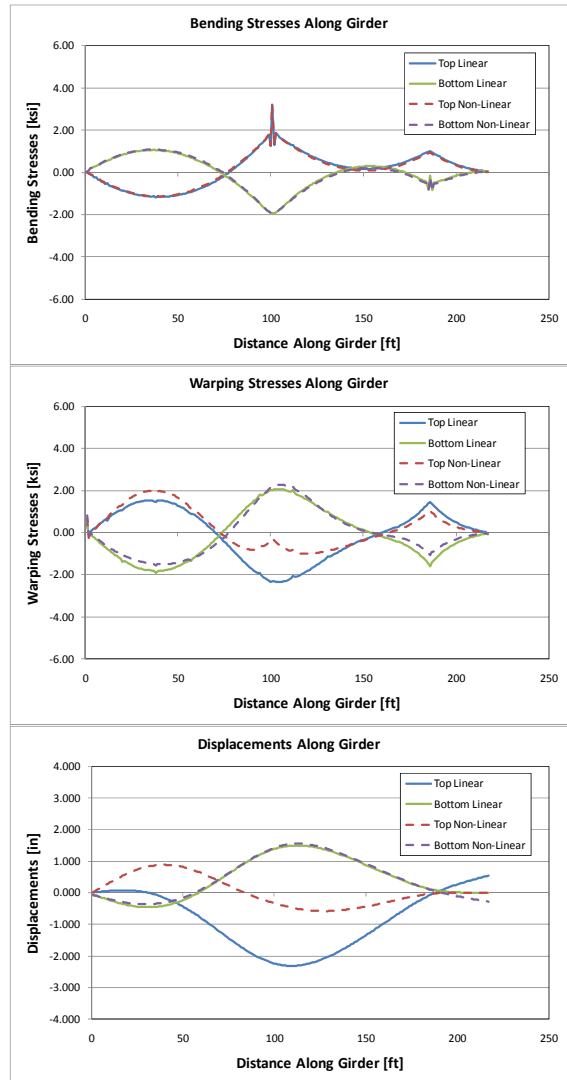


Figure B.26: Case 1: $x = 100$ ft : $F = 45.7$ kips : 0.15 Cantilever

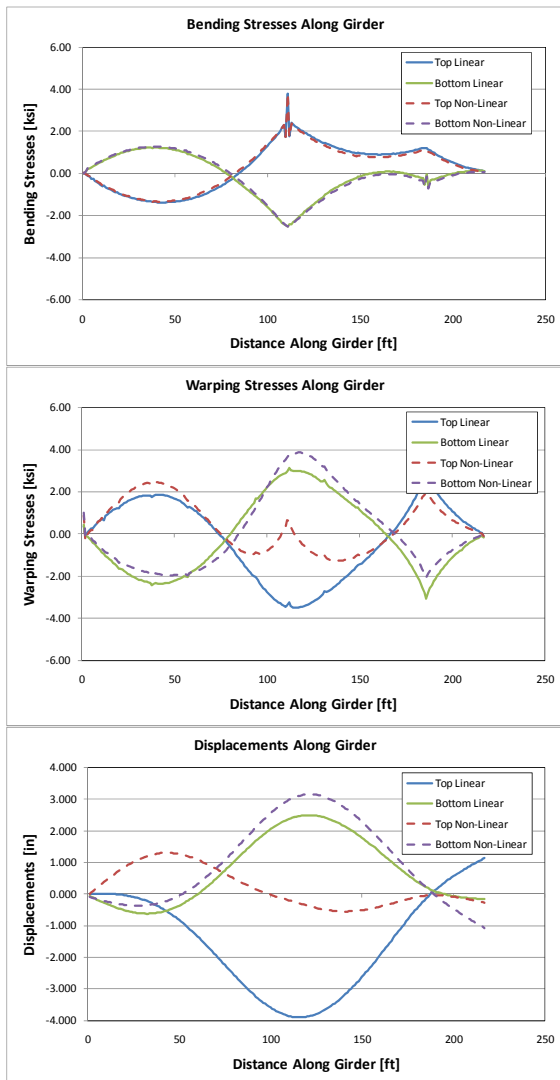


Figure B.27: Case 1: $x = 110$ ft : $F = 48.8$ kips : 0.15 Cantilever

B.1.3.3.2 Case 2

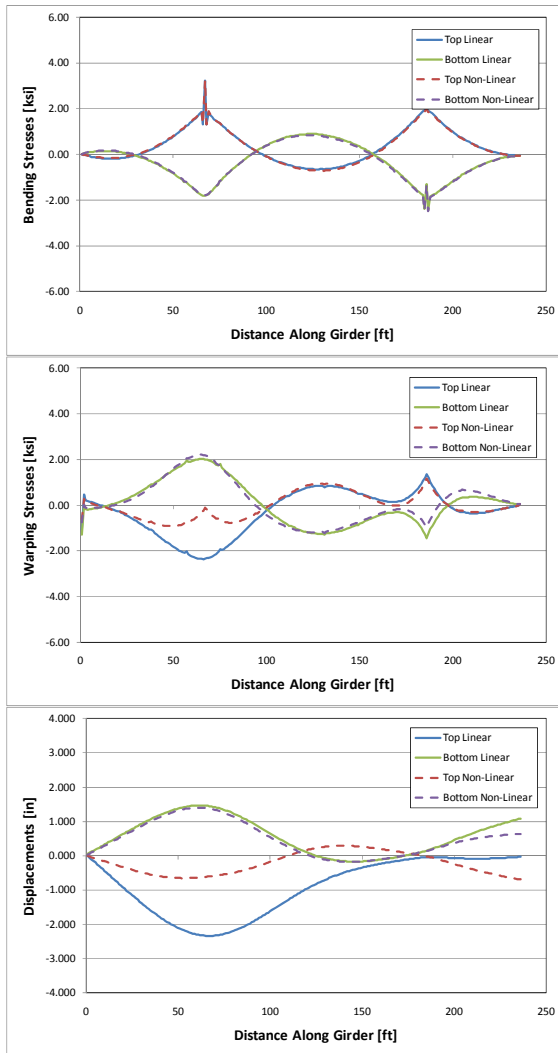


Figure B.28: Case 2: $x = 66 \text{ ft}$: $F = 44.3$ kips : 0.22 Cantilever

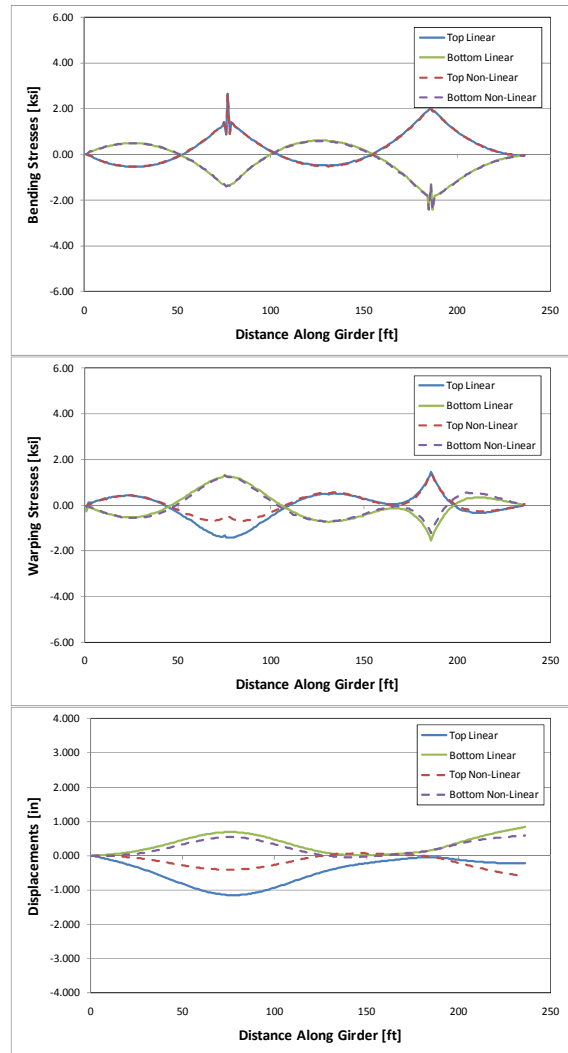


Figure B.29: Case 2: $x = 76 \text{ ft}$: $F = 40.7$ kips : 0.22 Cantilever

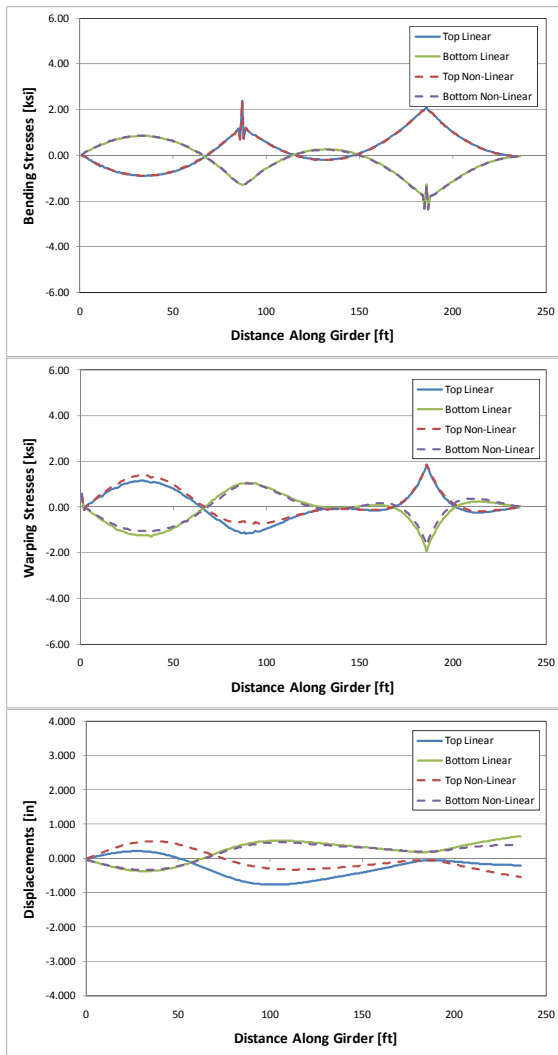


Figure B.30: Case 2: $x = 86$ ft : $F = 39.1$ kips : 0.22 Cantilever

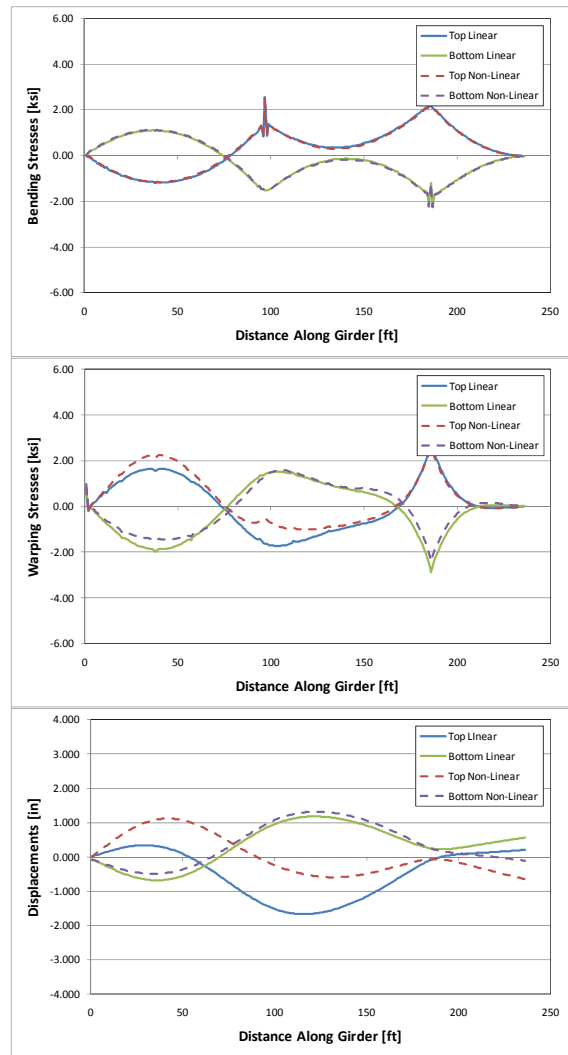


Figure B.31: Case 2: $x = 96$ ft : $F = 39.6$ kips : 0.22 Cantilever

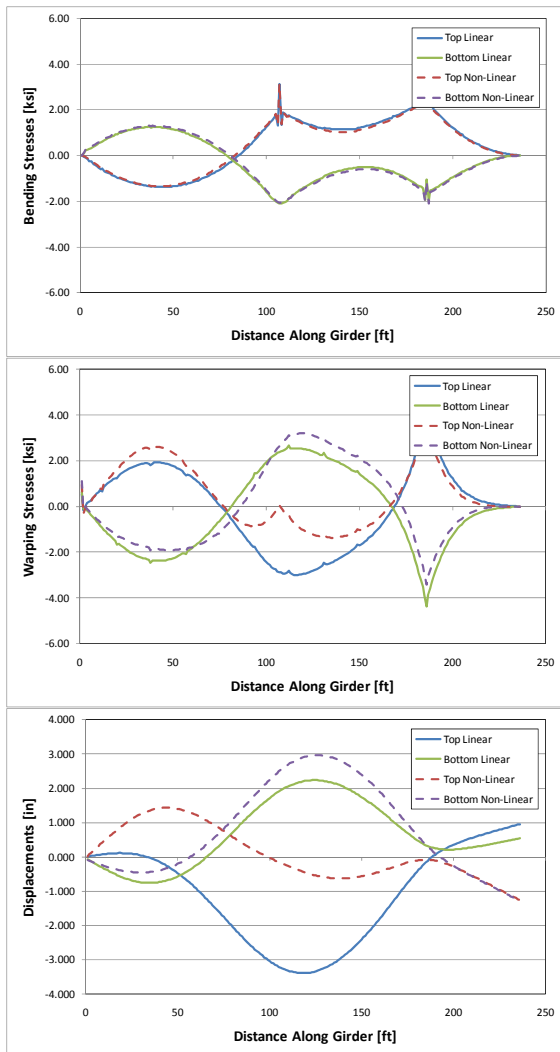


Figure B.32: Case 2: $x = 106$ ft : $F = 42.1$ kips : 0.22 Cantilever

B.1.3.3.3 Case 3

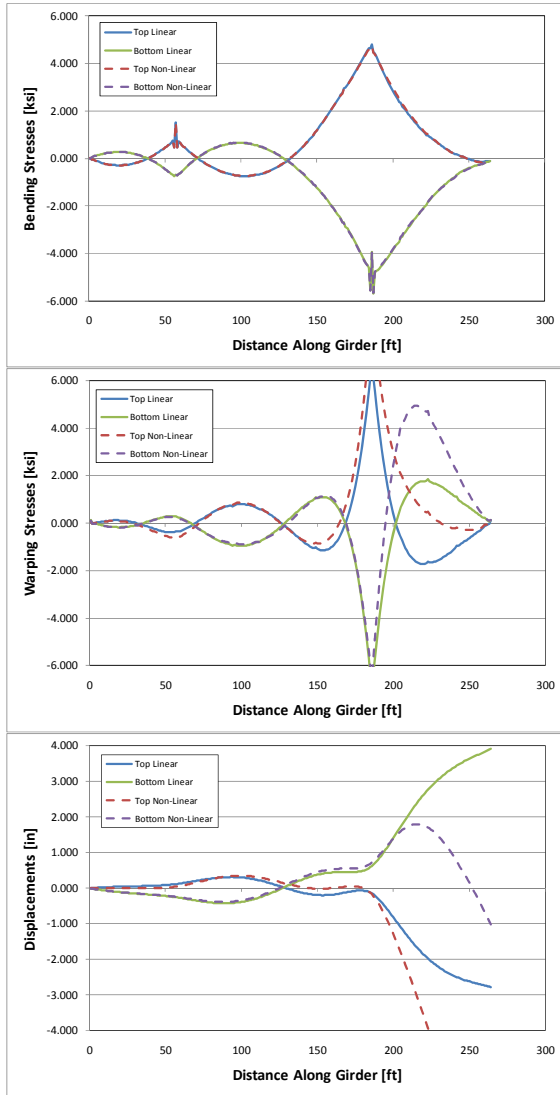


Figure B.33: Case 3: $x = 56$ ft : $F = 32.5$ kips : 0.30 Cantilever

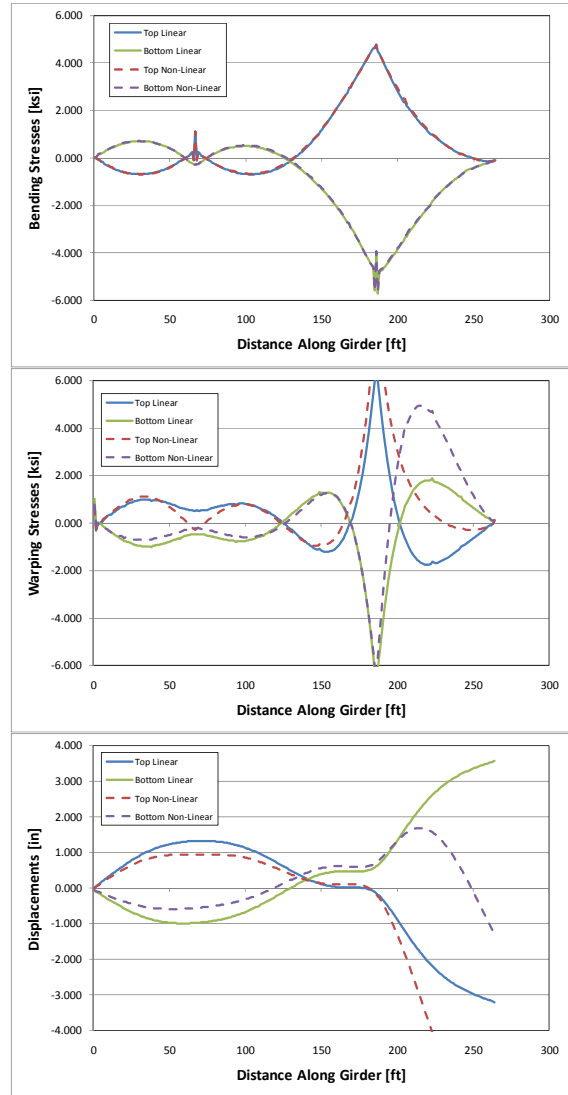
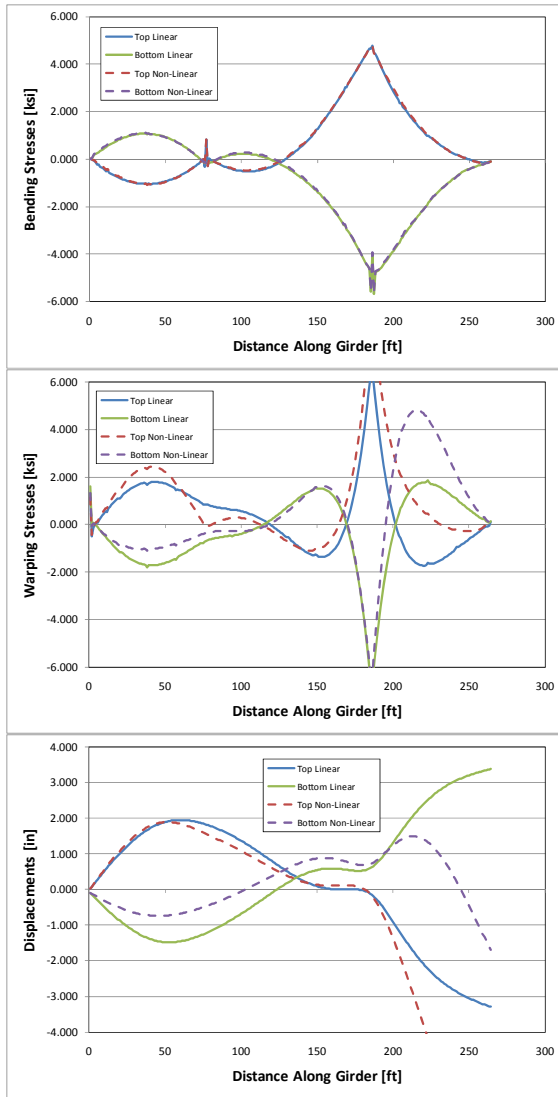
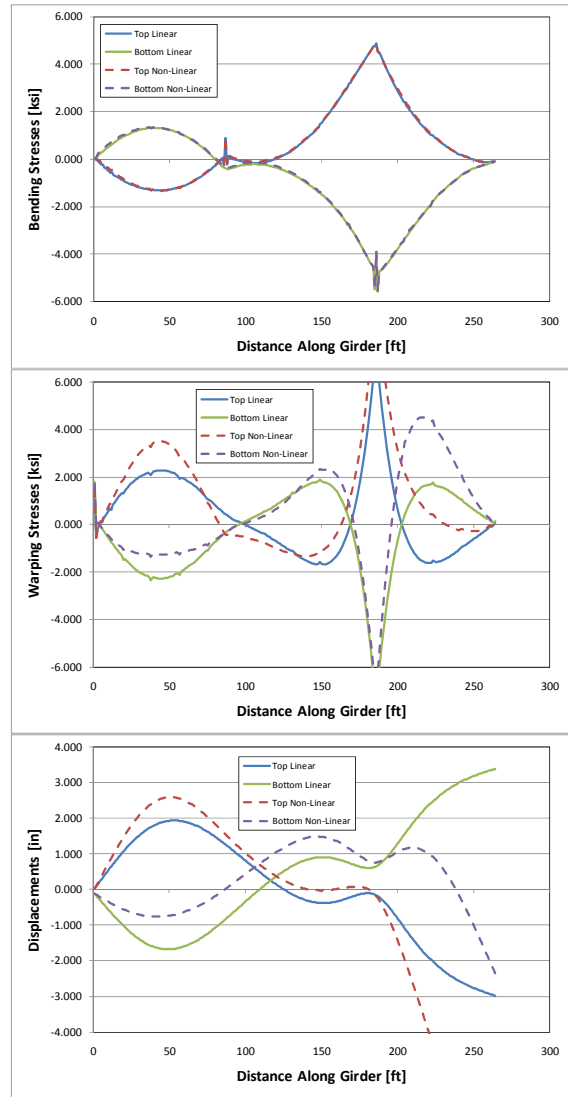


Figure B.34: Case 3: $x = 66$ ft : $F = 28.4$ kips : 0.30 Cantilever



**Figure B.35: Case 3: $x = 76 \text{ ft}$: $F = 26.3$
kips : 0.30 Cantilever**



**Figure B.36: Case 3: $x = 86 \text{ ft}$: $F = 25.9$
kips : 0.30 Cantilever**

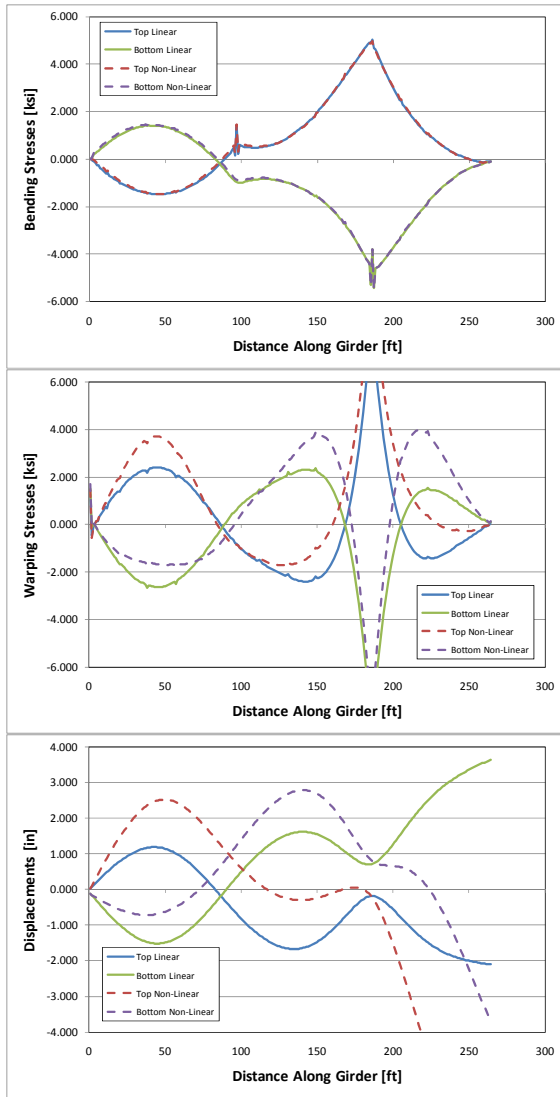


**Figure B.37: Case 3: $x = 96 \text{ ft}$: $F = 27.3$
kips : 0.30 Cantilever**

References

1. American Association of State Highway and Transportation Officials (AASHTO). Guide Specifications for Horizontally Curved Bridges. Washington, D.C., 2003.
2. American Associations of State Highway and Transportation Officials (AASHTO). AASHTO LRFD Bridge Design Specifications. Washington, D.C., 2007.
3. American Bridge Division. Handbook for Construction Engineers. Pittsburgh: United States Steel Corporation, 1983.
4. American Institute of Steel Construction, Inc. (AISC). Steel Construction Manual, 13th Edition. Chicago: American Institute of Steel Construction, Inc., 2005.
5. Brennan, P.J. "Horizontally Curved Bridges First Annual Report: Analysis of Horizontally Curved Bridges Through Three-Dimensional Mathematical Model and Small Scale Structural Testing." First Annual Report: Research Project HPR-2(111) (1970).
6. Canadian Institute of Steel Construction (CISC). Torsional Section Properties of Steel Sections. Markham: Canadian Institute of Steel Construction (CISC), 2002.
7. Earls, C J. "Observations on Eigenvalue Buckling Analysis Within a Finite Element Context." Proceedings - 2007 Annual Stability Conference (2007).
8. Farris, Jamie F. Behavior of Horizontally Curved Steel I-girders, Masters Thesis. Austin: University of Texas at Austin, 2008.
9. Howell, T D and C J Earls. "Curved Steel I-Girder Bridge Response during Construction Loading: Effects of Web Plumbness." Journal of Bridge Engineering (2007).
10. Mertz, Dennis R and Fred R Beckmann. "Steel Bridge Erection Practices." NCHRP Synthesis 345 (2005).
11. NCHRP Synthesis 345. Steel Bridge Erection Practices, A Synthesis of Highway Practice. Washington D.C.: Transportation Research Board of the National Academies, 2005.

12. Schuh, Andrew C. Behavior of Horizontally Curved Steel I-girders During Lifting, Masters Thesis. 2008: University of Texas at Austin, 2008.
13. Stith, Jason and Brian Petruzzi. "UT Bridge Beta 1.0 User Manual." Austin: University of Texas at Austin, 2009.
14. Stith, Jason C. The Behavior of Curved I-girder Bridges During Construction, PhD Dissertation. Austin: University of Texas at Austin, 2010.
15. Stith, Jason, et al. Guidence for Erection and Construction of Curved I-girder Bridges, FHWA/TX-09/0-5574. Austin: Center for Transportation Research, 2009.
16. Stith, Jason. "The Behavior of Horizontally Curved Plate Girders During Lifting." World Steel Bridge Symposium. San Antonio: American Institute of Steel Construction, 2009.
17. Texas Steel Quality Council. Preferred Practices for Steel Bridge Design Fabrication and Erection. Austin: Texas Department of Transportation (TxDOT), 2007.
18. Timoshenko, S P and J M Gere. Theory of Elastic Stability. 2nd Edition. New York: McGraw-Hill Book Company, Inc., 1961.
19. Topkaya, Cem. Behavior of Curved Steel Trapezoidal Box Girders During Construction, PhD Dissertation. Austin: University of Texas at Austin, 2002.
20. White, D W, et al. Development of Unified Equations for Design of Curved and Straight Steel Bridge I Girders. Prepared for American Iron and Steel Institute Transportation and Infrastructure Committee. Georgia Institute of Technology. Atlanta: Professional Service Industries, Inc. and Federal Highway Administration, 2001.
21. Zhao, Q, et al. "Monitoring Steel Girder Stability for Safer Bridge Erection." Journal of Performance of Constructed Facilities (2009).
22. Zhao, Qihong, et al. "Monitoring Steel Girder Stability for Safer Bridge Erection." World Steel Bridge Symposium. San Antonio, 2009.

Vita

Brian James Petruzzi, son of James and Carol Petruzzi and brother of Heather Petruzzi, was born in North Brunswick, New Jersey on February 23, 1986. At the age of five, his family moved from New Jersey to Dublin, Ohio where he spent the rest of his childhood. In May of 2008, Brian graduated from Dublin Coffman High School and in August of the same year enrolled at Virginia Polytechnic Institute and State University (Virginia Tech) in Blacksburg, Virginia. He graduated summa cum laude from Virginia Tech with a Bachelor of Science in Civil Engineering in May of 2008. In August of 2008, he enrolled in graduate school at The University of Texas at Austin, where he worked as a research assistant at the Phil M. Ferguson Structural Engineering Laboratory. Upon graduation from The University of Texas, he will be moving to Washington, DC to work for Weidlinger Associates, Inc.

Permanent Address:

135 Goldfinch Terrace
Hackettstown, NJ 07840

This document was typed by the author.